THE UNIVERSITY OF CHICAGO

# THE ROLE OF M6A MRNA METHYLATION IN OLIGODENDROCYTE DEVELOPMENT, CNS MYELINATION, AND REMYELIANTION

A DISSERTATION SUBMITTED TO

THE FACULTY OF THE DIVISION OF THE BIOLOGICAL SCIENCES

AND THE PRITZER SCHOOL OF MEDICINE

IN CANDIDACY FOR THE DEGREE OF

DOCTOR OF PHILOSOPHY

COMMITTEE ON NEUROBIOLOGY

BY

HUAN XU

CHICAGO, ILLINOIS

AUGUST 2021

For my dear friends, who accompanied me and made this journey so colorful and meaningful.

**Table of Contents**

**List of Figures**

**List of Tables**

**Acknowledgments**

In this journey, I was fortunate to encounter incredible mentors, colleagues, and friends, who had made positive, long-last impacts on many aspects of my life.

I want to particularly thank my Ph.D. mentor, Dr. Brian Popko. He is a brilliant and excellent scientist and a mentor for the rest of my life. Over the years, he patiently taught me many things that helped me to grow both professional and mentally. His dedication, humbleness, passion, and enthusiasm towards science inspire me on a day-to-day basis. His encouragement boosts my confidence to achieve higher and better. He nurtures an environment that I can freely ask questions and express my thoughts and ideas. He is always approachable when I need guidance and help. He generously shares his feedbacks whenever I have doubts and concerns. He trained me to think like a scientist, ask critical questions, write, and present science works outstandingly. Without Brian, it's impossible for me to arrive where I am. I feel wholeheartedly grateful of all the efforts, time, and trust Brian puts on me.

I also want to thank my committee members, who have guided and supported me all the way along my Ph.D. journey. Dr. Christopher Gomez is my thesis committee member and my mentor in the pathology and translational neuroscience (PTN) program. In the PTN program, Dr. Gomez designed and conducted a course called "Neurobiology diseases," in which physicians and scientists gather together to talk about the progress and integration of science and medicine based on different topics. It's the best course that I have ever attended in so many years of my study. I loved it so much that I took the course repeatedly more than three times. Even though the topics were similar each year, the knowledge of the course was constantly updated, so I learned new things every time I walked into the class. To motivate us, Dr. Gomez designed the clinical shadow sessions for us to closely observe the patients with neurobiology diseases and the strategies to help

them with translational neuroscience knowledge. I was fortunate to be shadowed by Dr. Gomez. I observed his outstanding communication skills to build deep connections with his patients and his endless efforts to design better diagnosis strategies and better treatments. Dr. Gomez's spirit and enthusiasm deeply inspire me, and he has become my role model to be a physician/scientist.

Dr. Xiaoxi Zhuang is an amazing mentor. He has mentored me in so many ways that I could not thank him enough with my words. Xiaoxi is an erudite expert in many science fields, and he is actively engaged in mentoring students. He has been on many students' thesis committees, including several of my close friends. When we talked about him, we all agreed that the way he treats his students is like treating his own children, which sometimes is really touching. He is one of the most wonderful human beings that I have ever encountered. From him, I learned how to become a better scientist, a better teacher, and a better person. I am grateful to have Dr. Tao Pan in my committee. He is a very cool professor and a brilliant scientist. He is always concise and straightforward to point out the key problems and solutions. Over the years, he has brought up many great questions and guidance that helped my project move forward. It's always delightful to have him in the same room to talk about science – it is like opening a box of chocolate, full of joy and surprises.

I want to thank my dear friends. They are my family in the U.S. I cannot imagine how this journey would look like without them. They are always on my back, support me, heal me and encourage me. We share food, thoughts, happiness, and sorrows. We deeply trust and appreciate the presence of each other. With them, I experience deep and satisfying human connections and understand what happiness feels like. Their kindness, compassion, grits, intelligence, and curiosities remind me time after time that I'm so lucky to be here, to have them in my life.

I want to thank my family. Their faith in me and love for me are the valuable assets that empower me to explore fearlessly, to achieve higher and further ambitiously. They encourage me to live happily and to be carefree, to pursue the things that I like and want for my life. It's liberating to have my family's support and encouragement. Without them, I won't be able to start this journey.

Last but not least, I want to thank all my lab members and colleagues who had helped me, guided me and inspired me along the journey. It was wonderful to work with them and learn from them every day.

**Abstract**

Oligodendrocytes are the myelin-forming cells in the central nervous system (CNS). Myelin is a multilayered membrane sheath structure that surrounds neuronal cell axons. Oligodendrocyte lineage cells and myelin are important for various CNS functions, such as electrical signal propagation and axonal metabolic support. Recent studies revealed oligodendrocyte lineage cells and myelin also play important roles in motor skill learning, memory and the aging process. Inherited and acquired myelination deficits such as leukodystrophies and multiple sclerosis result in severe neurological dysfunctions. At present, molecular mechanisms controlling oligodendrocyte differentiation and myelination are not comprehensively understood.

Recent evidence has shown that RNA modification is a dynamic and reversible process, which adds a new layer of understanding to epigenetic regulation in biological processes. N6-methyladenosine ($m^6A$), the most abundant internal modification site in eukaryotic messenger RNA (mRNA), is the first example of reversible RNA methylation. The conservative enrichment of $m^6A$ in stop codons, 3'-untranslated regions, and long internal exons in mice and humans suggest its fundamental importance in RNA biology. Discovery of $m^6A$ methyltransferase protein "writers," demethylase protein "erasers," and "readers" suggests their dynamic regulatory roles in reversible RNA modification. Many in vitro and in vivo studies have shown that reversible methylation of mRNA is essential for cell survival and cell differentation. Compared to DNA and protein methylation, RNA modification has the poteintial to have rapid influence on mRNA metabolism and gene expression, and thereby contribute to rapid cellular responses to cellular and environmental cues. In the CNS, studies have found $m^6A$ mRNA methylation is critical for embryonic neruogenesis and neural repair. In addition, $m^6A$ mRNA methylation plays a regulatory role in various CNS functions such as learning and memory. As a glia population, oligodendrocyts

share the same embryonic stem cell origin with neuorns, and actively interact with neurons to perform CNS functions. Therefore, it is highly important to understand whether $m^6A$ mRNA methylation plays a role in regulating oligodendrocytes lineage progression and function.

This thesis will focus on understanding the potential role that $m^6A$ mRNA regulation plays in oligodendrocyte development, CNS myelination, and remyelination. Chapter 1 will provide an overview of the current knowledge of molecular mechanisms regulating oligodendrocyte lineage progression. Chapter 2 will describe our discovery of $m^6A$ mRNA modification mechanism in regulating oligodendrocyte lineage development and the myelination process. In mouse models that specifically inactivate an essential $m^6A$ writer component, METTL14, we found an abnormal myelination process and disrupted oligodendrocyte differentiation. We also discovered that *Mettl14* deletion in oligodendrocyte lineage cells causes aberrant splicing of myriad RNA transcripts and disruption of gene expression, including an essential paranodal component neurofascin 155 (NF155). Chapter 3 will introduce the findings of $m^6A$ mRNA modification in the remyelination process in adult animals. We found that *Mettl14* deletion in oligodendrocyte precursor cells (OPCs) prevents proper remyelination after the demyelination event. Chapter 4 will discuss how we can further enhance our understandings based on the findings in chapters 2 and 3, in order to gain a complete mechanistic picture of oligodendrocyte biology and promote therapeutic discoveries for myelin diseases.

# CHAPTER 1

# The molecular mechanisms of oligodendrocyte Lineage progression

## 1.1 Abstract

Oligodendrocytes are myelin forming cells in the CNS. Recent evidence suggests oligodendrocyte lineage cells and CNS myelin contribute to CNS functions and pathological processes to a far greater extent than previously identified. Thus, it is critical to expand our knowledge to gain complete understanding of these processes and their regulatory mechanisms. Oligodendrocyte lineage progression is orchestrated by multiple layers of molecular regulations in time and space. In this chapter, I will review the recent findings of molecular mechanisms that regulate the oligodendrocyte lineage progression, including transcriptional factors, signaling pathways, and epigenetic regulatory mechanisms.

## 1.2 Oligodendrocyte lineage progression overview

Oligodendrocytes are glial cells that are responsible for myelination in the central nervous system (CNS). Myelin membrane sheath insulates the axons to allow rapid and efficient transduction of electrical signals and provides essential metabolic support to axons. With the advancement of technologies and available tools, it has been discovered that oligodendrocyte lineage cells and CNS myelin contribute to CNS functions and pathological processes to a far greater extent than formerly identified. Increasing evidence indicates that myelin sheath is more than an insulating membrane structure that plays a supportive role in the CNS. In fact, myelin plays an active role in CNS functions such as motor learning, social behavior, and sensory experience. These activity-

dependent, experience-driven myelination and myelin remodeling events suggest oligodendrocyte lineage cells' fundamental contribution to CNS complexity (Casaccia and Corfas, 2018). In addition, defects in the myelination process are associated with developmental disorders such as growth retardation, autism, heart disease, atresia choanae, genital hypoplasia, and ear abnormalities (CHARGE) syndrome, as well as neurodegenerative diseases such as multiple sclerosis (MS) and leukodystrophies (Berry et al., 2020). To decipher normal CNS functions and develop therapeutic strategies, we must gain complete understandings of molecular mechanisms that regulate the developmental myelination and remyelination process.

Oligodendrocytes develop from oligodendrocyte precursor cells (OPCs). OPCs arise from neuroepithelial cells in the ventral ventricular germinal zones at embryonic day 12.5(E12.5) in mice and gestational week 6.5 (~E45) in humans (Bergles and Richardson, 2015). Soon after OPCs appear, they proliferate rapidly, migrate and evenly distribute throughout CNS by E15 in mice. Unlike most progenitors, OPCs remain abundant in the adult CNS, proliferate and generate new oligodendrocytes to allow myelination upon pathological insults or aging, and change myelination patterns in response to life experience (Bergles and Richardson, 2015).

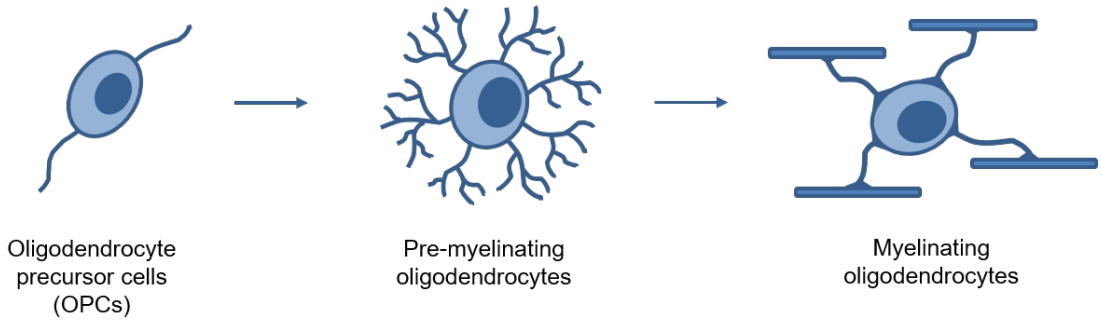


**Figure 1.1. Oligodendrocyte development paradigm**

To become mature myelinating oligodendrocytes, OPCs first exit the proliferation state and differentiate into pre-myelinating oligodendrocytes, resulting in the expression of major myelinating proteins such as myelin basic protein (MBP) and proteolipid-protein (PLP) (Zuchero and Barres, 2015). A series of morphological changes then allows these oligodendrocytes to extend many processes that wrap axons with the multilayered myelin sheaths (Figure1.1). Elucidating the key events involved in oligodendrocyte lineage progression is critical to understand the cellular and developmental biology of myelin production and regeneration in CNS diseases (Chamberlain et al., 2016). Following a defined series of steps, oligodendrocyte lineage progression is tightly controlled in time and space (Liu et al., 2016). However, the exact mechanism by which oligodendrocyte lineage progression is regulated has yet to be fully elucidated.

Over the past several decades, considerable insight has been gained into the molecular control of oligodendrocyte lineage progression. A number of intrinsic and extrinsic factors have been identified to be critical for regulating oligodendrocyte development. Growth factors, such as Sonic hedgehog (Shh), bone morphogenetic proteins (BMPs), and platelet-derived growth factor (PDGF), have been shown to influence the maturation of oligodendrocyte lineage cells from early progenitors to mature, myelinating cells (Nishiyama et al., 2009). Transcription factors, such as Nkx-2.2, Olig1, Olig2, Sox10, Myrf, and ZFP24, are required for the maturation of oligodendrocytes (Elbaz and Popko, 2019; Mitew et al., 2014). In addition, epigenetic mechanisms including chromatin remodeling by DNA methylation, histone deacetylases, and gene silencing by non-coding RNAs have been shown to play critical roles in oligodendrocyte differentiation and function during development and remyelination (Li and Richardson, 2009; Marin-Husstege et al., 2002; Moyon and Casaccia, 2017; Ye et al., 2009; Zhao et al., 2010b).

### 1.3 The mechanisms of oligodendrocyte lineage progression

### 1.3.1 Transcriptional regulation

During development, the commitment of oligodendrocyte lineage requires specified, tightly controlled feedback loops that involve key transcriptional factor networks (Elbaz and Popko, 2019). Following specification from neuroepithelial cells, OPCs express various transcriptional factors as they migrate out of their birthplace to colonize other CNS areas. These include continued expression of Olig1, Olig2, Nkx2-2, and Sox10, which are vital for the maintenance of OPCs. Controlled by Shh expression, Olig1 and Olig2 are key regulators of oligodendrocyte development (Lu et al., 2002). Throughout the CNS, Olig1 and Olig2 are required for the specification of oligodendrocytes progenitors. PDGF-α is critical for the survival and proliferation of OPCs (Emery and Lu, 2015). To maintain an undifferentiated state, OPCs express a repertoire of transcription factors that mediate the inhibitory extracellular signals to prevent differentiation. These factors include Id2, Id4, Sox5, Sox6, Hes5, all of which downregulate rapidly when OPCs enter the pre-myelinating stage (Emery and Lu, 2015). One of the most critical regulation points in oligodendrocyte lineage and CNS myelination is the stage that OPCs exit the cell cycle and differentiates into oligodendrocytes. It's a terminal event that requires to be tightly controlled to determine the timing of myelination during development and maintain OPCs for subsequent division and differentiation throughout life (Emery and Lu, 2015). In general, there is balanced proliferation/maintenance, and terminal differentiation signals maintained in OPCs. When this balance is tipped toward terminal differentiation, a cascade of myelination programs promotes differentiation and myelination. Recent evidence indicates that SOX10 is a major determinant of the terminal differentiation of oligodendrocyte lineage. SOX10 initiates transcriptional feedback loops for oligodendrocyte differentiation and activates a number of critical genes to the myelination process. For example, the myelin gene regulatory factor (*Myrf*) is one of the critical

transcriptional factors that locate in the SOX10 mediated differentiation feedback loop networks. Once *SOX10* activates *Myrf*, a number of myelin genes are activated and promote pre-myelinating oligodendrocytes' progress to a mature, myelinated state (Bujalka et al., 2013; Elbaz and Popko, 2019). In addition, SOX10 binds to the enhancer of *Zfp24*, an oligodendrocyte-specific zinc finger transcription factor that is required for CNS myelination. *Zfp24,* in turn, directly mediates the expression of *Sox10* and *Myrf* (Elbaz et al., 2018). Ther are similarities and differences of transcriptional regulation between myelination in early development and remyelination in adults. For example, Sox2, a transcription factor that has limited effects on OPC expansion during development plays prominent role in remyelination in the adult brains (Hoffmann et al., 2014; Sock and Wegner, 2019). It recruits Chd7-containing chromatin remodelers to positively augment proliferation of adult OPCs during remyelination (Doi et al., 2017).

### 1.3.2 Signaling pathways

The development of oligodendrocyte lineage and CNS myelination also requires coordinated signaling pathways (He and Lu, 2013). A number of signaling pathways are found critical for oligodendrocyte lineage progression and maturation. During early development, the sonic hedgehog (Shh) signal secreted from the notochord and ventral neural tube induces OPC specification. In the dorsal neural tube, bone morphogenetic protein (BMP) secretes Wnt signals to inhibit OPC generation and differentiation. Notch signaling pathway has been demonstrated to play an important role in oligodendrocyte differentiation. It plays a role in regulating OPC specification (Grandbarbe et al., 2003) and the timing of CNS myelination (Wang et al., 1998). Growth factors such as fibroblast growth factor (FGF) family and platelet-derived growth factor (PDGF) signaling are essential for OPC proliferation (van Tilborg et al., 2018); however, they inhibit OPC differentiation and maturation in a stage-specific manner development. Insulin-like

growth factor (IGF) promotes OPC differentiation and interacts with other growth factors such as FGF and BMP to regulate oligodendrocyte maturation (Wheeler and Fuss, 2016). The lingo-1 pathway is found to be an inhibitor for axonal growth and oligodendrocyte differentiation and maturation. Lingo-1 antagonists promote remyelination in the experimental autoimmune encephalomyelitis (EAE) mouse model of multiple sclerosis (Sun et al., 2015). Intrinsically, Wnt/β-catenin, PI3K/AKT/mTOR, and ERK/MAPK signaling pathways are crucial for the terminal differentiation of OPCs and myelin formation (Gaesser and Fyffe-Maricich, 2016). Wnt/β-catenin pathway regulates oligodendrocyte development in a stage-dependent manner. Before gliogenesis, activation of β-catenin inhibits the generation of OPCs. Once OPCs are formed, the Wnt/β-catenin signal plays an essential role in promoting oligodendrocyte differentiation (Dai et al., 2014). Akt/mTOR signaling pathway regulates the transition of the late progenitor stage to immature oligodendrocytes and promotes the commitment to oligodendrocyte differentiation before myelination (Tyler et al., 2009). During the remyelination process, the Akt pathway plays an important role in generating an adequate number of OPCs and appropriate differentiation of oligodendrocytes (Gaesser and Fyffe-Maricich, 2016). ERK/MAPK pathway can be activated by various growth factors such as PDGF and FGF-2. It has been implicated in many different aspects of OL development, including proliferation, migration, differentiation, and myelination (Gaesser and Fyffe-Maricich, 2016). In contrast to Akt/mTOR pathway, ERK/MAPK pathway is required for the transition of early progenitors to the late progenitor stage and immature stage, it is not required for the transition of immature oligodendrocytes to mature oligodendrocytes (Guardiola-Diaz et al., 2012).

### 1.3.3 Epigenetic regulation

Oligodendrocyte lineage cells and the myelination process are highly responsive to environmental cues. First, there are critical periods during development that oligodendrocyte lineage cells and myelin formation are highly receptive to the environmental cues (Liu et al., 2012; Makinodan et al., 2012). Second, neuronal activity or experience promotes OPC proliferation, oligodendrocytes differentiation, and synthesis of myelin(Gibson et al., 2014; Liu et al., 2012; Makinodan et al., 2012; McKenzie et al., 2014; Xiao et al., 2016a). Third, myelin plasticity and adaptive changes in myelin microstructure are crucial for neural circuit formation and CNS functions such as learning and cognition (Almeida and Lyons, 2017; Ford et al., 2015; Saab and Nave, 2017). These interactions and adaptations of oligodendrocyte lineage functions to the environment require dynamic regulation of gene expression and cell state transformation, suggesting epigenetic regulatory mechanisms play a role in these processes. Indeed, the importance of epigenetic mechanisms regulating oligodendrocyte lineage progression has been increasingly recognized by the field in the past decade.

Epigenetic regulation refers to the changes in the genome without affecting the nucleotide sequence. It influences a number of gene expression processes, such as DNA methylation, histone modification, ATP-dependent chromatin remodeling, and non-coding RNAs (long non-coding RNAs, microRNAs). There is emerging evidence that epigenetic regulation plays an important role in the oligodendrocyte lineage specification, development, myelination, and remyelination.

### 1.3.4 DNA methylation

DNA methylation is an important epigenetic mechanism that regulates CNS development. It is a multi-step modulation process of the local DNA markers. Moreover, it plays key roles in various cellular functions, such as aging, genomic imprinting, transposon silencing, and transcription

factor binding (Arthur-Farraj and Moyon, 2020). During oligodendrocyte lineage progression, the methylation levels have dynamic changes in different stages of development (Sanosaka et al., 2017). The dynamic levels of DNA methylation, hydroxymethylation and their respective catalytic enzymes, DNA methyltransferases (DNMTs), and ten-eleven translocations (TETs) in the oligodendrocyte lineage suggest their essential roles for oligodendrocyte development. At the early developmental stage, DNA methylation affects the lineage specification of oligodendrocytes. A recent methylome mapping study highlights the sequential demethylation of gliogenic genes such as gliogenic-specific nuclear factor I binding sites during neural stem cell differentiation. After glial cell fate choice is made, glial cells acquire methylation on neuronal genes (Sanosaka et al., 2017). De novo deficiency of a DNA methyltransferase, DNMT3a, leads to failure of differentiation of mouse embryonic stem cells (mESCs) to both neuronal and glial cell lineages in vitro (Wu et al., 2012). Selective ablation of DNA methyltransferase I gene (*Dnmt1*), but not *Dnmt3a,* in early oligodendrocyte progenitors in *Olig1-Cre* and *Cnp-Cre* lines impairs OPC proliferation and differentiation (Moyon et al., 2016). During differentiation, the methylation level of the 5-position of hydroxymethylcytocine by the TET family is highly correlated with the initial stage of the myelination process. siRNA inhibition of the TET family shows a decreased expression of myelin genes, indicating DNA methylation plays a key role in regulating the oligodendrocyte differentiation (Zhao et al., 2014a). In adults, DNA methylation regulation of oligodendrocyte lineage has also shown a critical role in the aging process. As introduced, OPCs maintain a progenitor pool in the adult CNS, performing essential functions such as CNS plasticity, immune homeostasis, adaptive myelination, learning, injury repair, and remyelination (Bergles and Richardson, 2015; Fernandez-Castaneda and Gaultier, 2016; Xiao et al., 2016a). Compared to OPCs during early development, adult OPCs have unique characteristics. The capacities of

proliferation, migration, differentiation and functional states of adult OPCs are distinct from their neonatal counterparts (Fernandez-Castaneda and Gaultier, 2016; Moyon et al., 2015; Spitzer et al., 2019). Various epitranscriptomic changes accompany these distinctions. However, DNA methylation has been shown as a strong predictor of aging (Arthur-Farraj and Moyon, 2020). It has been reported that TET1 level alternation results in defective remyelination in aging mice. Deletion of *Tet1* in young mice mimics aging phenotypes, which further emphasizes the role of DNA methylation during aging (Moyon et al., 2019).

Furthermore, DNA methylation plays an important role in regulating oligodendrocyte functions that contribute to CNS diseases. In multiple sclerosis (MS) patients, the DNMT family is upregulated, and TET families are downregulated in the demyelinated hippocampus (Chomyk et al., 2017). An epigenomic study of MS brains revealed that genes that regulate oligodendrocyte survival were found to hypermethylated and had lower expression levels compared to the age and gender-matched controlled brains. In comparison, genes related to proteolytic processing were hypomethylated and had higher expression levels (Huynh et al., 2014). Interestingly, a genome-wide analysis study of age-related methylation changes showed that the overall genomic methylation amounts did not change with aging, while specific genomic regions liable for aging changes in the hippocampus are sexually divergent. These findings suggest that DNA methylation changes are possible contributors to the sex influence on the MS occurrence.

### 1.3.5 Histone modification

Histones are a family of nuclear proteins that compact chromosomes and allow ribosomal access to the DNA. They are highly conserved throughout species and are subgrouped into core histones and linker histones. H1 family includes the linker histones that keep DNA correctly wrap with core

histones, including H2A, H2B, H3, H4 (Li et al., 2014). Since histones are enriched with basic lysine and arginine residues, they are accessible to multiple post-translational modifications, including acetylation, methylation, phosphorylation, ubiquitination, deamination, sumoylation, ADP ribosylation, and proline isomerization. These modification processes are highly involved with gene expression regulation. It is known that histone modification affects three-dimensional (3D) chromatin organization, which is involved in regulating many biological processes, including transcriptional regulation, gene silencing, cell cycle transformation, cell development, and disease pathogenesis (Pai and Engelke, 2010). In particular, histone acetylation and histone methylation are strongly implicated in regulating oligodendrocyte lineage development (Berry et al., 2020; Wang and Lu, 2020). Histone acetyltransferases (HAT) and histone deacetylases (HDACs) are two essential modifiers in histone modification. Mammalian HDACs consist of four classes: class I includes HDAC1-3 and 8, class II includes HDAC4-7 and 9-10, class III includes NAD-dependent sirtuins, SIRT1-7, and class IV includes HDAC, HDAC11(Glaser, 2007; Haberland et al., 2009). Pharmaceutical inhibition with valproic acid inhibits overall HDAC-induced inhibition of oligodendrogenesis from multipotent adult neural progenitor cells, indicating HDAC's key role in oligodendrocyte lineage specification(Hsieh et al., 2004). In addition, another HDAC inhibitor, trichostatin A (TSA), prevented the progression of neonatal cortical progenitors into mature oligodendrocytes in vitro and repressed the protein expression of myelin genes such as GalC and PLP, indicating HDACs are necessary for oligodendrocyte lineage progression(Glaser, 2007). Similarly, inhibition of HDACs by TSA and sodium butyrate in cultured human OPCs results in a reduction in OPC proliferation and inhibition of OPC differentiation, demonstrating the importance of HDACs' role in human oligodendrocyte lineage progression and potential role in human demyelinating disease repair (Conway et al., 2012). During oligodendrocyte development,

HDACs exert their functions in a specific time window (Emery and Lu, 2015). HDACs inhibitors impair the early phase of OPC differentiation rather than the post- myelination stage in the developing rat brains (Shen et al., 2005). Importantly, remyelination is regulated by HDACs such as HDAC1 and HDAC2 in an age-dependent manner in adult cuprizone treated demyelination model (Shen et al., 2008). HDAC1 and HDAC2 are also key players for OPC differentiation and myelination(Marin-Husstege et al., 2002). In addition, HDACs interact with HATs to regulate oligodendrocyte lineage development. For example, HDAC3 collaborates with HAT p300 to maintain oligodendrocyte identity while inhibiting astrogliogenesis during development (Zhang et al., 2016). Up to date, the specific role of how HDACs in regulating OL-specific gene expression still remains elusive.

### 1.3.6 MicroRNA

MicroRNAs (miRNAs) are small non-coding RNAs with an average of 22 base pairs in length (Ameres and Zamore, 2013). Their biogenesis and functions are highly regulated within cells, and they emerge as a key post-transcriptional mechanism of gene expression in almost all known biological processes and essential for mammalian development and homeostasis. (Gebert and MacRae, 2019; Landgraf et al., 2007). miRNA is generated through canonical and non-canonical pathways. In the canonical pathway, miRNA genes are transcripted to primary miRNAs (pri-miRNAs), then cleaved by Drosha, a ribonuclease III enzyme, and its cofactor DiGeorge Syndrome Critical Region 8 (DGCR8) into characteristic hairpin shaped precursor-miRNA (pre-miRNA). Pre-miRNAs are then transported from the nucleus to the cytoplasm by exportin-5/RanGTP complex, followed by the other process by an RNase III endonuclease Dicer, into mature miRNAs. Depending on the directions of pre-RNAs that mature miRNAs generated, they are classified into 5p miRNAs, which arise from 5’ end of pre-miRNA hairpin or 3p miRNA,

which arises from 3' end of pre-miRNA. In the non-canonical pathway, miRNAs are processed in Drosha/ DGCR8-independent or Dicer-independent manner.

Mature miRNAs mediate gene silencing by guiding Argonaute (AGO) proteins to complementary mRNAs, inducing translational repression and mRNA degradation (Gebert and MacRae, 2019; Ha and Kim, 2014). It has been suggested that in mammalian cells, microRNAs regulate up to 50% of all genes post-transcriptionally, and they primarily impact gene expression by destabilization of mRNA to reduce protein translation (Guo et al., 2010). With the advance of technologies, more than two thousand mature miRNAs have been identified in homo sapiens (Landgraf et al., 2007), and 60% of human coding genes contain conserved miRNA-binding sites (Friedman et al., 2009).

It was estimated that 70% of miRNAs are expressed in the brain, which is important in neural development and gliogenesis (Chen and Qin, 2015). miRNA profiling has shown that miRNAs are dynamically expressed during oligodendrocyte lineage cell development and regulate oligodendrocyte lineage transcriptome in a spatiotemporal pattern (Lau et al., 2008). The functional role of miRNA in oligodendrocyte development was initially suggested in a study that inactivated Dicer, an endonuclease essential for miRNA maturation in the *Nestin-Cre* line. *Nestin-Cre-Dicer* affects late-born neurons and is embryonic lethal. While motor neuron development in these mice appears normal in the spinal cord, oligodendrocyte precursors that occur after motor neuron show decreased expansion and differentiation deficits into mature oligodendrocytes (Kawase-Koga et al., 2009). Oligodendrocyte conditional Dicer knockout studies further demonstrate that Dicer mediated miRNA is essential for oligodendrocyte development and maintenance (Dugas et al., 2010; Shin et al., 2009). Shin et al. showed that oligodendrocyte-specific Dicer deletion in proteolipid protein (PLP) *Cre* (CreERT) postnatal mice leads to CNS demyelination and inflammatory gliosis and eventually leads to neuronal impairment, indicating

Dicer plays an important role in myelin maintenance. miRNA microarray profiling of *Dicer1-PLP CreERT* whole-brain showed robust downregulation of various microRNAs, including the most abundant miRNA in mature oligodendrocytes: miR-219. By deleting Dicer1 in oligodendrocyte lineage transcription factor 2(Olig2) Cre mice (*Dicer-Olig2 Cre*) and 2′,3′-cyclic nucleotide 3′phosphodiesterase (CNP) Cre (*Dicer-Cnp cre*) mice, Dugas et al. demonstrated that mature miRNA impairment led to CNS myelin deficits and shivering phenotype from early postnatal days. While both CNS myelin pathology and phenotype eventually turned normal at P60 in *Dicer-Olig2 cre* mice, *Dicer-Cnp cre* mice did not survive passing one month old (Dugas et al., 2010). Deleting Dicer in another oligodendrocyte lineage Olig1-Cre line, *Dicer-Olig1 Cre* mice showed miRNAs are required for the initiation of OPC generation and promoting OPC maturation in the spinal cord (Zhao et al., 2010b; Zheng et al., 2012).

While these studies showed that mature miRNA generation by Dicer is required for oligodendrocyte lineage progression, a recent study demonstrated miRNA dysregulation is an essential mechanism in autoimmune demyelination. By profiling oligodendrocyte Argonaut 2(AGO2) tagged miRNA of experimental autoimmune encephalomyelitis (EAE) mouse model (Ma et al., 2020) in *AGO2-Olig1* cre line, the study identified distinct miRNA groups that mediated either protective or detrimental signals in neuroinflammatory injury.

Both Dicer and AGO deletion studies revealed that the expression of miRNAs is post-transcriptional “brake” of gene expression(Nave, 2010), which governs the key downstream targets to regulate oligodendrocyte development and myelination. For example, miR-219 and miR-338 negatively regulate oligodendrocyte differentiation inhibitors, including transcription inhibitors Sox6 and Hes5 and OPC proliferation factors PDGF-α (Dugas et al., 2010; Zhao et al., 2010b) to control the transition of proliferative OPCs to differentiated oligodendrocytes. In

addition, studies have reported that miRNAs interplay with various post-transcriptional mechanisms at different stages of oligodendrocyte lineage (Emery and Lu, 2015; Hernandez and Casaccia, 2015; Li et al., 2014). Nevertheless, the big picture of how miRNAs regulate oligodendrocyte lineage progress in time and space remains incomplete.

### 1.3.7 Long non-coding RNAs (LncRNAs)

ncRNAs are non-protein-coding RNAs that are longer than 200 nucleotides. They function as modular scaffolds to form ribonucleoprotein complexes with other chromatin regulators to modulate genome architecture (Rinn and Chang, 2012). The ncRNAs regulate gene expression at various levels, including epigenetic, transcriptional, and post-transcriptional, with multiple action modes. They are important regulators of diverse biological processes, and the alternation of their expression causes diseases such as cancer and neurodegenerative diseases (Peinado et al., 2018; Wei et al., 2018). In the CNS, studies have shown that LncRNAs expression is essential to regulate the neuronal-glial fate specification and oligodendrocyte lineage progression(He et al., 2017; Mercer et al., 2010). There is a stage-specific LncRNAs network that is accompanied by oligodendrocyte maturation and myelination. *Inc158*, a LncRNA was found to promote the differentiation of mouse neural precursor cells into oligodendrocytes. It acts as an antisense transcript of nuclear factor-IB to promote the differentiation of mouse neural precursor cells into oligodendrocytes (Li et al., 2018b). A cluster of LncRNAs called *LncOL1-4* are specifically enriched during OPC differentiation. In vivo evidence suggest *LncOL1* is crucial for the timing of oligodendrocyte differentiation and the onset of myelination, but not myelin maintenance. In addition, *LncOL1* is found essential for the oligodendrocyte remyelination after lysolecithin (LPC) induced white matter injury (He et al., 2017). Mechanically, *LncOL1* forms complex with a polycomb repressive complex 2 Suz12 to repress an inhibitory differentiation network (He et al.,

2017). Recently, a novel LncRNA called *Pcdh17it* was found as a maker for premylinating oligodendrocytes, adding an extra tool for mapping the differentiating oligodendrocytes in various time and space (Kasuga et al., 2019). Although LncRNAs are identified as important regulators for the oligodendrocyte lineage progression, their functions in oligodendrocyte development and myelination remain to be elucidated. Until now, very few LncRNAs have been experimentally validated, while most of LncRNAs are annotated via bioinformatics (Wei et al., 2018). Extensive mechanistic studies are required to identify how LncRNAs cooperate as a signaling network and how they collaborate with other molecular mechanisms to regulate oligodendrocytes' fate specification and differentiation.

### 1.3.8 *N*$^6$-methyladenosine (m$^6$A)

Although epigenetic regulatory mechanisms such as DNA methylation, histone acetylation, miRNA modification, LncRNAs modification are known to influence gene expression and a multitude of biological processes, a similar role for the chemical modification of RNA has only recently been identified (Fu et al., 2014). The discovery of reversible *N*$^6$-methyladenosine (m$^6$A) mRNA methylation has revealed a new dimension of post-transcriptional regulation of gene expression (Yue et al., 2015). m$^6$A is a chemical derivative of adenosine (A) in RNA. It is the most prevalent mRNA modification in mammals, occurring at a frequency of ~1-2 m$^6$A per 1000 mRNA nucleotides (nt) (Ke et al., 2015). In the transcriptome, m$^6$A to A ratio in the mRNA population is about 0.15-0.6%, and the percentage of m$^6$A marked transcripts is about 25-60%. About 7,000 genes have been identified to contain m$^6$A in the human transcriptome. However, due to the limitation of the techniques and analysis, the number of m$^6$A marked transcripts is likely underestimated (Dominissini et al., 2012; He and He, 2021; Liu et al., 2020; Wang et al., 2014b). The m$^6$A mRNA methyltransferase complex (m$^6$A writer) was first purified in the 1990s, with the

discovery of METTL3 as a key component (Bokar et al., 1994; Desrosiers et al., 1974; He and He, 2021). In 2014, a second key component of $m^6A$, methyltransferase, METTL14, was discovered (Liu et al., 2014). METTL3 and METTL14 form a stable heterodimer that functions as a catalytic enzyme to deposit $m^6A$ in mammalian nuclear RNAs. In addition, WTAP, a pre-mRNA splicing factor, was found to recruit METTL3-14 heterodimer and act as a regulatory subunit in the $m^6A$ methyltransferase complex (Liu et al., 2014; Ping et al., 2014). Emerging studies have demonstrated this $m^6A$ "mark" influences various aspects of mRNA metabolism, including stability, translation, localization, and splicing (Roundtree et al., 2017; Wang et al., 2014a; Xiao et al., 2016b; Zhao et al., 2014b; Zhou et al., 2018). M6A "reader" proteins that selectively bind $m^6A$ primarily mediate the wide-ranging effects of $m^6A$ mark in gene expression and exert functions. The YTH domain-containing proteins were first identified as $m^6A$ readers that bind RNA in an $m^6A$ –dependent manner (Dominissini et al., 2012; Zaccara et al., 2019; Zhu et al., 2014). In addition, $m^6A$ recruit RNA-binding proteins indirectly to execute functions. For example, $m^6A$ can form RNA folding structures to influence RNA-binding protein access and efficiency (Liu et al., 2015, 2017). An important characteristic of the $m^6A$ methylation regulatory system is its reversibility (He and He, 2021). $M^6A$ "eraser" proteins execute the demethylation of $m^6A$. FTO, a fat mass and obesity-associated protein, was discovered as the first known $m^6A$ eraser(Jia et al., 2011). ALKBH5 functions as a testes-enriched $m^6A$ eraser and is crucial for spermatogenesis (Zheng et al., 2013). Until now, there are controversies about $m^6A$ erasers' role in regulating physiological cellular functions, and more studies are required to uncover the targets and mechanisms of these enzymes (Zaccara et al., 2019).

With the advancement of technologies and extensive collaborations, $m^6A$ modification has been shown to be an important post-transcriptional mechanism in mammalian cell functions. By

controlling the turnover and translation of transcripts during cell-state transitions, $m^6A$ modification of mRNA plays key regulatory roles during embryonic and adult stem cell differentiation (Frye et al., 2018). Recent studies have highlighted the function of $m^6A$ in lineage fate decisions during cell development. For example,embryonic stem cell pluripotency exit, T cell differentiation, hematopoietic fate transition, and gametogenesis (Batista et al., 2014; Geula et al., 2015; Ivanova et al., 2017; Li et al., 2017; Weng et al., 2018b; Xu et al., 2017; Zhang et al., 2017a). Importantly, a recent study in neural stem cells revealed that conditional inactivation of METTL14 disrupts cortical neurogenesis (Yoon et al., 2017), thus revealing a critical role of the $m^6A$ mark in the CNS neuronal development. Nevertheless, the role of $m^6A$ mRNA methylation in oligodendrocyte lineage regulation is unclear. In order to advance the understanding of $m^6A$'s role in oligodendrocyte lineage progression and its potential impacts on human neurobiology diseases, my Ph.D. work is focused on answering the following scientific questions: 1. Does $m^6A$ play a role in regulating oligodendrocyte development and CNS myelination? 2. How does $m^6A$ regulates oligodendrocyte development and CNS myelination? 3. Does $m^6A$ play a role in remyelination?

### 1.4 References


Almeida, R.G., and Lyons, D.A. (2017). On myelinated axon plasticity and neuronal circuit formation and function. J. Neurosci. *37*, 10023–10034.

Ameres, S.L., and Zamore, P.D. (2013). Diversifying microRNA sequence and function. Nat. Rev. Mol. Cell Biol. *14*, 475–488.

Arthur-Farraj, P., and Moyon, S. (2020). DNA methylation in Schwann cells and in oligodendrocytes. Glia *68*, 1568–1583.

Batista, P.J., Molinie, B., Wang, J., Qu, K., Zhang, J., Li, L., Bouley, D.M., Lujan, E., Haddad, B., Daneshvar, K., et al. (2014). m(6)A RNA modification controls cell fate transition in mammalian embryonic stem cells. Cell Stem Cell *15*, 707–719.

Bergles, D.E., and Richardson, W.D. (2015). Oligodendrocyte development and plasticity. Cold Spring Harb. Perspect. Biol. *8*, a020453.

Berry, K., Wang, J., and Lu, Q.R. (2020). Epigenetic regulation of oligodendrocyte myelination in developmental disorders and neurodegenerative diseases. [version 1; peer review: 2 approved]. F1000Res. *9*.

Bokar, J.A., Rath-Shambaugh, M.E., Ludwiczak, R., Narayan, P., and Rottman, F. (1994). Characterization and partial purification of mRNA N6-adenosine methyltransferase from HeLa cell nuclei. Internal mRNA methylation requires a multisubunit complex. J. Biol. Chem. *269*, 17697–17704.

Bujalka, H., Koenning, M., Jackson, S., Perreau, V.M., Pope, B., Hay, C.M., Mitew, S., Hill, A.F., Lu, Q.R., Wegner, M., et al. (2013). MYRF is a membrane-associated transcription factor that autoproteolytically cleaves to directly activate myelin genes. PLoS Biol. *11*, e1001625.

Casaccia, P., and Corfas, G. (2018). Introduction to the special issue on myelin plasticity in the central nervous system. Dev. Neurobiol. *78*, 65–67.

Chamberlain, K.A., Nanescu, S.E., Psachoulia, K., and Huang, J.K. (2016). Oligodendrocyte regeneration: Its significance in myelin replacement and neuroprotection in multiple sclerosis. Neuropharmacology *110*, 633–643.

Chen, W., and Qin, C. (2015). General hallmarks of microRNAs in brain evolution and development. RNA Biol. *12*, 701–708.

Chomyk, A.M., Volsko, C., Tripathi, A., Deckard, S.A., Trapp, B.D., Fox, R.J., and Dutta, R. (2017). DNA methylation in demyelinated multiple sclerosis hippocampus. Sci. Rep. *7*, 8696.

Conway, G.D., O'Bara, M.A., Vedia, B.H., Pol, S.U., and Sim, F.J. (2012). Histone deacetylase activity is required for human oligodendrocyte progenitor differentiation. Glia *60*, 1944–1953.

Dai, Z.-M., Sun, S., Wang, C., Huang, H., Hu, X., Zhang, Z., Lu, Q.R., and Qiu, M. (2014). Stage-specific regulation of oligodendrocyte development by Wnt/β-catenin signaling. J. Neurosci. *34*, 8467–8473.

Desrosiers, R., Friderici, K., and Rottman, F. (1974). Identification of methylated nucleosides in messenger RNA from Novikoff hepatoma cells. Proc. Natl. Acad. Sci. USA *71*, 3971–3975.

Doi, T., Ogata, T., Yamauchi, J., Sawada, Y., Tanaka, S., and Nagao, M. (2017). Chd7 Collaborates with Sox2 to Regulate Activation of Oligodendrocyte Precursor Cells after Spinal Cord Injury. J. Neurosci. *37*, 10290–10309.

Dominissini, D., Moshitch-Moshkovitz, S., Schwartz, S., Salmon-Divon, M., Ungar, L., Osenberg, S., Cesarkas, K., Jacob-Hirsch, J., Amariglio, N., Kupiec, M., et al. (2012). Topology of the human and mouse m6A RNA methylomes revealed by m6A-seq. Nature *485*, 201–206.

Dugas, J.C., Cuellar, T.L., Scholze, A., Ason, B., Ibrahim, A., Emery, B., Zamanian, J.L., Foo, L.C., McManus, M.T., and Barres, B.A. (2010). Dicer1 and miR-219 Are required for normal oligodendrocyte differentiation and myelination. Neuron *65*, 597–611.

Elbaz, B., and Popko, B. (2019). Molecular control of oligodendrocyte development. Trends Neurosci. *42*, 263–277.

Elbaz, B., Aaker, J.D., Isaac, S., Kolarzyk, A., Brugarolas, P., Eden, A., and Popko, B. (2018). Phosphorylation state of ZFP24 controls oligodendrocyte differentiation. Cell Rep. *23*, 2254–2263.

Emery, B., and Lu, Q.R. (2015). Transcriptional and epigenetic regulation of oligodendrocyte development and myelination in the central nervous system. Cold Spring Harb. Perspect. Biol. *7*, a020461.

Fernandez-Castaneda, A., and Gaultier, A. (2016). Adult oligodendrocyte progenitor cells - Multifaceted regulators of the CNS in health and disease. Brain Behav. Immun. *57*, 1–7.

Ford, M.C., Alexandrova, O., Cossell, L., Stange-Marten, A., Sinclair, J., Kopp-Scheinpflug, C., Pecka, M., Attwell, D., and Grothe, B. (2015). Tuning of Ranvier node and internode properties in myelinated axons to adjust action potential timing. Nat. Commun. *6*, 8073.

Friedman, R.C., Farh, K.K.-H., Burge, C.B., and Bartel, D.P. (2009). Most mammalian mRNAs are conserved targets of microRNAs. Genome Res. *19*, 92–105.

Frye, M., Harada, B.T., Behm, M., and He, C. (2018). RNA modifications modulate gene expression during development. Science *361*, 1346–1349.

Fu, Y., Dominissini, D., Rechavi, G., and He, C. (2014). Gene expression regulation mediated through reversible $m^6A$ RNA methylation. Nat. Rev. Genet. *15*, 293–306.

Gaesser, J.M., and Fyffe-Maricich, S.L. (2016). Intracellular signaling pathway regulation of myelination and remyelination in the CNS. Exp. Neurol. *283*, 501–511.

Gebert, L.F.R., and MacRae, I.J. (2019). Regulation of microRNA function in animals. Nat. Rev. Mol. Cell Biol. *20*, 21–37.

Geula, S., Moshitch-Moshkovitz, S., Dominissini, D., Mansour, A.A., Kol, N., Salmon-Divon, M., Hershkovitz, V., Peer, E., Mor, N., Manor, Y.S., et al. (2015). m6A mRNA methylation facilitates resolution of naïve pluripotency toward differentiation. Science *347*, 1002–1006.

Gibson, E.M., Purger, D., Mount, C.W., Goldstein, A.K., Lin, G.L., Wood, L.S., Inema, I., Miller, S.E., Bieri, G., Zuchero, J.B., et al. (2014). Neuronal activity promotes oligodendrogenesis and adaptive myelination in the mammalian brain. Science *344*, 1252304.

Glaser, K.B. (2007). HDAC inhibitors: clinical update and mechanism-based potential. Biochem. Pharmacol. *74*, 659–671.

Grandbarbe, L., Bouissac, J., Rand, M., Hrabé de Angelis, M., Artavanis-Tsakonas, S., and Mohier, E. (2003). Delta-Notch signaling controls the generation of neurons/glia from neural stem cells in a stepwise process. Development *130*, 1391–1402.

Guardiola-Diaz, H.M., Ishii, A., and Bansal, R. (2012). Erk1/2 MAPK and mTOR signaling sequentially regulates progression through distinct stages of oligodendrocyte differentiation. Glia *60*, 476–486.

Guo, H., Ingolia, N.T., Weissman, J.S., and Bartel, D.P. (2010). Mammalian microRNAs predominantly act to decrease target mRNA levels. Nature *466*, 835–840.

Ha, M., and Kim, V.N. (2014). Regulation of microRNA biogenesis. Nat. Rev. Mol. Cell Biol. *15*, 509–524.

Haberland, M., Montgomery, R.L., and Olson, E.N. (2009). The many roles of histone deacetylases in development and physiology: implications for disease and therapy. Nat. Rev. Genet. *10*, 32–42.

He, L., and Lu, Q.R. (2013). Coordinated control of oligodendrocyte development by extrinsic and intrinsic signaling cues. Neurosci. Bull. *29*, 129–143.

He, P.C., and He, C. (2021). m6 A RNA methylation: from mechanisms to therapeutic potential. EMBO J. *40*, e105977.

He, D., Wang, J., Lu, Y., Deng, Y., Zhao, C., Xu, L., Chen, Y., Hu, Y.-C., Zhou, W., and Lu, Q.R. (2017). lncRNA Functional Networks in Oligodendrocytes Reveal Stage-Specific Myelination Control by an lncOL1/Suz12 Complex in the CNS. Neuron *93*, 362–378.

Hernandez, M., and Casaccia, P. (2015). Interplay between transcriptional control and chromatin regulation in the oligodendrocyte lineage. Glia *63*, 1357–1375.

Hoffmann, S.A., Hos, D., Küspert, M., Lang, R.A., Lovell-Badge, R., Wegner, M., and Reiprich, S. (2014). Stem cell factor Sox2 and its close relative Sox3 have differentiation functions in oligodendrocytes. Development *141*, 39–50.

Hsieh, J., Nakashima, K., Kuwabara, T., Mejia, E., and Gage, F.H. (2004). Histone deacetylase inhibition-mediated neuronal differentiation of multipotent adult neural progenitor cells. Proc. Natl. Acad. Sci. USA *101*, 16659–16664.

Huynh, J.L., Garg, P., Thin, T.H., Yoo, S., Dutta, R., Trapp, B.D., Haroutunian, V., Zhu, J., Donovan, M.J., Sharp, A.J., et al. (2014). Epigenome-wide differences in pathology-free regions of multiple sclerosis-affected brains. Nat. Neurosci. *17*, 121–130.

Ivanova, I., Much, C., Di Giacomo, M., Azzi, C., Morgan, M., Moreira, P.N., Monahan, J., Carrieri, C., Enright, A.J., and O'Carroll, D. (2017). The RNA m6A Reader YTHDF2 Is Essential for the Post-transcriptional Regulation of the Maternal Transcriptome and Oocyte Competence. Mol. Cell *67*, 1059–1067.e4.

Jia, G., Fu, Y., Zhao, X., Dai, Q., Zheng, G., Yang, Y., Yi, C., Lindahl, T., Pan, T., Yang, Y.-G., et al. (2011). N6-methyladenosine in nuclear RNA is a major substrate of the obesity-associated FTO. Nat. Chem. Biol. *7*, 885–887.

Kasuga, Y., Fudge, A.D., Zhang, Y., and Li, H. (2019). Characterization of a long noncoding RNA Pcdh17it as a novel marker for immature premyelinating oligodendrocytes. Glia *67*, 2166–2177.

Kawase-Koga, Y., Otaegi, G., and Sun, T. (2009). Different timings of Dicer deletion affect neurogenesis and gliogenesis in the developing mouse central nervous system. Dev. Dyn. *238*, 2800–2812.

Ke, S., Alemu, E.A., Mertens, C., Gantman, E.C., Fak, J.J., Mele, A., Haripal, B., Zucker-Scharff, I., Moore, M.J., Park, C.Y., et al. (2015). A majority of m6A residues are in the last exons, allowing the potential for 3' UTR regulation. Genes Dev. *29*, 2037–2053.

Landgraf, P., Rusu, M., Sheridan, R., Sewer, A., Iovino, N., Aravin, A., Pfeffer, S., Rice, A., Kamphorst, A.O., Landthaler, M., et al. (2007). A mammalian microRNA expression atlas based on small RNA library sequencing. Cell *129*, 1401–1414.

Lau, P., Verrier, J.D., Nielsen, J.A., Johnson, K.R., Notterpek, L., and Hudson, L.D. (2008). Identification of dynamically regulated microRNA and mRNA networks in developing oligodendrocytes. J. Neurosci. *28*, 11720–11730.

Li, J., Ding, Y., and Zheng, L. (2014). Histone-Mediated Transgenerational Epigenetics. In Transgenerational Epigenetics, (Elsevier), pp. 87–103.

Li, Y., Guo, B., Yang, R., Xiao, Z., Gao, X., Yu, J., Li, S., and Luo, Y. (2018). A novel long noncoding RNA lnc158 promotes the differentiation of mouse neural precursor cells into oligodendrocytes by targeting nuclear factor-IB. Neuroreport *29*, 1121–1128.

Li, Z., Weng, H., Su, R., Weng, X., Zuo, Z., Li, C., Huang, H., Nachtergaele, S., Dong, L., Hu, C., et al. (2017). FTO plays an oncogenic role in acute myeloid leukemia as a N6-methyladenosine RNA demethylase. Cancer Cell *31*, 127–141.

Liu, J., Dietz, K., DeLoyht, J.M., Pedre, X., Kelkar, D., Kaur, J., Vialou, V., Lobo, M.K., Dietz, D.M., Nestler, E.J., et al. (2012). Impaired adult myelination in the prefrontal cortex of socially isolated mice. Nat. Neurosci. *15*, 1621–1623.

Liu, J., Yue, Y., Han, D., Wang, X., Fu, Y., Zhang, L., Jia, G., Yu, M., Lu, Z., Deng, X., et al. (2014). A METTL3-METTL14 complex mediates mammalian nuclear RNA N6-adenosine methylation. Nat. Chem. Biol. *10*, 93–95.

Liu, L., Wang, Y., Wu, J., Liu, J., Qin, Z., and Fan, H. (2020). N6-Methyladenosine: A Potential Breakthrough for Human Cancer. Mol. Ther. Nucleic Acids *19*, 804–813.

Liu, N., Dai, Q., Zheng, G., He, C., Parisien, M., and Pan, T. (2015). N(6)-methyladenosine-dependent RNA structural switches regulate RNA-protein interactions. Nature *518*, 560–564.

Liu, N., Zhou, K.I., Parisien, M., Dai, Q., Diatchenko, L., and Pan, T. (2017). N6-methyladenosine alters RNA structure to regulate binding of a low-complexity protein. Nucleic Acids Res. *45*, 6051–6063.

Lu, Q.R., Sun, T., Zhu, Z., Ma, N., Garcia, M., Stiles, C.D., and Rowitch, D.H. (2002). Common developmental requirement for Olig function indicates a motor neuron/oligodendrocyte connection. Cell *109*, 75–86.

Ma, Q., Matsunaga, A., Ho, B., Oksenberg, J.R., and Didonna, A. (2020). Oligodendrocyte-specific Argonaute profiling identifies microRNAs associated with experimental autoimmune encephalomyelitis. J. Neuroinflammation *17*, 297.

Makinodan, M., Rosen, K.M., Ito, S., and Corfas, G. (2012). A critical period for social experience-dependent oligodendrocyte maturation and myelination. Science *337*, 1357–1360.

Marin-Husstege, M., Muggironi, M., Liu, A., and Casaccia-Bonnefil, P. (2002). Histone deacetylase activity is necessary for oligodendrocyte lineage progression. J. Neurosci. *22*, 10333–10345.

McKenzie, I.A., Ohayon, D., Li, H., de Faria, J.P., Emery, B., Tohyama, K., and Richardson, W.D. (2014). Motor skill learning requires active central myelination. Science *346*, 318–322.

Mercer, T.R., Qureshi, I.A., Gokhan, S., Dinger, M.E., Li, G., Mattick, J.S., and Mehler, M.F. (2010). Long noncoding RNAs in neuronal-glial fate specification and oligodendrocyte lineage maturation. BMC Neurosci. *11*, 14.

Moyon, S., Dubessy, A.L., Aigrot, M.S., Trotter, M., Huang, J.K., Dauphinot, L., Potier, M.C., Kerninon, C., Melik Parsadaniantz, S., Franklin, R.J.M., et al. (2015). Demyelination causes adult CNS progenitors to revert to an immature state and express immune cues that support their migration. J. Neurosci. *35*, 4–20.

Moyon, S., Huynh, J.L., Dutta, D., Zhang, F., Ma, D., Yoo, S., Lawrence, R., Wegner, M., John, G.R., Emery, B., et al. (2016). Functional characterization of DNA methylation in the oligodendrocyte lineage. Cell Rep. *15*, 748–760.

Moyon, S., Frawley, R., Marshall-Phelps, K.L., Kegel, L., Bøstrand, S.M., Sadowski, B., Huang, D., Jiang, Y.-H., Lyons, D., Möbius, W., et al. (2019). TET1-mediated DNA hydroxy-methylation regulates adult remyelination. BioRxiv.

Nave, K.-A. (2010). Oligodendrocytes and the “micro brake” of progenitor cell proliferation. Neuron *65*, 577–579.

Pai, D.A., and Engelke, D.R. (2010). Spatial organization of genes as a component of regulated expression. Chromosoma *119*, 13–25.

Peinado, P., Herrera, A., Baliñas, C., Martín-Padrón, J., Boyero, L., Cuadros, M., Coira, I.F., Rodriguez, M.I., Reyes-Zurita, F.J., Rufino-Palomares, E.E., et al. (2018). Long noncoding rnas as cancer biomarkers. In Cancer and noncoding rnas, (Elsevier), pp. 95–114.

Ping, X.-L., Sun, B.-F., Wang, L., Xiao, W., Yang, X., Wang, W.-J., Adhikari, S., Shi, Y., Lv, Y., Chen, Y.-S., et al. (2014). Mammalian WTAP is a regulatory subunit of the RNA N6-methyladenosine methyltransferase. Cell Res. *24*, 177–189.

Rinn, J.L., and Chang, H.Y. (2012). Genome regulation by long noncoding RNAs. Annu. Rev. Biochem. *81*, 145–166.

Roundtree, I.A., Luo, G.-Z., Zhang, Z., Wang, X., Zhou, T., Cui, Y., Sha, J., Huang, X., Guerrero, L., Xie, P., et al. (2017). YTHDC1 mediates nuclear export of N6-methyladenosine methylated mRNAs. Elife *6*, e31311.

Saab, A.S., and Nave, K.-A. (2017). Myelin dynamics: protecting and shaping neuronal functions. Curr. Opin. Neurobiol. *47*, 104–112.

Sanosaka, T., Imamura, T., Hamazaki, N., Chai, M., Igarashi, K., Ideta-Otsuka, M., Miura, F., Ito, T., Fujii, N., Ikeo, K., et al. (2017). DNA Methylome Analysis Identifies Transcription Factor-Based Epigenomic Signatures of Multilineage Competence in Neural Stem/Progenitor Cells. Cell Rep. *20*, 2992–3003.

Shen, S., Li, J., and Casaccia-Bonnefil, P. (2005). Histone modifications affect timing of oligodendrocyte progenitor differentiation in the developing rat brain. J. Cell Biol. *169*, 577–589.

Shen, S., Sandoval, J., Swiss, V.A., Li, J., Dupree, J., Franklin, R.J.M., and Casaccia-Bonnefil, P. (2008). Age-dependent epigenetic control of differentiation inhibitors is critical for remyelination efficiency. Nat. Neurosci. *11*, 1024–1034.

Shin, D., Shin, J.-Y., McManus, M.T., Ptácek, L.J., and Fu, Y.-H. (2009). Dicer ablation in oligodendrocytes provokes neuronal impairment in mice. Ann. Neurol. *66*, 843–857.

Sock, E., and Wegner, M. (2019). Transcriptional control of myelination and remyelination. Glia *67*, 2153–2165.

Spitzer, S.O., Sitnikov, S., Kamen, Y., Evans, K.A., Kronenberg-Versteeg, D., Dietmann, S., de Faria, O., Agathou, S., and Káradóttir, R.T. (2019). Oligodendrocyte Progenitor Cells Become Regionally Diverse and Heterogeneous with Age. Neuron *101*, 459–471.e5.

Sun, J.-J., Ren, Q.-G., Xu, L., and Zhang, Z.-J. (2015). LINGO-1 antibody ameliorates myelin impairment and spatial memory deficits in experimental autoimmune encephalomyelitis mice. Sci. Rep. *5*, 14235.

Tyler, W.A., Gangoli, N., Gokina, P., Kim, H.A., Covey, M., Levison, S.W., and Wood, T.L. (2009). Activation of the mammalian target of rapamycin (mTOR) is essential for oligodendrocyte differentiation. J. Neurosci. *29*, 6367–6378.

Van Tilborg, E., de Theije, C.G.M., van Hal, M., Wagenaar, N., de Vries, L.S., Benders, M.J., Rowitch, D.H., and Nijboer, C.H. (2018). Origin and dynamics of oligodendrocytes in the developing brain: Implications for perinatal white matter injury. Glia *66*, 221–238.

Wang, J., and Lu, Q.R. (2020). Convergent epigenetic regulation of glial plasticity in myelin repair and brain tumorigenesis: A focus on histone modifying enzymes. Neurobiol. Dis. *144*, 105040.

Wang, S., Sdrulla, A.D., diSibio, G., Bush, G., Nofziger, D., Hicks, C., Weinmaster, G., and Barres, B.A. (1998). Notch receptor activation inhibits oligodendrocyte differentiation. Neuron *21*, 63–75.

Wang, X., Lu, Z., Gomez, A., Hon, G.C., Yue, Y., Han, D., Fu, Y., Parisien, M., Dai, Q., Jia, G., et al. (2014a). N6-methyladenosine-dependent regulation of messenger RNA stability. Nature *505*, 117–120.

Wang, Y., Li, Y., Toth, J.I., Petroski, M.D., Zhang, Z., and Zhao, J.C. (2014b). N6-methyladenosine modification destabilizes developmental regulators in embryonic stem cells. Nat. Cell Biol. *16*, 191–198.

Wei, C.-W., Luo, T., Zou, S.-S., and Wu, A.-S. (2018). The role of long noncoding rnas in central nervous system and neurodegenerative diseases. Front. Behav. Neurosci. *12*, 175.

Weng, Y.-L., Wang, X., An, R., Cassin, J., Vissers, C., Liu, Y., Liu, Y., Xu, T., Wang, X., Wong, S.Z.H., et al. (2018). Epitranscriptomic m6a regulation of axon regeneration in the adult mammalian nervous system. Neuron *97*, 313–325.e6.

Wheeler, N.A., and Fuss, B. (2016). Extracellular cues influencing oligodendrocyte differentiation and (re)myelination. Exp. Neurol. *283*, 512–530.

Wu, Z., Huang, K., Yu, J., Le, T., Namihira, M., Liu, Y., Zhang, J., Xue, Z., Cheng, L., and Fan, G. (2012). Dnmt3a regulates both proliferation and differentiation of mouse neural stem cells. J. Neurosci. Res. *90*, 1883–1891.

Xiao, L., Ohayon, D., McKenzie, I.A., Sinclair-Wilson, A., Wright, J.L., Fudge, A.D., Emery, B., Li, H., and Richardson, W.D. (2016a). Rapid production of new oligodendrocytes is required in the earliest stages of motor-skill learning. Nat. Neurosci. *19*, 1210–1217.

Xiao, W., Adhikari, S., Dahal, U., Chen, Y.-S., Hao, Y.-J., Sun, B.-F., Sun, H.-Y., Li, A., Ping, X.-L., Lai, W.-Y., et al. (2016b). Nuclear m(6)A Reader YTHDC1 Regulates mRNA Splicing. Mol. Cell *61*, 507–519.

Xu, K., Yang, Y., Feng, G.-H., Sun, B.-F., Chen, J.-Q., Li, Y.-F., Chen, Y.-S., Zhang, X.-X., Wang, C.-X., Jiang, L.-Y., et al. (2017). Mettl3-mediated m6A regulates spermatogonial differentiation and meiosis initiation. Cell Res. *27*, 1100–1114.

Yoon, K.-J., Ringeling, F.R., Vissers, C., Jacob, F., Pokrass, M., Jimenez-Cyrus, D., Su, Y., Kim, N.-S., Zhu, Y., Zheng, L., et al. (2017). Temporal control of mammalian cortical neurogenesis by m6a methylation. Cell *171*, 877–889.e17.

Yue, Y., Liu, J., and He, C. (2015). RNA N6-methyladenosine methylation in post-transcriptional gene expression regulation. Genes Dev. *29*, 1343–1355.

Zaccara, S., Ries, R.J., and Jaffrey, S.R. (2019). Reading, writing and erasing mRNA methylation. Nat. Rev. Mol. Cell Biol. *20*, 608–624.

Zhang, C., Chen, Y., Sun, B., Wang, L., Yang, Y., Ma, D., Lv, J., Heng, J., Ding, Y., Xue, Y., et al. (2017). m6A modulates haematopoietic stem and progenitor cell specification. Nature *549*, 273–276.

Zhang, L., He, X., Liu, L., Jiang, M., Zhao, C., Wang, H., He, D., Zheng, T., Zhou, X., Hassan, A., et al. (2016). Hdac3 Interaction with p300 Histone Acetyltransferase Regulates the Oligodendrocyte and Astrocyte Lineage Fate Switch. Dev. Cell *36*, 316–330.

Zhao, X., He, X., Han, X., Yu, Y., Ye, F., Chen, Y., Hoang, T., Xu, X., Mi, Q.-S., Xin, M., et al. (2010). MicroRNA-mediated control of oligodendrocyte differentiation. Neuron *65*, 612–626.

Zhao, X., Dai, J., Ma, Y., Mi, Y., Cui, D., Ju, G., Macklin, W.B., and Jin, W. (2014a). Dynamics of ten-eleven translocation hydroxylase family proteins and 5-hydroxymethylcytosine in oligodendrocyte differentiation. Glia *62*, 914–926.

Zhao, X., Yang, Y., Sun, B.-F., Shi, Y., Yang, X., Xiao, W., Hao, Y.-J., Ping, X.-L., Chen, Y.-S., Wang, W.-J., et al. (2014b). FTO-dependent demethylation of N6-methyladenosine regulates mRNA splicing and is required for adipogenesis. Cell Res. *24*, 1403–1419.

Zheng, G., Dahl, J.A., Niu, Y., Fedorcsak, P., Huang, C.-M., Li, C.J., Vågbø, C.B., Shi, Y., Wang, W.-L., Song, S.-H., et al. (2013). ALKBH5 is a mammalian RNA demethylase that impacts RNA metabolism and mouse fertility. Mol. Cell *49*, 18–29.

Zheng, K., Li, H., Huang, H., and Qiu, M. (2012). MicroRNAs and glial cell development. Neuroscientist *18*, 114–118.

Zhou, J., Wan, J., Shu, X.E., Mao, Y., Liu, X.-M., Yuan, X., Zhang, X., Hess, M.E., Brüning, J.C., and Qian, S.-B. (2018). N6-Methyladenosine Guides mRNA Alternative Translation during Integrated Stress Response. Mol. Cell *69*, 636–647.e7.

Zhu, T., Roundtree, I.A., Wang, P., Wang, X., Wang, L., Sun, C., Tian, Y., Li, J., He, C., and Xu, Y. (2014). Crystal structure of the YTH domain of YTHDF2 reveals mechanism for recognition of N6-methyladenosine. Cell Res. *24*, 1493–1496.

Zuchero, J.B., and Barres, B.A. (2015). Glia in mammalian development and disease. Development *142*, 3805–3809.

# CHAPTER 2

# $M^6A$ mRNA methylation is essential for Oligodendrocyte maturation and CNS myelination

This chapter is a full reprint of *Xu el al., Neuron*, 2020, in which I am the primary author.

**Relevant Publication**

Xu H, Dzhashiashvili Y, Shah A, Kunjamma RB., Weng YL, Elbaz B, Fei QL, Jones JS, Li Y, Zhuang XX, Ming GL, He C, Popko B. "$m^6A$ mRNA methylation is essential for oligodendrocyte maturation and CNS myelination." *Neuron,* 2020 Jan 22;105(2):293-309. PMID: 31901304.

## 2.1 Abstract

The molecular mechanisms that govern the maturation of oligodendrocyte lineage cells remain unclear. Emerging studies have shown that $N^6$-methyladenosine ($m^6A$), the most common internal RNA modification of mammalian mRNA, plays a critical role in various developmental processes. Here, we demonstrate that oligodendrocyte lineage progression is accompanied by dynamic changes in $m^6A$ modification on numerous transcripts. *In vivo* conditional inactivation of an essential $m^6A$ writer component, METTL14, results in decreased oligodendrocyte numbers and CNS hypomyelination, although oligodendrocyte precursor cell (OPC) numbers are normal. *In vitro Mettl14* ablation disrupts post-mitotic oligodendrocyte maturation and has distinct effects on OPC and oligodendrocyte transcriptomes. Moreover, the loss of *Mettl14* in oligodendrocyte lineage cells causes aberrant splicing of myriad RNA transcripts, including that which encodes the essential paranodal component neurofascin 155 (NF155). Together, our findings indicate that

dynamic RNA methylation plays an important regulatory role in oligodendrocyte development and CNS myelination.

**Key words**: Mettl14; m(6)A; mRNA methylation; RNA epigenetic regulation; oligodendrocyte precursor cells; oligodendrocytes; oligodendrocyte development; alternative splicing; NF155

## 2.2 Introduction

Oligodendrocytes are glial cells in the CNS that are responsible for myelination of axons, which allows for rapid saltatory conduction (Nave and Werner, 2014; Simons and Nave, 2015). Oligodendrocytes develop from oligodendrocyte precursor cells (OPCs), which originate from discrete regions of the embryonic neural tube (Rowitch, 2004). To become mature myelinating oligodendrocytes, OPCs first exit the proliferation state and differentiate into pre-myelinating oligodendrocytes, resulting in the expression of major myelinating proteins such as myelin basic protein (MBP) and proteolipid protein (PLP). A series of morphological changes then allows these oligodendrocytes to extend a number of processes that wrap axons with the multilayered myelin sheath (Zuchero and Barres, 2015). Elucidating the key events involved in oligodendrocyte lineage progression is critical to understand the cellular and developmental biology of myelin production and regeneration.

Following a defined series of steps, oligodendrocyte lineage progression is tightly controlled in time and space (Liu et al., 2016). The exact mechanism by which oligodendrocyte lineage progression is regulated, however, has yet to be fully elucidated. A number of intrinsic and extrinsic factors have been found to be critical for regulating oligodendrocyte development.

Growth factors, such as Sonic Hedgehog (SHH), bone morphogenetic proteins (BMPs), and platelet-derived growth factor (PDGF), have been shown to influence the maturation of oligodendrocyte lineage cells from early progenitors to mature, myelinating cells (Nishiyama et al., 2009). Transcription factors, such as Nkx-2.2, Olig1, Olig2, Sox10, Myrf and ZFP24, are required for maturation of oligodendrocytes (Elbaz and Popko, 2019; Mitew et al., 2014). In addition, epigenetic mechanisms including chromatin remodeling by DNA methylation, histone deacetylases, and gene silencing by non-coding RNAs have been shown to play critical roles in oligodendrocyte differentiation and function during development and remyelination (Li and Richardson, 2009; Marin-Husstege et al., 2002; Moyon and Casaccia, 2017; Ye et al., 2009; Zhao et al., 2010b).

Although reversible chemical modification of DNA and histone proteins is known to influence gene expression and a multitude of biological processes, a similar role for the chemical modification of RNA has only recently been identified (Fu et al., 2014). The discovery of reversible $N^6$-methyladenosine ($m^6A$) mRNA methylation has revealed a new dimension of post-transcriptional regulation of gene expression (Yue et al., 2015). Emerging studies have demonstrated this $m^6A$ "mark" influences various aspects of mRNA metabolism, including stability, translation, localization, and splicing (Roundtree et al., 2017; Wang et al., 2014a; Xiao et al., 2016b; Zhao et al., 2014b; Zhou et al., 2018). By controlling the turnover and/or translation of transcripts during cell-state transitions, $m^6A$ modification of mRNA plays key regulatory roles during embryonic and adult stem cell differentiation (Frye et al., 2018). Recent studies have highlighted the function of $m^6A$ in lineage fate decisions during cell development, such as embryonic stem cell pluripotency exit, T cell differentiation, hematopoietic fate transition, and gametogenesis (Batista et al., 2014; Geula et al., 2015; Ivanova et al., 2017; Li et al., 2017; Weng

et al., 2018b; Xu et al., 2017; Zhang et al., 2017a). Importantly, a recent study in neural stem cells revealed that conditional inactivation of the gene that encodes METTL14, a core component of the m$^6$A methyltransferase complex (Liu et al., 2014), disrupts cortical neurogenesis (Yoon et al., 2017), thus revealing a critical role of the m$^6$A mark in CNS neuronal development.

In this study, we sought to elucidate the role that m$^6$A mRNA methylation plays in oligodendrocyte lineage progression by conditionally inactivating the *Mettl14* gene specifically in these cells using a *Mettl14* conditional (floxed) mouse line in combination with oligodendrocyte Cre driver lines. *In vivo*, we found myelin abnormalities and altered oligodendrocyte numbers in the *Mettl14* mutants. Despite these findings, OPC numbers were not affected. *In vitro*, OPCs lacking *Mettl14* did not properly differentiate into mature oligodendrocytes, suggesting that m$^6$A plays a critical role in oligodendrocyte differentiation. RNA-seq and m$^6$A -seq revealed that OPC and oligodendrocyte transcripts encoding transcription factors, DNA epigenetic regulators and signaling pathways that are critical for oligodendrocyte lineage progression were m$^6$A marked, and differentially affected by the *Mettl14* deletion. We also found pervasive, aberrant mRNA splicing in the *Mettl14*-deleted OPCs and oligodendrocytes. Importantly, we discovered that the critical paranode component, NF155, is differentially spliced and significantly disrupted during myelination in the *Mettl14* ablated mutants.

## 2.3 Results

### 2.3.1 Oligodendrocyte lineage progression is accompanied by changes in m$^6$A modification on numerous transcripts

To characterize changes of the m$^6$A mark and its role in gene expression during oligodendrocyte lineage progression, we performed m$^6$A-seq and RNA-seq on both purified OPCs and mature, cultured oligodendrocytes. Using an immunopanning approach (Emery and Dugas, 2013), we

purified OPCs from neonatal mouse pups. These cells were maintained under proliferating conditions with the addition of the OPC mitogen PDGF-AA. We obtained mature oligodendrocytes by promoting OPC differentiation via removal of PDGF-AA and addition of the T3 hormone to the culture media (Fig.2.1 A). SMART2 single cell RNA-seq was used for $m^6A$ mRNA profiling (Picelli et al., 2014; Weng et al., 2018b), which detected 3,554 $m^6A$ marked transcripts in OPCs and 2606 $m^6A$ marked transcripts in oligodendrocytes. Gene ontology analyses indicated that these $m^6A$ marked transcripts have important functions for cell development in both OPCs (Fig.2.1 B) and oligodendrocytes (Fig.2.1 C). The $m^6A$-seq data also revealed transcripts present in both OPCs and oligodendrocytes that were differentially marked by $m^6A$, demonstrating the dynamic nature of this mRNA modification. We found 2,806 transcripts with the $m^6A$ mark in OPCs that were present but not marked in oligodendrocytes (Fig.2.1 D), and 1,626 transcripts that possessed the $m^6A$ mark in oligodendrocytes but not in OPCs (Fig.2.1 E). Only 23 of the shared transcripts (Fig.2.1 F), showed the $m^6A$ mark in both OPCs and oligodendrocytes. The dynamic nature of the $m^6A$ mark in oligodendrocyte lineage cells suggests that it may play an important role in regulating oligodendrocyte differentiation and CNS myelination.

In order to investigate the role of the $m^6A$ mark in CNS myelinating cells, we generated mouse lines in which the gene encoding an essential $m^6A$ writer component, METTL14, was conditionally inactivated at distinct oligodendrocyte developmental stages. We crossed mice carrying a conditional allele of *Mettl14* (*Mettl14*$^{fl/fl}$) (Koranda et al., 2018) with mice expressing the Cre recombinase under the transcriptional control of oligodendrocyte transcription factor 2 (Olig2), which is expressed throughout the oligodendrocyte lineage (Schüller et al., 2008) (Fig.2.1 G). The *Mettl14*$^{fl/fl}$*;Olig2*-Cre mouse line allows us to study the role of $m^6A$ in developing oligodendrocyte lineage cells (Bergles and Richardson, 2015). We also generated *Mettl14*$^{fl/fl}$*;CNP-*

Cre mice (Fig.2.1 G), in which *Mettl14* is conditionally eliminated by Cre under the transcriptional control of the myelin protein CNP primarily in post-mitotic oligodendrocytes (Lappe-Siefke et al., 2003), allowing us to study the role of $m^6A$ in maturing oligodendrocytes.

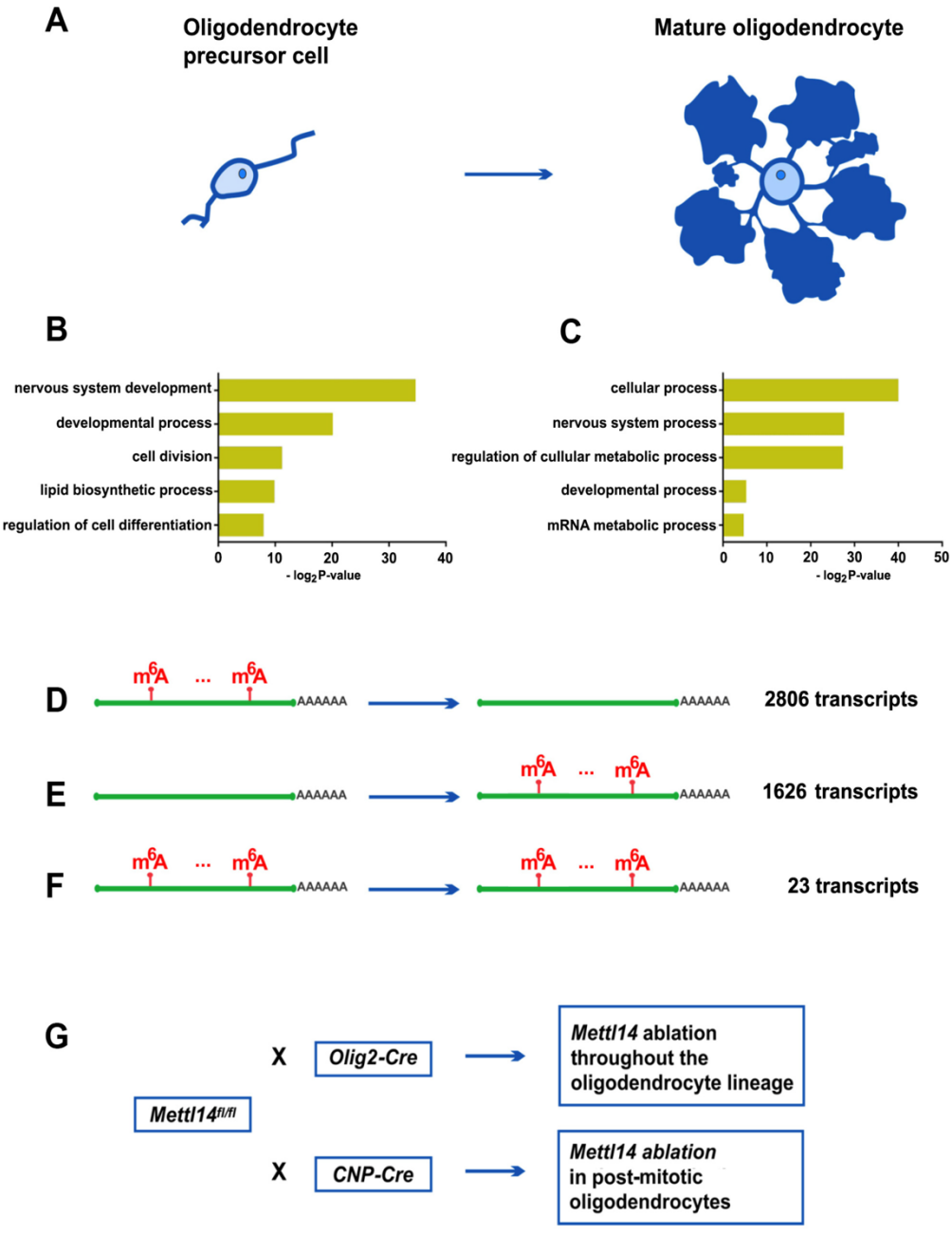

**Figure 2.1. Oligodendrocyte lineage progression is accompanied by changes in m$^6$A modification on numerous transcripts.**

(A) Schematic drawing of an OPC and mature oligodendrocyte. (B-C) The gene ontology categories of the m$^6$A marked transcripts that belong to OPCs (B) and oligodendrocytes (C) ($log_2$ |CPM|>1, Z-score>0). (D) Of the 11,502 transcripts that are expressed both in OPCs and oligodendrocytes, 2806 transcripts bear the m$^6$A mark in OPCs, but not in oligodendrocytes. ($log_2$ |CPM|>1, Z score>0). (E) Of the 11,502 transcripts that are expressed both in OPCs and oligodendrocytes, 1626 transcripts bear the m$^6$A mark in oligodendrocytes, but not in OPCs. (F) Of the 11,502 transcripts that are expressed both in OPCs and oligodendrocytes, 23 transcripts bear the m$^6$A mark in both OPCs and oligodendrocytes. (G) Mouse lines generated for this study. *Mettl14*$^{fl/fl}$ mouse line was crossed with *Olig2*-Cre and *CNP*-Cre mouse lines, to conditional eliminate *Mettl14* in oligodendrocyte lineage cells and post-mitotic cells, respectively.

### 2.3.2 *Mettl14* ablation leads to reduction of mature oligodendrocytes but not OPCs

We first examined whether the *Mettl14* gene was efficiently inactivated via the Cre-*loxP* genetic strategy by examining METTL14 expression in the CNS using immunohistochemistry. We observed a reduction of METTL14 expression in both *Mettl14*$^{fl/fl}$*;Olig2*-Cre and *Mettl14*$^{fl/fl}$*;CNP*-Cre mutants, compared to their *Mettl14*$^{fl/fl}$ littermate controls at postnatal day P12 (Fig.S2.5 A-F), and across different CNS white matter regions at postnatal day18 (P18) (data not shown), a time point at which myelin is still undergoing development.

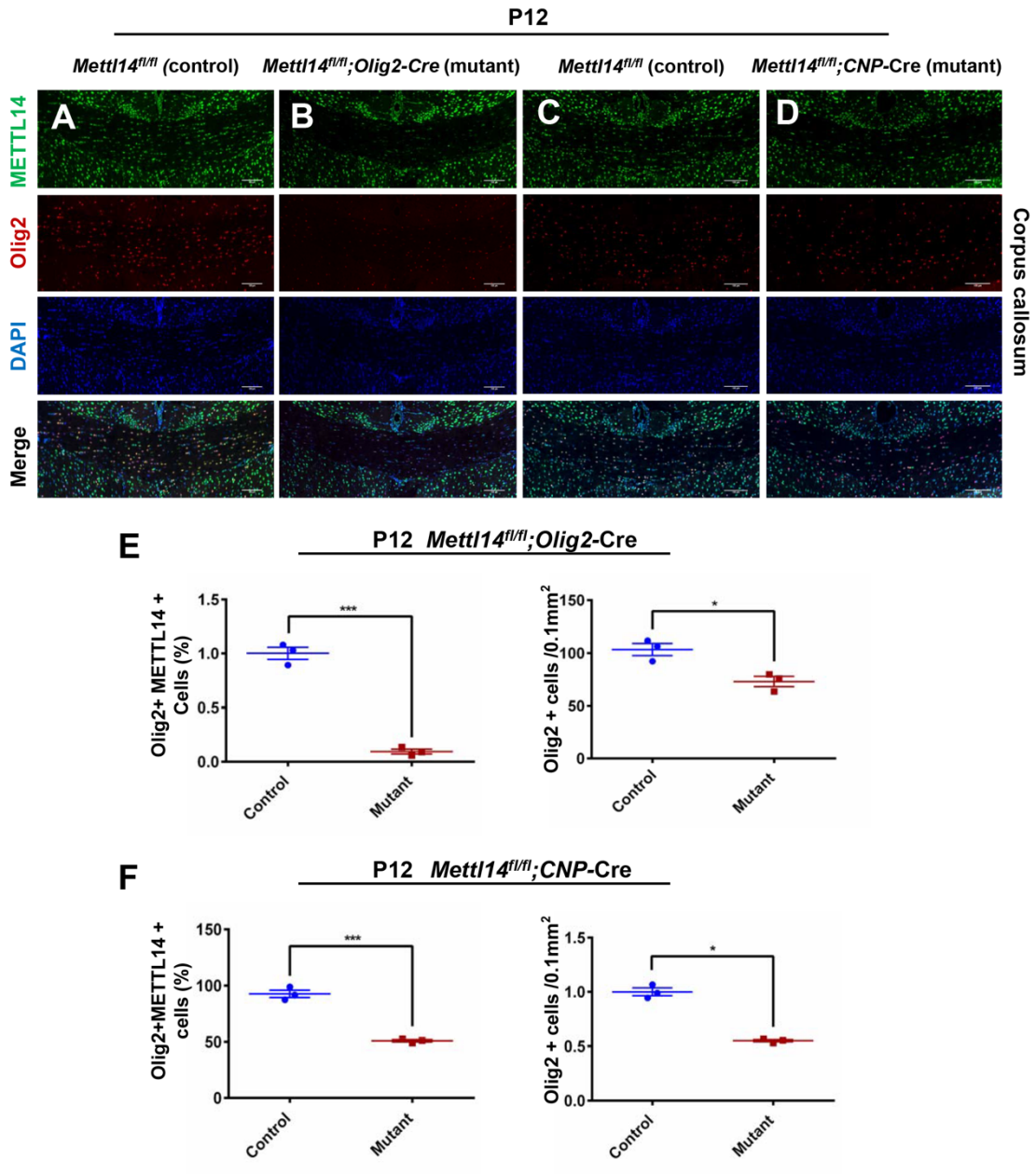


**Figure S2.5. Efficient *Mettl14* ablation in oligodendrocyte lineage cells in *Mettl14*$^{fl/fl}$;*Olig2*-Cre and *Mettl14*$^{fl/fl}$;*CNP*-Cre animals (P12). Relate to Figure 2.2**

**(A-B)** Representative METTL14 (green) and Olig2 (red) immunostaining in the corpus callosum of P12 *Mettl14*$^{fl/fl}$;*Olig2*-Cre mutant and control mice. (Scale bar=100µm). **(C-D)** Representative METTL14 (green) and Olig2 (red) immunostaining in the corpus callosum of P12 *Mettl14*$^{fl/fl}$;*CNP*-Cre mutant and control mice. (Scale bar=100µm). **(E)** Quantification analysis showing a significantly reduced percentage of Olig2$^{+}$/METTL14$^{+}$ double-positive cells, as wells as reduced Olig2-positive cells in the P12 *Mettl14*$^{fl/fl}$;*Olig2*-Cre mutants. Values represent mean ± SEM (n=3; $^{*}p<0.05$, $^{***}p<0.001$; unpaired Student's t-test). **(F)** Quantification analysis showing a significantly reduced percentage of Olig2$^{+}$/METTL14$^{+}$ double-positive cells, as wells as reduced

Olig2-positive cells in the P12 *Mettl14*$^{fl/fl}$*;CNP*-Cre mutants. Values represent mean ± SEM (n=3; $^{*}p<0.05$, $^{***}p<0.001$; unpaired Student's t-test).

To gain insight into how *Mettl14* inactivation affects oligodendrocyte lineage cell development, we used immunohistochemistry to detect the oligodendrocyte lineage cell marker Olig2 in P18 mice (Fig.2.2 A, B). We found a decreased percentage of Olig2/METTL14 double positive cells (Fig.2.2 C) accompanied by a reduction of Olig2+ cell numbers in the corpus callosum in *Mettl14*$^{fl/fl}$*;Olig2*-Cre (Fig.2.2 D) mutants. Similarly, P18 *Mettl14*$^{fl/fl}$*;CNP*-Cre (Fig.S2.1 A,B) mutants also showed decreased percentage of Olig2/METTL14 double positive cells (Fig.S2.1 C) and decreased Olig2+ cell numbers (Fig.S2.1 D) and in the corpus callosum. The reduction of oligodendrocyte lineage cells in both *Mettl14*$^{fl/fl}$*;Olig2*-Cre and *Mettl14*$^{fl/fl}$*;CNP*-Cre mutant corpus callosum indicates that *Mettl14* is important in oligodendrocyte lineage development.

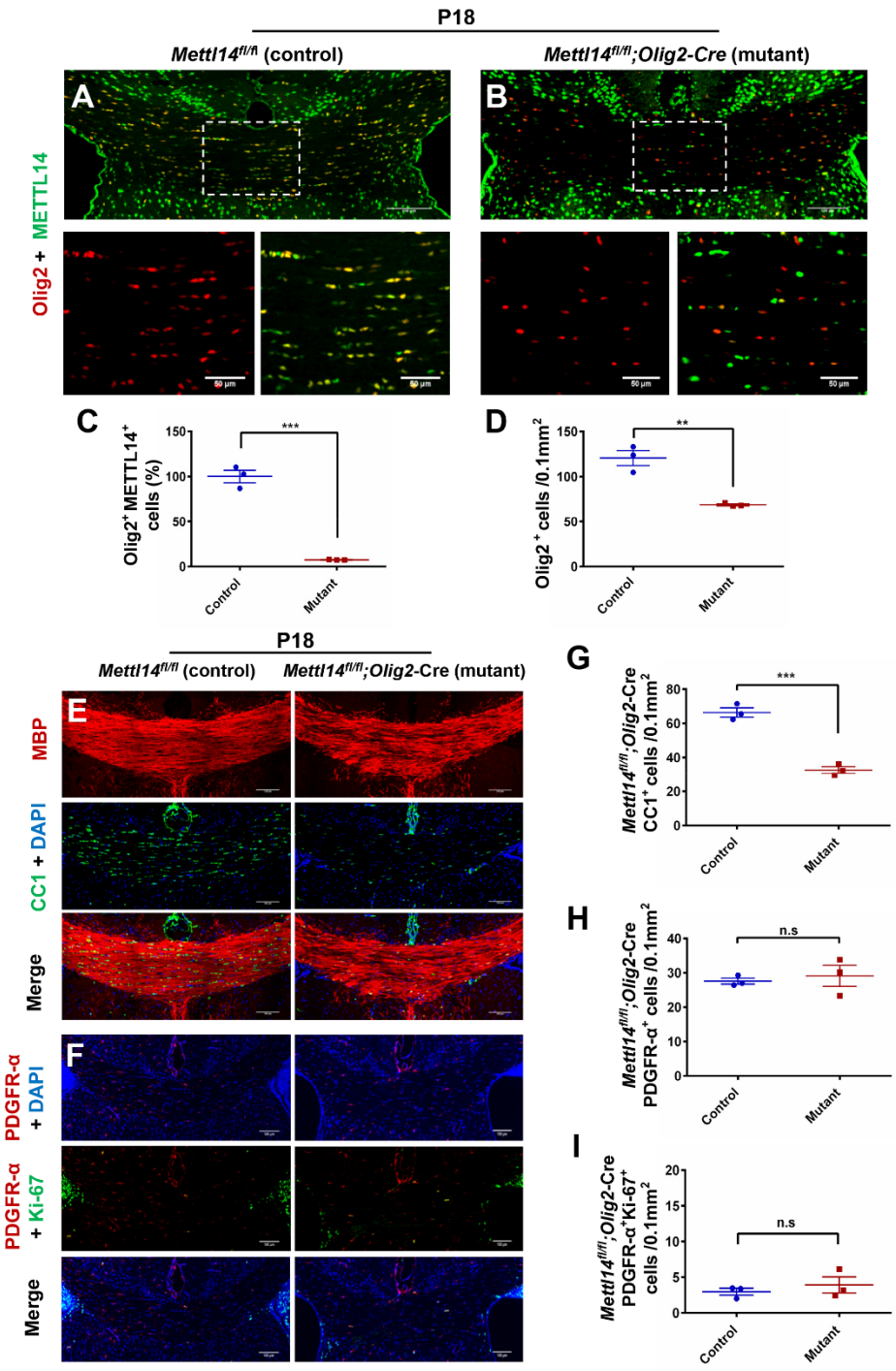


**Figure 2.2. Oligodendrocyte lineage cell-specific ablation of *Mettl14* results in loss of oligodendrocytes.**

**(A-B)** Representative METTL14 (green) and Olig2 (red) immunostaining in the corpus callosum of P18 *Mettl14*$^{fl/fl}$*;Olig2*-Cre control (A) and mutant (B) mice (Scale bar=100µm, 50µm). **(C)** Quantification analysis showing a significantly reduced percentage of Olig2$^{+}$/METTL14$^{+}$ double

positive cells in the mutants. Values represent mean ± SEM (n=3; ***p<0.001; unpaired Student's t-test). **(D)** Quantification analysis showing a statistically significant reduction of total oligodendrocyte lineage cells (Olig2$^+$ cells). Values represent mean ± SEM (n=3; **p<0.01; unpaired Student's t- test). **(E)** Representative CC1 (green) and MBP (red) immunostaining in the corpus callosum of P18 *Mettl14$^{fl/fl}$;Olig2*-Cre control and mutant mice. Mutant corpus callosum showed visible reduction of oligodendrocytes (CC1$^+$ cells) and patchy myelin (MBP) (Scale bar=100µm). **(F)** Representative PDGFR-α (red) and Ki-67 (green) immunostaining in the corpus callosum of P18 *Mettl14$^{fl/fl}$;Olig2*-Cre control and mutant mice (Scale bar=100µm). **(G)** Quantification showing a significant reduction of CC1$^+$ cells (OLs) in P18 *Mettl14$^{fl/fl}$;Olig2*-Cre mutant corpus callosum. Values represent mean ± SEM (n=3; ***p<0.001; unpaired Student's t-test). **(H)** Quantification showing no significant difference between control and mutant numbers of PDGFR-α$^+$ cells (OPCs) in P18 *Mettl14$^{fl/fl}$;Olig2*-Cre mice. Values represent mean ± SEM (n=3; p>0.05; unpaired Student's t-test). **(I)** Quantification showing no significant difference between control and mutant numbers of PDGFR-α$^+$ and Ki67$^+$ double positive cells in P18 *Mettl14$^{fl/fl}$;Olig2*-Cre mice. Values represent mean ± SEM (n=3; p>0.05; unpaired Student's t-test).

**See also Figure S2.1, Figure S2.5-S2.7.**

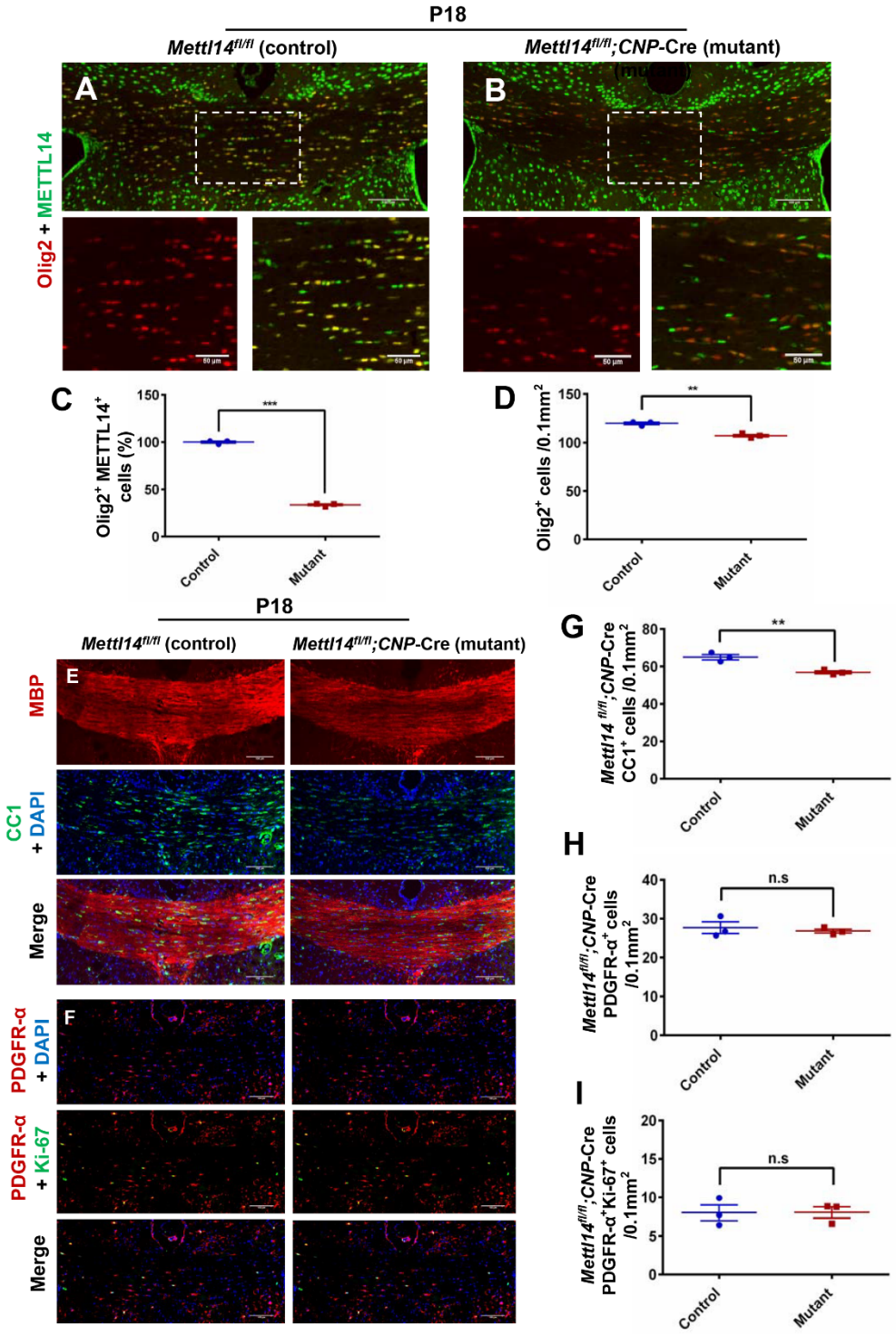


**Figure S2.1 *Mettl14* ablation in post mitotic oligodendrocytes results in loss of oligodendrocytes. Relate to Figure 2.2.**

**(A-B)** Representative METTL14 (green) and Olig2 (red) immunostaining in the corpus callosum of P18 *Mettl14$^{fl/fl}$;CNP*-Cre mutant and control mice (scale bar=100µm, 50µm). **(C)** Quantification

analysis showing a significantly reduced percentage of Olig2$^{+}$/METTL14$^{+}$ double positive cells in the *Mettl14$^{fl/fl}$;CNP*-Cre mutants. Values represent mean ± SEM (n=3; $^{***}p<0.001$; unpaired Student's t-test). **(D)** Quantification analysis showing a statistically significant reduction of total oligodendrocyte lineage cells (Olig2$^{+}$ cells) in the *Mettl14$^{fl/fl}$;CNP*-Cre mutants. Values represent mean ± SEM (n=3; $^{**}p<0.01$; unpaired Student's t- test). **(E)** Representative CC1 (green) and MBP (red) immunostaining in the corpus callosum of P18 control and *Mettl14$^{fl/fl}$*;*CNP*-Cre mutant mice. Mutant corpus callosum showed visible reduction of oligodendrocytes (CC1$^{+}$ cells) and patchy myelin (MBP) (scale bar=100µm). **(F)** Representative PDGFR-α (red) and Ki-67 (green) immunostaining in the corpus callosum of P18 *Mettl14$^{fl/fl}$;CNP*-Cre mutant and control mice (scale bar=100µm). **(G)** Quantification showing a significant reduction of CC1$^{+}$ cells (OLs) in P18 *Mettl14$^{fl/fl}$;CNP*-Cre mutant corpus callosum (n=3; $^{**}p<0.01$;$^{***}p<0.001$, unpaired Student's t-test). **(H)** Quantification showing no significant difference between control and mutant numbers of PDGFR-α$^{+}$ cells (OPCs) in P18 *Mettl14$^{fl/fl}$;CNP*-Cre mice (n=3; $p>0.05$; unpaired Student's t-test). **(I)** Quantification showing no significant difference between control and mutant numbers of PDGFR-α$^{+}$ and Ki-67$^{+}$ double positive cells in P18 *Mettl14$^{fl/fl}$;CNP*-Cre mice (n=3; $p>0.05$; unpaired Student's t-test).

During early development, Olig2+ pMN progenitors produce both motor neurons and oligodendrocytes (Ravanelli and Appel, 2015). Therefore, we explored whether the *Mettl14* deletion affects motor neuron development. We used choline acetyltransferase (ChAT) immunohistochemistry to identify motor neurons in the lumbar spinal cord at P12, and we found no difference in motor neuron numbers in both *Mettl14$^{fl/fl}$;Olig2*-Cre (Fig.S2.7 A,B,E) and *Mettl14$^{fl/fl}$;CNP*-Cre (Fig.S2.7 C,D,F) mutant mice compared to controls. In addition, motor neurons express METTL14 in the mutants of both strains (Fig.S2.7 B,D), suggesting that Cre recombination has limited effect in motor neurons.

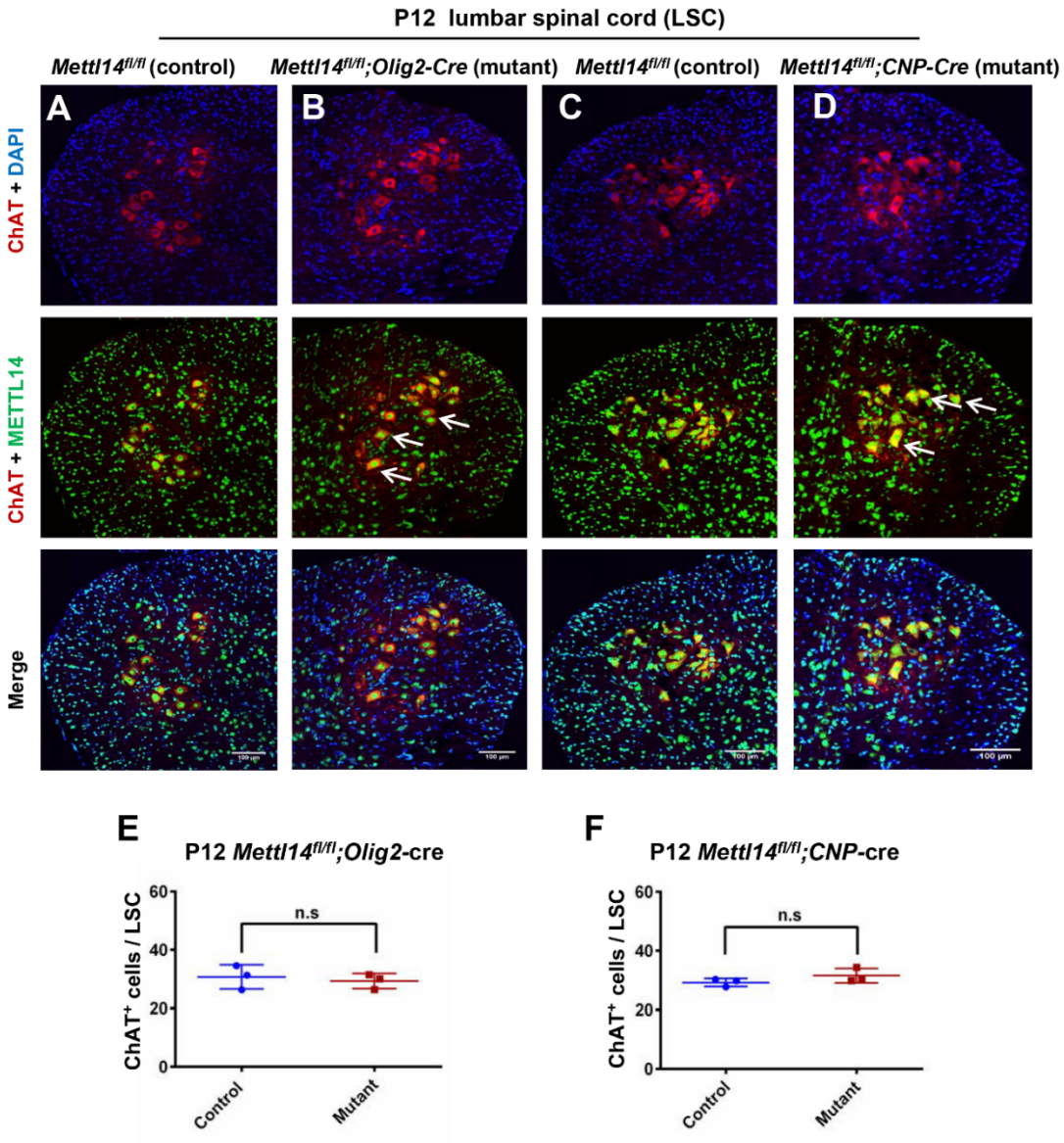


**Figure S2.7. *Mettl14* deletion has no effect on motor neuron numbers. Relate to Figure 2.2.**

**(A-B)** Representative ChAT and METTL14 immunostaining in P12 *Mettl14*$^{fl/fl}$*;Olig2*-Cre control and mutant lumbar spinal cord (LSP). Arrows showing motor neurons are ChAT and METTL14 double positive in the mutants (Scale bar=100µm). **(C-D)** Representative ChAT and METTL14 immunostaining in P12 *Mettl14*$^{fl/fl}$*;CNP*-Cre control and mutant LSP. Arrows showing motor neurons are ChAT and METTL14 double positive in the mutants (Scale bar=100µm). **(E-F)** Quantification results of motor neurons in both *Mettl14*$^{fl/fl}$*;Olig2*-Cre (E) and *Mettl14*$^{fl/fl}$*;CNP*-Cre (F) LSP showed no difference in the mutants compared to controls. (n=3; p>0.05; unpaired Student's t test)

To identify the oligodendrocyte lineage stage(s) that was affected by *Mettl14* inactivation, we examined the number of OPCs and post-mitotic oligodendrocytes in P18 *Mettl14$^{fl/fl}$;Olig2*-Cre and *Mettl14$^{fl/fl}$;CNP*-Cre corpus callosum. CC1 antibody immunostaining specific for mature oligodendrocytes, showed that the mutants had significantly fewer mature oligodendrocytes as compared to controls in the corpus callosum of both *Mettl14$^{fl/fl}$;Olig2*-Cre (Fig.2.2 E,G) and *Mettl14$^{fl/fl}$;CNP*-Cre mice (Fig.S2.1 E,G). Interestingly, the number of cells positive for PDGF-receptor-alpha (PDGFR-α), a marker for OPCs, showed no difference in the mutants in both *Mettl14$^{fl/fl}$;Olig2*-Cre (Fig.2.2 F,H) and *Mettl14$^{fl/fl}$;CNP*-Cre mice (Fig.S2.1 F,H), indicating that the loss of *Mettl14* does not disrupt OPC formation.

To investigate *Mettl14'*s role in OPC proliferation, we co-stained CNS tissue sections with Ki-67, a marker of cellular proliferation, and PDGFR-α to detect OPCs. We found no significant difference in the numbers of proliferating OPCs between mutants and controls in both P18 *Mettl14$^{fl/fl}$;Olig2*-Cre (Fig.2.2 F,I) and P18 *Mettl14$^{fl/fl}$;CNP*-Cre mice (Fig.S2.1 F,I). We further examined the effects of *Mettl14* ablation on OPCs and proliferating OPCs at an earlier time point P12, when a larger percentage of OPCs are normally proliferative compared to P18. The quantitative analysis of P12 sections revealed results similar to those seen at P18, with no significant difference of OPC and proliferating OPC numbers between mutants and controls in both *Mettl14$^{fl/fl}$;Olig2*-Cre (Fig. S2.6 C, D, K, M) and *Mettl14$^{fl/fl}$;CNP*-Cre mice (Fig.S2.6 G, H, L, N). In addition, similarly to P18 mutants, both P12 *Mettl14$^{fl/fl}$;Olig2*-Cre (Fig.S2.6 A, B, I) and *Mettl14$^{fl/fl}$;CNP*-Cre (Fig.S2.6 E, F, J) mice showed reduced numbers of $CC1^{+}$ mature oligodendrocytes in the corpus callosum.

Together, our findings demonstrate that *Mettl14* ablation leads to the reduction of oligodendrocyte lineage cells, in which mature oligodendrocyte numbers, as opposed to OPC numbers, are predominantly affected.

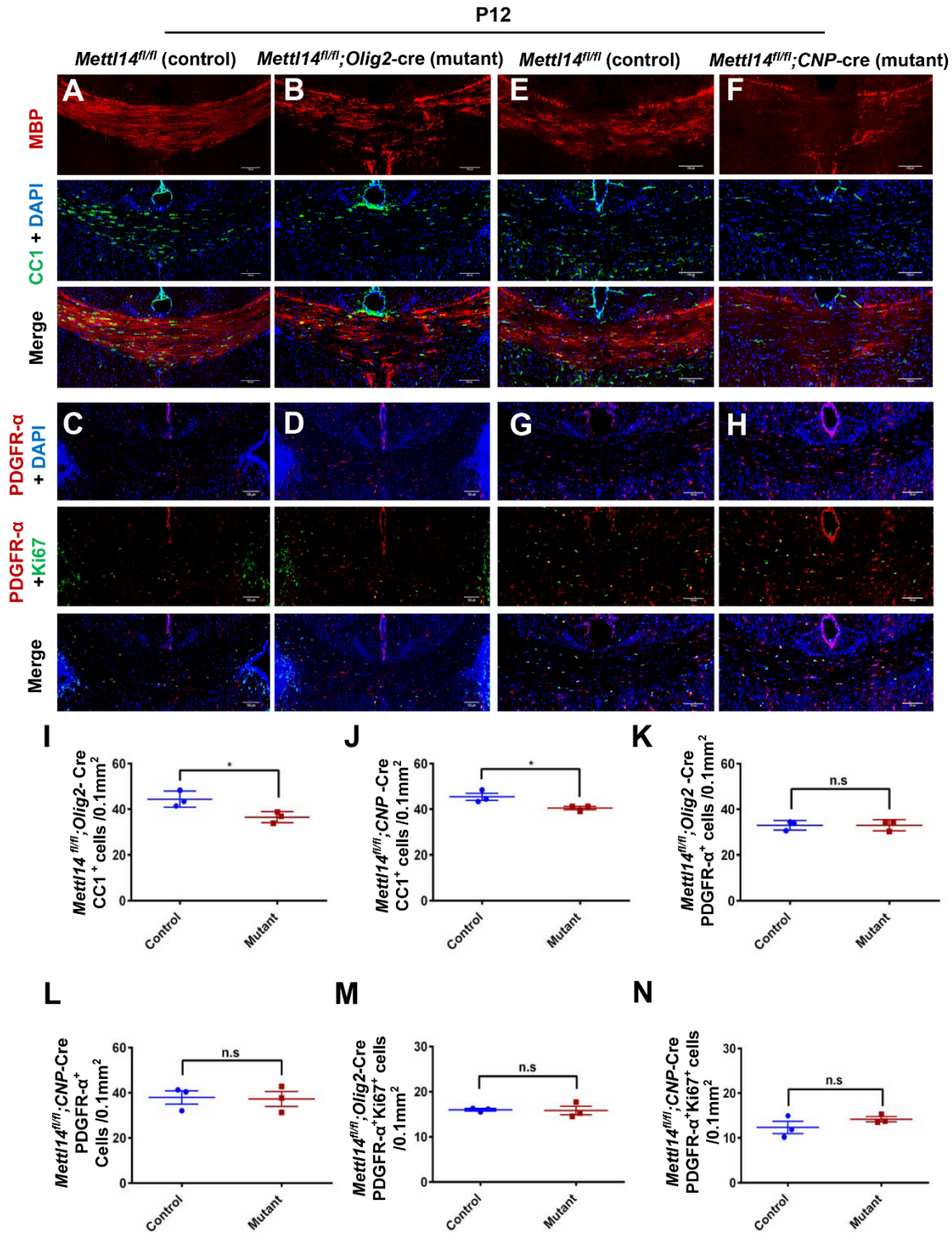
P12
Mettl14fl/fl (control)
Mettl14fl/fl;Olig2-cre (mutant)
Mettl14fl/fl (control)
Mettl14fl/fl;CNP-cre (mutant)
A
B
E
F
MBP
CC1 + DAPI
Merge
C
D
G
H
PDGFR-α + DAPI
PDGFR-α +Ki67
Merge
I
J
K
Mettl14 fl/fl;Olig2- Cre CC1+ cells /0.1mm2
Mettl14fl/fl;CNP -Cre CC1+ cells /0.1mm2
Mettl14fl/fl;Olig2 -Cre PDGFR-α+ cells /0.1mm2
*
*
n.s
Control
Mutant
L
M
N
Mettl14fl/fl;CNP-Cre PDGFR-α+ Cells /0.1mm2
Mettl14fl/fl;Olig2-Cre PDGFR-α+Ki67+ cells /0.1mm2
Mettl14fl/fl;CNP-Cre PDGFR-α+Ki67+ cells /0.1mm2
n.s
n.s
n.s
Control
Mutant

**Figure S2.6. Oligodendrocyte-specific ablation of *Mettl14* results in reduced number of oligodendrocytes. Relate to Figure 2.2.**

**(A-B)** Representative CC1 and MBP immunostaining in the corpus callosum of P12 control and *Mettl14*$^{fl/fl}$*;Olig2*-Cre mutant animals. Mutant corpus callosum showed visible reduction of oligodendrocytes (CC1+cells), and patchy myelin (MBP) (Scale bar=100μm). **(C-D)** Representative PDGFR-α and Ki67 immunostaining in the corpus callosum of P12 control and *Mettl14*$^{fl/fl}$*;Olig2*-Cre mutant animals (Scale bar=100μm). **(E-F)** Representative CC1 and MBP immunostaining in the corpus callosum of P12 control and mutant *Mettl14*$^{fl/fl}$*;CNP*-Cre animals. Mutant corpus callosum showed visible reduction of oligodendrocytes (CC1+cells), and patchy myelin (MBP) (Scale bar=100μm). **(G-H)** Representative PDGFR-α and Ki67 immunostaining in the corpus callosum of P12 control and *Mettl14*$^{fl/fl}$*;CNP*-Cre mutant animals (Scale bar=100μm). **(I-J)** Quantification showing a significant reduction of CC1 positive cells (oligodendrocytes) in P12 *Mettl14*$^{fl/fl}$*;Olig2*-Cre (I) and *Mettl14*$^{fl/fl}$*;CNP*-Cre mutant (J) corpus callosum. (n=3; $^{*}p<0.05$; unpaired Student's t test). **(K-L)** Quantification showing no difference of PDGFR-α positive cells (OPCs) in P12 *Mettl14*$^{fl/fl}$;Olig2-Cre (K) and *Mettl14*$^{fl/fl}$*;CNP*-Cre mutant (L) corpus callosum. (n=3; $p>0.05$; unpaired Student's t test). **(M-N)** Quantification showing no difference of PDGFR-α and Ki-67 double positive cells (proliferating OPCs) in P12 *Mettl14*$^{fl/fl}$;*Olig2*-Cre (L) and *Mettl14*$^{fl/fl}$*;CNP*-Cre mutant (N) corpus callosum. (n=3; $p>0.05$; unpaired Student's t test)

### 2.3.3 *Mettl14* ablation in oligodendrocyte lineage cells leads to hypomyelination

To characterize the pathological consequences caused by *Mettl14* ablation during myelin development, we examined two different CNS regions, the corpus callosum and optic nerve, in both P18 *Mettl14*$^{fl/fl}$*;Olig2*-Cre and *Mettl14*$^{fl/fl}$*;CNP*-Cre mice using electron microscopy (EM). We found hypomyelination in both corpus callosum and optic nerve in *Mettl14*$^{fl/fl}$*;Olig2*-Cre (Fig.2.3 A) and *Mettl14*$^{fl/fl}$*;CNP*-Cre P18 mutants (Fig.S2.2 A), indicating that pathological changes start when myelin is developing. Quantitative analyses showed significantly increased g-ratios, the ratio between the inner axonal and outer total diameter of the myelin sheath, of myelinated axons (Fig.2.3 B, Fig.S2.2 B) and a significantly increased percentage of unmyelinated axons in both P18 *Mettl14*$^{fl/fl}$*;Olig2*-Cre (corpus callosum: Fig.2.3 D, optic nerve: Fig.2.3 E) and *Mettl14*$^{fl/fl}$*;CNP*-Cre (corpus callosum: Fig.S2.2 D, optic nerve: Fig.S2.2 E) mutants. These results revealed decreased thickness of the myelin sheath and fewer myelinated axons upon *Mettl14*

ablation. CNS hypomyelination was further supported by Western blot analysis, which revealed significant reductions of the myelin proteins MBP and myelin-associated glycoprotein (MAG) expression levels in the *Mettl14*$^{fl/fl}$*;Olig2*-Cre (Fig.3 H, I), and *Mettl14*$^{fl/fl}$*;CNP*-Cre (Fig. S2.2 H, I) P18 mutant brains.

To explore whether the pathological change caused by *Mettl14* ablation persists in adulthood, we analyzed adult CNS regions using EM. The *Mettl14*$^{fl/fl}$*;Olig2*-Cre mutant animals are clinically normal until about 6 months (P180) of age, when they begin to display occasional hind limb flexion, slight ataxia, and mild tremor. The *Mettl14*$^{fl/fl}$*;CNP*-Cre mutant animals start to display tremor and hind limb clenching at around 4 months of age, with symptoms becoming progressively worse (e.g. ataxic phenotype). The earlier appearance of clinical symptoms in the *Mettl14*$^{fl/fl}$*;CNP*-Cre mutant animals is likely the result of Cre expression in Schwann cells in the peripheral nervous system of the CNP-Cre mice (Brockschnieder et al., 2004). Similar to P18 animals, both *Mettl14*$^{fl/fl}$*;Olig2*-Cre (P180) and *Mettl14*$^{fl/fl}$*;CNP*-Cre (P150) adult mutants displayed myelin abnormalities (Fig.2.3 A, Fig.S2.2 A), with increased g-ratios (Fig.2.3 C) and non-myelinated axon percentages in both corpus callosum (Fig.2.3 F, Fig.S2.2 F) and optic nerve (Fig.2.3 G, Fig.S2.2 G). Western blot analysis also revealed decreased myelin protein levels in both P180 *Mettl14*$^{fl/fl}$*;Olig2*-Cre (Fig.2.3 H, J) and P150 *Mettl14*$^{fl/fl}$*;CNP*-Cre (Fig.S2.2 H, J) mutants. Together, our results demonstrate that *Mettl14* is important in CNS myelination.

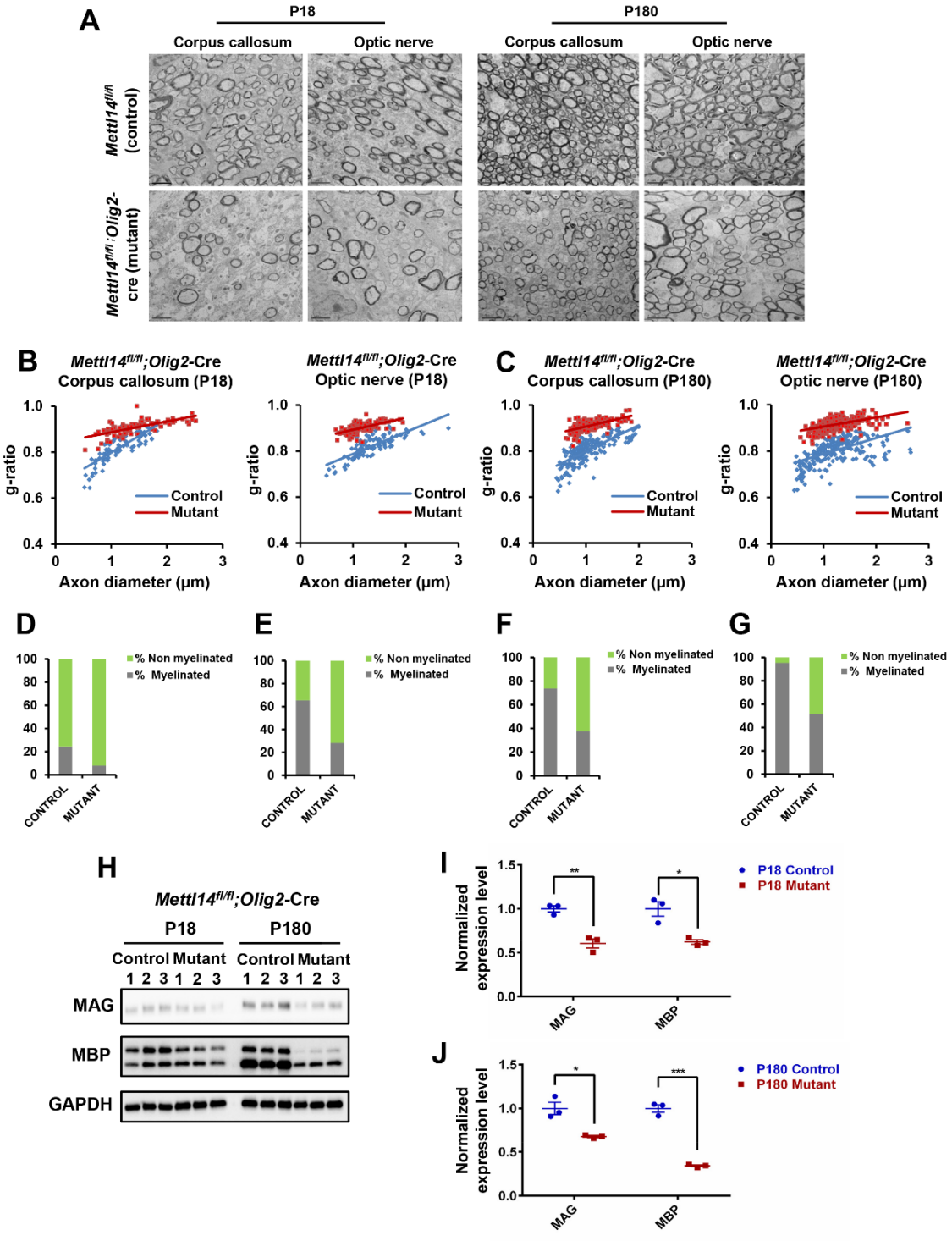


**Figure 2.3. *Mettl14* ablation leads to hypomyelination.**

**(A)** Representative EM images of corpus callosum and optic nerve in P18 and P180 *Mettl14*$^{fl/fl}$*;Olig2*-Cre control and mutant animals. Mutant corpus callosum and optic nerve had

thinner myelin and fewer myelinated axons in both ages (Scale bar=2μm). **(B)** g-ratio analyses showing significantly higher g-ratios in both P18 *Mettl14$^{fl/fl}$;Olig2*-Cre mutant corpus callosum (Mutant g ratio=0.91, control g ratio=0.80) and optic nerve (mutant g ratio= 0.90, control g ratio= 0.82), (n=3; $^{***}p<0.001$; unpaired Student's t test). **(C)** g-ratio analyses showing significantly higher g-ratios in both P180 *Mettl14$^{fl/fl}$;Olig2*-Cre mutant corpus callosum (Mutant g ratio=0.91, control g ratio=0.80) and optic nerve (mutant g ratio= 0.91, control g ratio= 0.83), (n=3; $^{***}p<0.001$; unpaired Student's t test). **(D-G)** Percentage of myelinated axons in corpus callosum and optic nerve (D. P18 *Mettl14$^{fl/fl}$;Olig2*-Cre corpus callosum, E. P18 *Mettl14$^{fl/fl}$;Olig2*-Cre optic nerve, F. P180 *Mettl14$^{fl/fl}$;Olig2*-Cre corpus callosum, G. P180 *Mettl14$^{fl/fl}$;Olig2*-Cre optic nerve). (n=3, $^{***}p<0.001$; unpaired Student's t test). **(H)** Western blot showing myelin protein expression (MAG, MBP) levels in both P18 and P180 *Mettl14$^{fl/fl}$;Olig2*-Cre control and mutant animals (n=3). **(I-J)** Quantification of immunoblots. MAG and MBP expression levels were normalized to GAPDH expression levels. Both MAG and MBP were significantly reduced in P18 (I) and P180 (J) *Mettl14$^{fl/fl}$;Olig2*-Cre mutants. Values represent mean ± SEM (n=3; $^{*}p<0.05$; $^{**}p<0.01$; $^{***}p<0.001$; unpaired Student's t test). **See also Figure S2.2.**

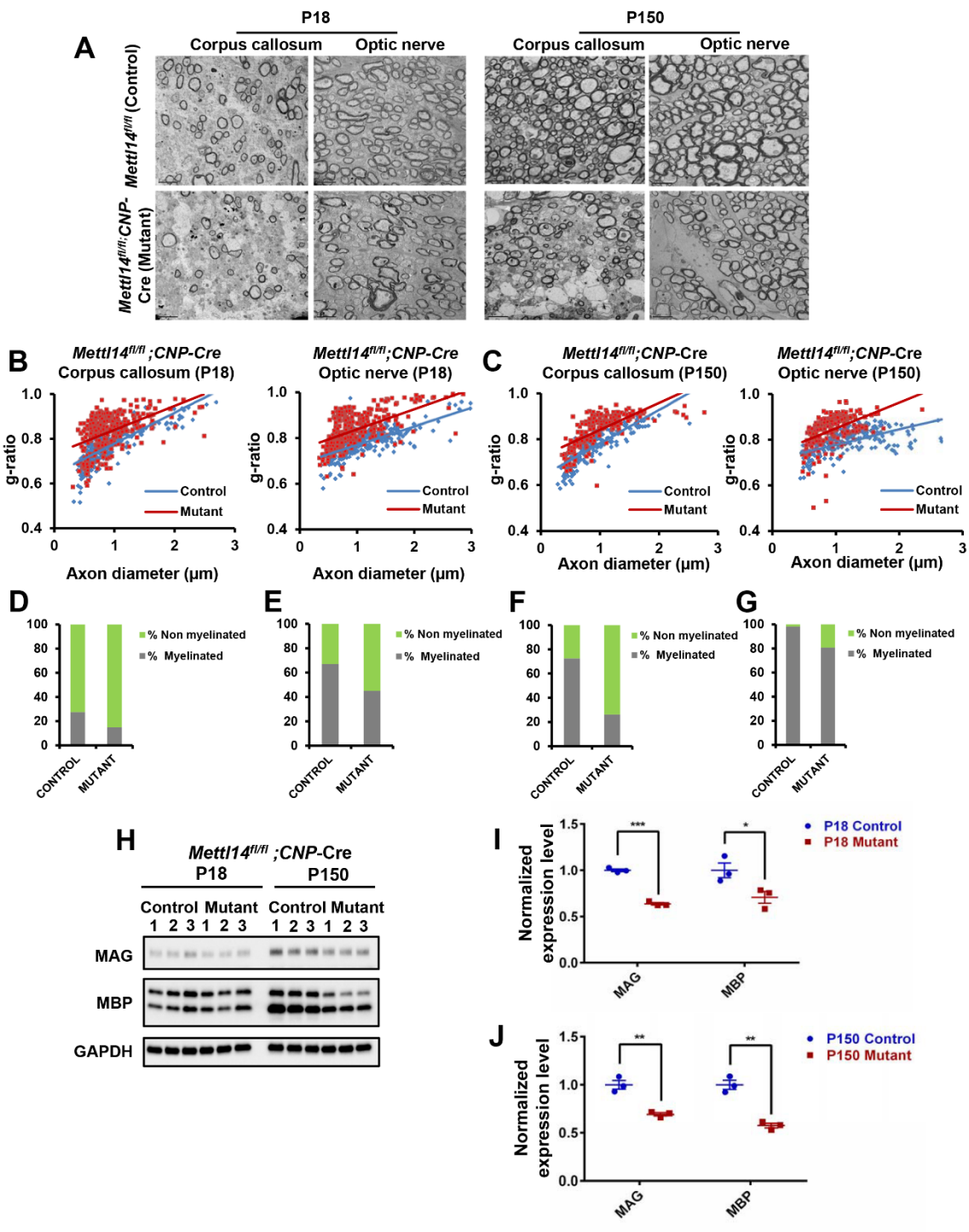


**Figure S2.2. *Mettl14* ablation in post mitotic oligodendrocytes leads to hypomyelination. Relate to Figure 2.3.**

**(A)** Representative EM images of corpus callosum and optic nerve in P18 and P150 control and *Mettl14*$^{fl/fl}$*;CNP*-Cre mutant animals. Mutant corpus callosum and optic nerve had thinner myelin

and fewer myelinated axons in both ages (Scale bar=2μm). **(B)** g-ratio analyses showing significantly higher g-ratios in both P18 *Mettl14*$^{fl/fl}$*;CNP*-Cre mutant corpus callosum (mutant g ratio=0.86, control g ratio=0.81) and optic nerve (mutant g ratio=0.85, control g ratio= 0.82), (n=3; $^{***}p<0.001$; unpaired Student's t test). **(C)** g-ratio analyses showing significantly higher g-ratios in both P150 *Mettl14*$^{fl/f}$*;CNP*-Cre mutant corpus callosum (mutant g ratio=0.84, control g ratio=0.77) and optic nerve (mutant g ratio=0.84, control g ratio= 0.79), (n=3; $^{***}p<0.001$; unpaired Student's t test). **(D-G)** Percentage of myelinated axons in corpus callosum and optic nerve (D. P18 *Mettl14*$^{fl/fl}$*;CNP*-Cre corpus callosum, E. P18 *Mettl14*$^{fl/fl}$*;CNP*-Cre optic nerve, F. P150 *Mettl14*$^{fl/fl}$*;CNP*-Cre corpus callosum, G. P150 *Mettl14*$^{fl/fl}$*;CNP*-Cre optic nerve). (n=3, $^{***}p<0.001$). **(H)** Western blot showing myelin protein expression (MAG,MBP) levels in both P18 and P150 *Mettl14*$^{fl/fl}$*;CNP*-Cre control and mutant animals (n=3). **(I-J)** Quantification of immunoblots. MAG and MBP expression levels were normalized to GAPDH expression levels. Both MAG and MBP displayed significant reductions in P18 (I) and P150 (J) *Mettl14*$^{fl/fl}$*;CNP*-Cre mutants. Values represent mean ± SEM (n=3; $^{*}p<0.05$; $^{**}p<0.01$; $^{***}p<0.001$, unpaired Student's t test).

### 2.3.4 *Mettl14* ablation prevents oligodendrocyte differentiation

To further determine the role of *Mettl14* in different oligodendrocyte lineage stages, we turned to *in vitro* cultures. We found that the *Mettl14* mutant OPCs were isolated as efficiently as control OPCs, and that the mutant cells displayed similar mitotic activity and bipolar morphology in the presence of PDGF-AA (Fig.2.4 A, B). Interestingly, the *Mettl14* deleted cells did not develop into MBP$^{+}$ mature oligodendrocytes after 5 days of differentiation following removal of PDGF-AA from the culture media (Fig.2.4 D). The mutant cells did not send out the extensive membrane structure seen with control oligodendrocytes (Fig.2.4 C). Indeed, only rare cells (less than 7%, data not shown) that escaped Cre recombination and were METTL14$^{+}$ in the mutant cell cultures developed into MBP$^{+}$ cells (Fig.2.4 E). Our Western blot data confirmed the almost complete elimination of METTL14 in the mutant oligodendrocytes, as well as the dramatic reduction of major myelin protein (MAG and MBP) expression (Fig.2.4 F, G). These results correlate with our *in vivo* findings, strongly suggesting that *Mettl14* is critical for oligodendrocyte maturation.

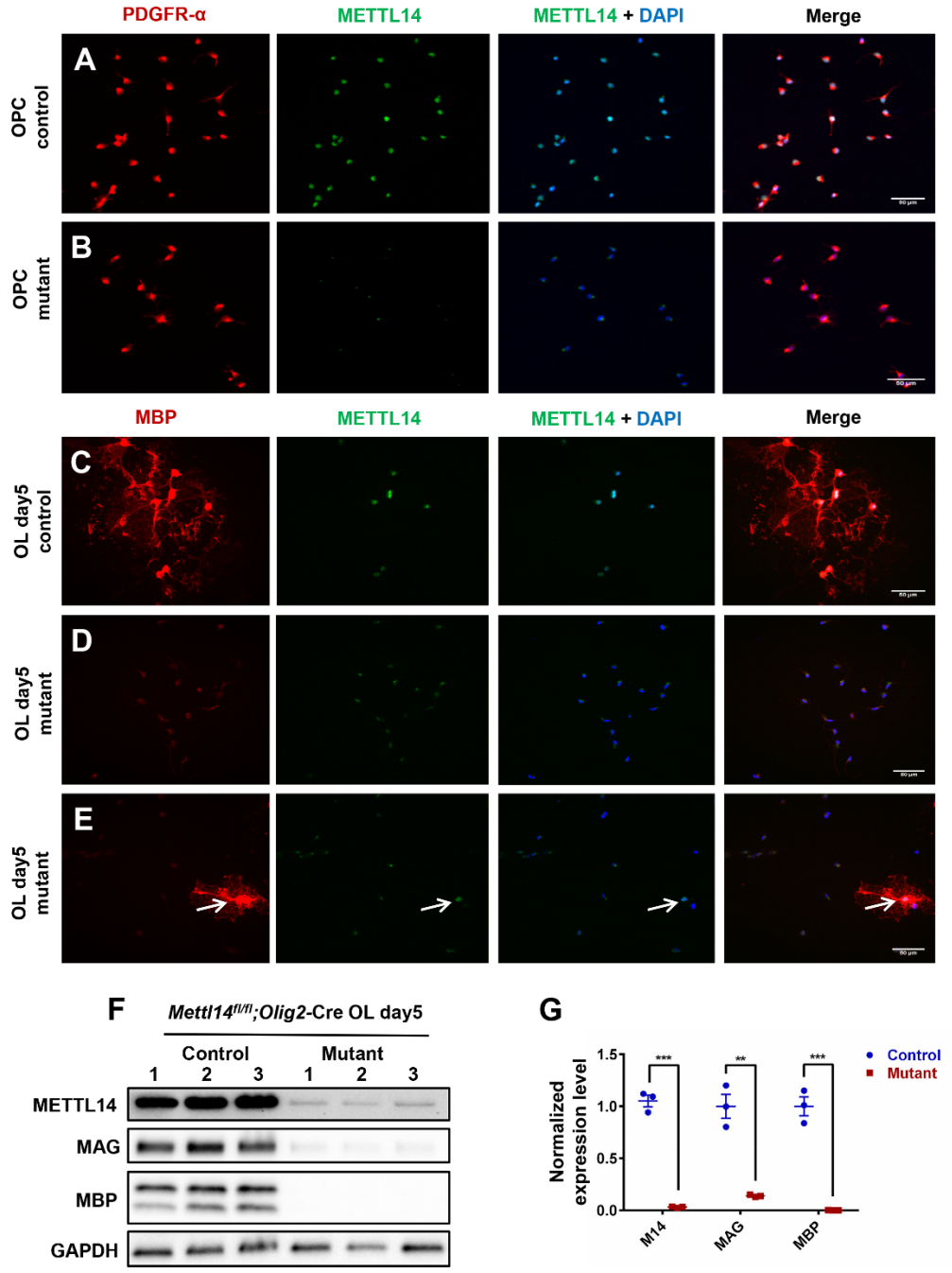


**Figure 2.4. *Mettl14* ablated OPCs fail to develop into mature oligodendrocytes *in vitro.***

**(A-B)** PDGFR-α and METTL14 immunostaining of *Mettl14*$^{fl/fl}$*;Olig2*-Cre control and mutant OPCs in culture. METTL14 was eliminated from the mutant OPCs, which showed no morphological changes compared to control OPCs (Scale bar=50μm). **(C-D)** MBP and METTL14 immunostaining of *Mettl14*$^{fl/fl}$*;Olig2*-Cre control and mutant oligodendrocytes that had been

cultured in differentiation media for 5 days (oligodendrocyte day5). Mutant cells fail to develop into MBP-positive cells (Scale bar=50µm). **(E)** Only rare cells (white arrow pointed) that had escaped Cre-mediated recombination and thus expressed METTL14 in the mutant day5 OL group successfully differentiated into MBP expressing oligodendrocytes (Scale bar=50µm). **(F)** Western blot showing METTL14, MAG, MBP and GAPDH expression levels in control and mutant OL day5 groups. **(G)** Quantification of immunoblots showing significant reduction of METTL14, MAG and MBP expression in mutant OL day5 group. METTL14, MAG and MBP expression levels were normalized to GAPDH expression level. Values represent mean ± SEM (n=3; $^{**}p<0.01$; $^{***}p<0.001$, unpaired Student's t test). **See also Figure S2.4.**

We next examined cell morphology and maturation from early to late post-mitotic differentiation stages of oligodendrocytes *in vitro* to further explore the effects of Mettl14 on oligodendrocyte lineage cell maturation. We used O1, an antibody specific for the myelin galactolipid galactocerebroside, to detect oligodendrocyte morphology (Sommer and Schachner, 1981) from day 1 to day 5 after cells were plated in differentiation media. Interestingly, *Mettl14* deleted cells (Fig.2.5 C) showed O1 immunoreactivity but did not display the morphological changes of control cells, which progressively extended their membrane structures to form complex membrane sheets (Fig.2.5 A). The *Mettl14* ablated cells did not express appreciable levels of MBP (Fig.2.5 D), whereas control cells matured gradually from day 1 to day 5 with increasing MBP expression (Fig.2.5 B). These results together with our *in vivo* data strongly suggest that *Mettl14* plays an important role in post mitotic oligodendrocyte maturation.

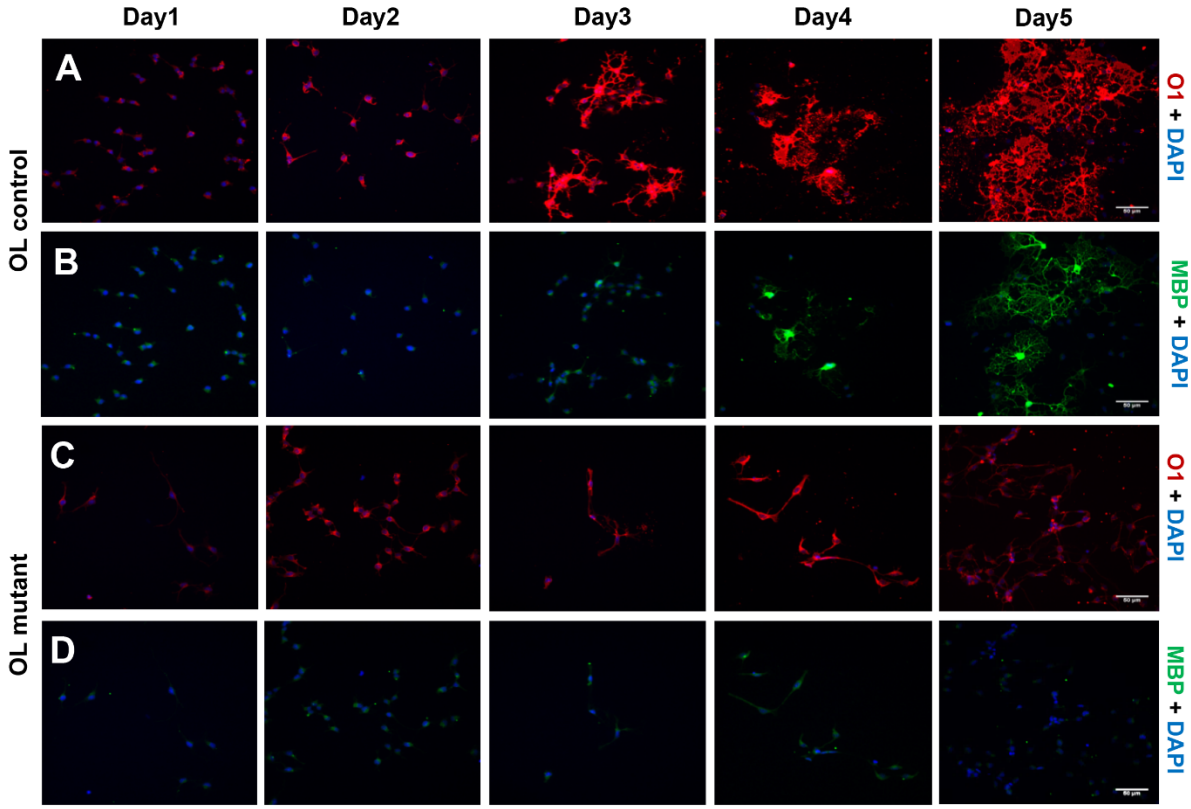


**Figure 2.5. *Mettl14* ablation prevents oligodendrocyte differentiation.**

**(A-B)** O1 and MBP immunostaining of *Mettl14*$^{fl/fl}$ (control) oligodendrocytes that had been seeded in differentiation media for 1-5 days (day1-5). Control cells progressively differentiated into mature oligodendrocytes (Scale bar=50µm). **(C-D)** O1 and MBP immunostaining of *Mettl14*$^{fl/fl}$*;Olig2*-Cre (mutant) oligodendrocytes that had been seeded in differentiation media for 1-5 days (day1-5). Mutant cells did not differentiate into MBP positive oligodendrocytes, and never formed membrane sheath structures like control cells (Scale bar=50µm).

### 2.3.5 *Mettl14* ablation differentially alters the OPC and oligodendrocyte transcriptomes

To elucidate the effects of *Mettl14* on oligodendrocyte lineage cell gene expression during development at the transcriptome level, we performed RNA-seq with both purified OPCs and cultured mature oligodendrocytes from *Mettl14*$^{fl/fl}$*;Olig2*-Cre control and mutant mice. The quantification of differential expression in the *Mettl14* mutant transcriptome revealed distinct differences in the OPCs and myelinating oligodendrocytes. For quantification analysis we defined

significance of differentially expressed transcripts using the following three criteria: 1. a 99.9% confidence interval, adjusted for false discovery, as a q-value using methods previously described (Benjamini and Yekutieli, 2005); 2. fold changes (FC) that exceeded 2.0 fold ($\log_2$ |FC|>1) in expression and 3. an expression level that exceeded two counted transcripts per million ($\log_2$ |CPM| >1) . Of the 11,809 transcripts present in the OPC transcriptome, 586 were expressed at significantly higher levels and 177 were expressed at significantly lower levels in the mutant cells (Fig.2.6 A). Among the 12,542 transcripts present in mature oligodendrocytes, 1,388 transcripts were significantly upregulated and 1,247 were downregulated in the mutant cells (Fig.2.6 B). Interestingly, among the significantly downregulated oligodendrocyte transcripts, many are normally highly expressed in myelinating oligodendrocytes, such as *Mbp, Mog, Mag, Plp1, and Cnp* (Fig.2.6 B). The downregulation of these myelin transcripts correlates with the downregulation of myelin protein expression observed in the *Mettl14* ablated mutant animals.

The m$^6$A mark has been shown to play a role in reducing the stability of m$^6$A-containing transcripts (Wang et al., 2014a, 2018; Weng et al., 2018a; Yoon et al., 2017; Zhang et al., 2017a). Accordingly, many transcripts in the *Mettl14$^{fl/fl}$;Olig2*-Cre mutants had higher relative expression levels. We compared the m$^6$A-seq data and RNA-seq data, and found that among the 3,554 m$^6$A marked OPC transcripts, 46 transcripts had significantly downregulated expression levels, and 108 transcripts had significantly upregulated expression levels (Fig.2.6 C). Among the 2,606 m$^6$A marked oligodendrocyte transcripts, 221 had significantly downregulated expression levels, and 217 transcripts had significantly upregulated expression levels (Fig.2.6 D). Gene ontology analysis of significantly altered m$^6$A marked transcripts revealed many important functions such as glia cell development in OPCs (Fig.2.6 E) and myelination in oligodendrocytes (Fig.2.6 F). These results indicate that the m$^6$A mark differentially regulates the OPC and oligodendrocyte transcriptomes.

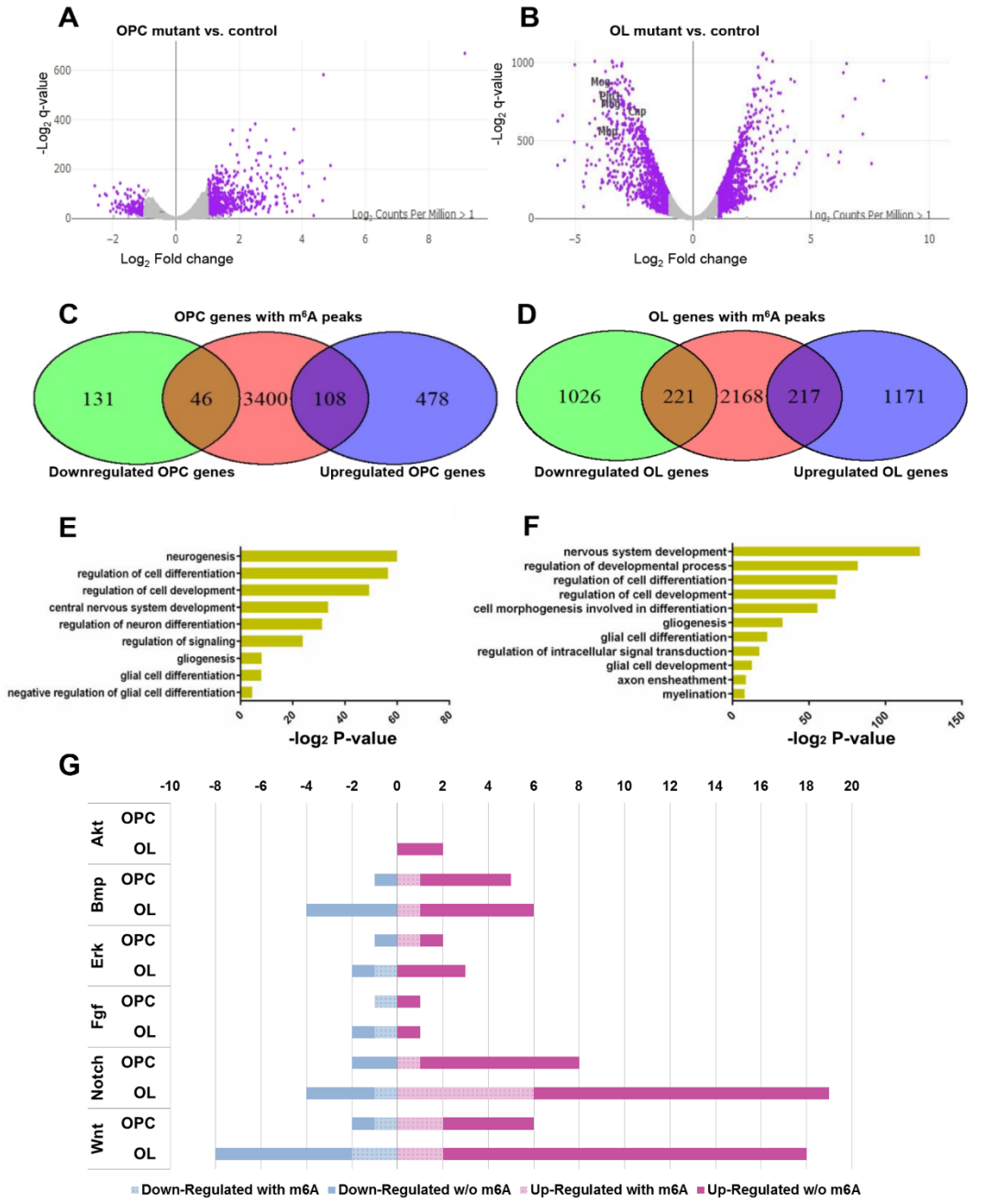


**Figure 2.6. *Mettl14* deletion differentially alters OL and OPC transcriptome.**

**(A-B)** Volcano plots display the differentially expressed genes in the *Mettl14*$^{fl/fl}$*;Olig2*-Cre OPCs (A) and oligodendrocytes (B) mutants versus controls (n=3). The highlighted genes (purple) are significantly (q-value<0.001, $\log_2$ |CPM|>1) regulated and have a notable fold change ($\log_2$ |FC|>1) in their expression in the mutants. Selected myelin genes are labeled. **(C-D)** Venn diagram shows the numbers of significantly downregulated or upregulated OPC (C) and oligodendrocyte (OL) (D) transcripts that also have the m$^6$A mark. **(E-F)** The ontology categories of the m$^6$A marked

transcripts that are significantly altered in the OPCs (E) and oligodendrocytes (F). ($log_2$ |FC|>1, $log_2$ |CPM|>1, q-value <0.001, Z-score>0). **(G)** Bar graph shows the number of $m^6A$ marked transcripts in the selected altered signaling pathways in OPCs and oligodendrocytes. ($log_2$ |FC|>1, $log_2$ |CPM|>1, q-value<0.001, Z-score>0). **See also Figure S2.8, Table 2.1–2.5**

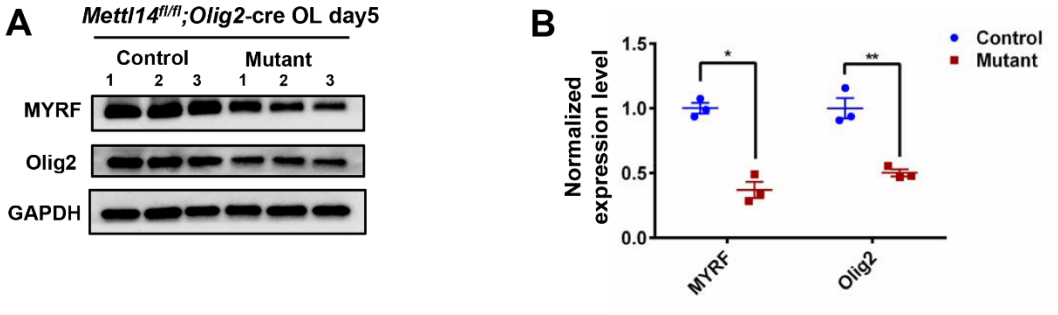


**Figure S2.8. Expression level of important oligodendrocyte transcription factors. Relate to Figure 2.6.**

**(A)** Western blot result of MYRF and Olig2 in *Mettl14$^{fl/fl}$;Olig2*-Cre day5 control and mutant oligodendrocytes. **(B)** Quantification of MYRF and Olig2 expression. MYRF and Olig2 expression levels were normalized to GAPDH expression levels. Both MYRF and Olig2 had significant reduction in P18 and P150 *Mettl14$^{fl/fl}$;CNP-Cre* mutants. Values represent mean ± SEM (n=3; $^{*}p<0.05$; $^{**}p<0.01$, unpaired Student's t test).

### 2.3.6 *Mettl14* regulates OPC and oligodendrocyte transcripts that are critical for oligodendrocyte lineage progression

In order to find clues of how the $m^6A$ mark regulates oligodendrocyte lineage development, we examined the expression of factors that play a critical cell-autonomous role in oligodendrocyte lineage progression by cross-comparing our $m^6A$-seq and RNA-seq datasets. We identified a number of transcripts that encode transcriptional factors implicated in oligodendrocyte lineage progression as being dynamically marked by $m^6A$ at different oligodendrocyte lineage stages. For example, *Hey1, Klf19, Sox2, Sox5, Srebf1, Tcf19, Zeb2* are marked by $m^6A$ in OPCs, but not in oligodendrocytes; *Hes1*, *Nkx6.2, Olig2* and *Yy1* are marked by $m^6A$ only in oligodendrocytes, but

not in OPCs (Table 2.1). The dynamic m$^6$A marked status of these transcription factor transcripts suggests a time-specific, post-transcriptional regulatory role of m$^6$A during oligodendrocyte lineage progression and may contribute to the differentially altered transcriptome in OPCs and oligodendrocytes following *Mettl14* deletion.

Studies have shown that DNA epigenetic regulatory mechanisms, such as chromatin remodeling and histone modifications, are important for oligodendrocyte lineage progression (Koreman et al., 2018). Our RNA-seq and m$^6$A-seq analyses revealed that many transcripts encoding histone modification regulators bear an m$^6$A mark, and were significantly differentially expressed in the mutant transcriptome (Table 2.2). We detected transcripts of histone "writers" such as histone acetyltransferases (HATs) *Hat1,* histone methyltransferases (HMTs) *Smyd2, Prdm2, Setdb1, Suv39h1, Ash1l, Dot1l;* histone "erasers" such as histone deacetylases (HDACs) *Hdac3, Hdac7, Hdac8, Hdac9,* and lysine demethylases (KDMs) *Kdm2b*, *Kdm5c, Kdm3b , Kdm4a, Kdm4c, Kdm6a* that had the m$^6$A mark and had significantly altered mRNA levels in the *Mettl14* ablated mutants: these transcripts encode proteins with important regulator functions in oligodendrocyte development (Hernandez and Casaccia, 2015). Thus, our findings suggest a possible link between m$^6$A RNA modification and histone modifications in the regulation of oligodendrocyte lineage development.

We also examined key signaling pathways that are critically involved in oligodendrocyte lineage progression. We found transcripts that were significantly altered by *Mettl14* ablation in the bone morphogenetic proteins (BMPs), ERK/MAPK, fibroblast growth factor families (FGFs), Notch/Delta, Sonic hedgehog (Shh) and Wnt signaling pathways in OPCs (Table 2.3); and P13K/AKT/mTOR, BMPs, ERK/MAPK, insulin-like growth factor-1 (IGF-1), Notch/Delta, Shh and Wnt signaling pathways in oligodendrocytes (Table 2.4). The alternation of critical gene

expression levels in these signaling pathways provided us with important clues regarding disruption of oligodendrocyte maturation displayed by the *Mettl14*$^{fl/fl}$*;Olig2*-Cre and *Mettl14*$^{fl/fl}$*;CNP*-Cre animals. Indeed, many transcripts that encode critical components of these signaling pathways have the m$^6$A mark (Fig.2.6 G) (Table 2.3, 2.4), suggesting that m$^6$A may regulate these signaling pathways to promote oligodendrocyte lineage progression.

**Table 2.1. Transcription factor transcripts that are dynamically marked by m$^6$A in oligodendrocyte lineage cells. Relate to Figure 2.6.**

| Gene name | m$^6$A mark | | Expression level (Control) | | Fold change (Mutant/Control) | | | |
|---|---|---|---|---|---|---|---|---|
| | OPC | OL | OPC $log_2$CPM | OL $log_2$CPM | OPC $log_2$FC | OPC q-value | OL $log_2$FC | OL q-value |
| *Hey1* | Yes | No | 4.31 | 6.84 | 0.61 | 1.22E-05 | 0.93 | 3.43E-36 |
| *Klf9* | Yes | No | -1.55 | 2.84 | -0.29 | 7.9E-01 | -0.55 | 7.81E-6 |
| *Sox2* | Yes | No | 8.32 | 7.84 | 0.57 | 2.23E-10 | 0.43 | 5.72E-08 |
| *Sox5* | Yes | No | 5.57 | 4.94 | -0.17 | 3.79E-01 | 0.82 | 1.20E-28 |
| *Srebf2* | Yes | No | 8.75 | 8.23 | -0.12 | 4.19E-01 | 5E-03 | 1.00E+00 |
| *Tcf19* | Yes | No | 6.28 | 4.74 | -0.50 | 3.35E-09 | -0.28 | 6.92E-04 |
| *Zeb2* | Yes | No | 7.93 | 8.75 | 0.58 | 4.32E-15 | -0.57 | 6.11E-15 |
| *Hes1* | No | Yes | 2.65 | 0.63 | 0.08 | 9.97E-01 | 0.59 | 1.30E-03 |
| *Nkx6.2* | No | Yes | -1.75 | 6.98 | 3.73 | 3.00E-28 | -3.31 | 1.64E-229 |
| *Olig2* | No | Yes | 9.70 | 8.25 | -0.83 | 1.71E-24 | -0.66 | 3.72E-20 |
| *Yy1* | No | Yes | 6.32 | 5.83 | 0.06 | 7.01E-01 | 0.23 | 2.82E-03 |

**Table 2.1.** m$^6$A-seq and RNA-seq results showing oligodendrocyte transcription factor transcripts that have dynamic m$^6$A marked status, accompanied by altered mRNA levels at different oligodendrocyte lineage stages (n=3; CPM: counts per million; Z score>0).

**Table 2.2. DNA epigenetic regulator transcripts that are dynamically marked by m$^6$A in oligodendrocyte lineage cells. Relate to Figure 2.6.**

| Gene name | m$^6$A mark | | Expression level (Control) | | Fold change (Mutant/Control) | | | |
|---|---|---|---|---|---|---|---|---|
| | OPC | OL | OPC $log_2$CPM | OL $log_2$CPM | OPC $log_2$FC | OPC q-value | OL $log_2$FC | OL q-value |
| *Ash1l* | Yes | No | 6.84 | 6.18 | 0.72 | 7.44E-18 | 1.64 | 3.56E-101 |
| *Dot1l* | Yes | No | 7.41 | 6.91 | 0.52 | 4.80E-10 | 0.54 | 2.80E-12 |
| *Hdac3* | Yes | No | 7.18 | 6.45 | -0.20 | 1.31E-02 | -0.26 | 6.00E-04 |
| *Hdac8* | Yes | No | 4.26 | 4.59 | 0.04 | 1.00E+00 | -0.14 | 1.01E-01 |
| *Hdac9* | Yes | No | 0.81 | -3.26 | 1.43 | 2.69E-08 | -0.46 | 1.20E-05 |
| *Kdm2b* | Yes | No | 6.49 | 4.82 | 0.23 | 5.37E-03 | 0.64 | 2.46E-17 |
| *Kdm3b* | Yes | No | 7.36 | 6.5 | 0.15 | 7.03E-02 | 0.66 | 5.42E-20 |
| *Kdm4a* | Yes | No | 7.38 | 6.82 | 0.10 | 3.59E-01 | 0.05 | 6.54E-01 |
| *Kdm5c* | Yes | No | 7.96 | 7.04 | -0.16 | 1.81E-01 | 0.29 | 3.24E-04 |
| *Kdm6a* | Yes | No | 6.19 | 5.57 | -0.34 | 3.79E-02 | -5.8E-03 | 1.00E+00 |
| *Prdm2* | Yes | No | 6.35 | 5.97 | 0.54 | 2.02E-12 | 0.53 | 6.06E-13 |
| *Setd1b* | Yes | No | 5.86 | 5.03 | 1.03 | 9.77E-29 | 1.30 | 2.45E-68 |
| *Smyd2* | Yes | No | 6.32 | 4.62 | 0.23 | 7.51E-03 | 0.65 | 5.83E-18 |
| *Hdac7* | No | Yes | 4.44 | 4.59 | 1.09 | 1.87E-22 | 1.42 | 4.59E-83 |
| *Kdm4c* | No | Yes | 6.00 | 5.53 | -0.69 | 5.48E-05 | -0.14 | 9.92E-02 |
| *Hat1* | No | Yes | 6.42 | 4.42 | -0.37 | 8.21E-06 | 0.07 | 5.68E-01 |
| *Suv39h1* | No | Yes | 6.74 | 4.58 | -0.08 | 5.32E-01 | 0.56 | 8.72E-13 |

**Table 2.2.** m$^6$A-seq and RNA-seq results showing histone modifiers have dynamic m$^6$A marked status, accompanied by altered mRNA levels at different oligodendrocyte lineage stages (n=3; Z score>0).

**Table 2.3. Transcripts involved in oligodendrocyte development signaling pathways are significantly altered by *Mettl14* ablation (OPCs). Relate to Figure 2.6.**

| Signaling Pathways | Gene name | $Log_2FC$ | $log_2CPM$ | m$^6$A mark |
|---|---|---|---|---|
| BMP | | | | |
| | *Bmp4* | 3.50 | 1.65 | |
| | *Rgmb* | 1.82 | 4.17 | |
| | *Bambi* | 1.26 | 3.04 | Yes |
| | *Chrdl1* | -1.18 | 5.31 | |
| | *Rgma* | 1.26 | 5.92 | |
| | *Smad7* | 1.02 | 2.10 | |
| ERK/MAPK | | | | |
| | *Egfr* | 1.72 | 4.01 | Yes |
| | *Igf1r* | 1.04 | 6.86 | |
| | *Ptprr* | -1.46 | 1.28 | |
| FGF | | | | |
| | *Camk2a* | -1.91 | 2.78 | Yes |
| | *Fgfr2* | 2.58 | 4.24 | |
| Notch/Delta | | | | |
| | *Cdk6* | 1.11 | 2.44 | |
| | *Cntn6* | 4.00 | 3.00 | Yes |
| | *Dll3* | -2.24 | 5.25 | |
| | *Maml3* | 1.39 | 2.60 | |
| | *Hes5* | -1.25 | 3.49 | |
| | *Mdk* | 2.66 | 2.84 | |
| | *Notch3* | 3.22 | 4.19 | |
| | *Rbm15* | 1.06 | 6.32 | |
| | *Susd5* | 1.78 | 1.16 | |
| | *Tgfbr2* | 2.82 | 2.34 | |
| Shh | | | | |
| | *Gli3* | 2.98 | 1.40 | |
| Wnt | | | | |
| | *Camk2a* | -1.91 | 2.78 | Yes |
| | *Ccnd2* | 1.01 | 6.82 | |
| | *Daam2* | 2.86 | 2.84 | |
| | *Fzd4* | 1.78 | 5.54 | Yes |
| | *Nfatc2* | -1.06 | 2.20 | |
| | *Smad3* | 1.75 | 5.04 | |
| | *Tcf7l1* | 1.62 | 4.61 | |
| | *Wnt5a* | 2.10 | 2.41 | Yes |

**Table 2.3.** m$^6$A-seq and RNA-seq results showing transcripts involved in key oligodendrocyte signaling pathways were significantly altered and m$^6$A marked in OPCs (n=3; $log_2$ |FC|>1, $log_2$ |CPM|>1, q-value<0.001, Z-score>0).

**Table 2.4. Transcripts involved in oligodendrocyte development signaling pathways are significantly altered by *Mettl14* ablation (oligodendrocytes). Relate to Figure 2.6.**

| Signaling Pathways | Gene name | $Log_2FC$ | $log_2CPM$ | $m^6A$ mark |
|---|---|---|---|---|
| P13K/AKT/ mTOR | | | | |
| | *Foxo1* | 1.56 | 5.84 | |
| | *Foxo3* | 1.58 | 7.71 | |
| BMP | | | | |
| | *Bambi* | 1.99 | 3.55 | |
| | *Bmp2* | -2.43 | 1.15 | |
| | *Bmp4* | -1.75 | 3.47 | |
| | *Bmpr2* | 1.44 | 8.14 | |
| | *Chrd* | 1.80 | 2.66 | |
| | *Fst* | 4.27 | 2.24 | Yes |
| | *Rgmb* | 1.16 | 4.46 | |
| | *Smad7* | -2.36 | 5.30 | |
| | *Smad9* | -1.72 | 4.11 | |
| | *Smurf1* | -1.16 | 7.20 | |
| ERK/MAPK | | | | |
| | *Egfr* | 1.08 | 6.27 | |
| | *Igf1r* | 2.02 | 6.05 | |
| | *Mapk3* | -1.40 | 7.13 | Yes |
| | *Myc* | 1.06 | 5.97 | |
| | *Ngfr* | -2.14 | 1.69 | |
| IGF-1 | | | | |
| | *Igf1r* | 2.02 | 6.05 | |
| FGF | | | | |
| | *Fgfr2* | -1.14 | 6.68 | |
| | *Mapk3* | -1.40 | 7.13 | Yes |
| | *Ptpn11* | -1.23 | 8.61 | |
| | *Ssh1* | 1.22 | 5.50 | |
| Notch/Delta | | | | |
| | *Angpt4* | -4.62 | 1.10 | Yes |
| | *Cntn6* | 3.17 | 5.51 | Yes |
| | *Crebbp* | 1.11 | 6.21 | Yes |
| | *Dll3* | -1.69 | 1.62 | |
| | *Dner* | -1.29 | 7.73 | |
| | *Dtx4* | 1.21 | 7.35 | |
| | *Hes5* | -3.22 | 1.22 | |
| | *Kcna5* | 1.72 | 5.73 | Yes |
| | *Maml2* | 1.15 | 6.07 | |
| | *Maml3* | 2.83 | 3.30 | |
| | *Mdk* | 2.49 | 3.75 | |
| | *Myc* | 1.06 | 5.97 | |
| | *Neurl1b* | 1.44 | 2.89 | |
| | *Notch1* | 1.28 | 7.96 | |
| | *Notch2* | 1.98 | 6.37 | Yes |
| | *Notch3* | 2.27 | 5.68 | |
| | *Nrarp* | 1.32 | 4.80 | Yes |
| | *Ptp4a3* | 1.14 | 4.78 | |
| | *Rbm15* | 1.64 | 5.87 | |
| | *Spen* | 1.48 | 7.05 | |
| | *Susd5* | 2.64 | 3.81 | |
| | *Tgfbr2* | 2.19 | 3.83 | Yes |
| | *Tmem100* | 1.18 | 5.26 | |

**Table 2.4 (continued)**

| Signaling Pathways | Gene name | $Log_2FC$ | $log_2CPM$ | $m^6A$ mark |
|---|---|---|---|---|
| Wnt | | | | |
| | *Camk2b* | -1.25 | 3.73 | |
| | *Ccnd1* | 1.02 | 7.46 | |
| | *Ccnd2* | 1.21 | 7.48 | |
| | *Crebbp* | 1.11 | 6.21 | Yes |
| | *Ctbp2* | 1.02 | 5.82 | |
| | *Cxxc4* | 1.89 | 3.82 | |
| | *Daam2* | 1.09 | 9.44 | |
| | *Fzd2* | 1.88 | 4.08 | |
| | *Fzd6* | 1.58 | 3.34 | |
| | *Fzd7* | 2.31 | 4.59 | |
| | *Fzd9* | 1.22 | 4.45 | |
| | *Lrp5* | 1.63 | 4.77 | Yes |
| | *Lrp6* | 1.21 | 7.56 | |
| | *Myc* | 1.06 | 5.97 | |
| | *Plcb4* | 1.22 | 4.25 | |
| | *Ppp2r5a* | -1.03 | 6.81 | |
| | *Ppp2r5b* | -1.23 | 6.51 | |
| | *Prickle1* | -2.99 | 7.00 | |
| | *Prkcb* | -1.20 | 5.03 | |
| | *Prkcg* | 2.07 | 3.95 | |
| | *Sfrp1* | 1.26 | 6.34 | |
| | *Sfrp5* | 3.12 | 5.29 | |
| | *Tcf7l2* | -1.01 | 5.40 | |
| | *Vangl2* | 1.17 | 7.30 | |
| | *Wnt3* | -3.66 | 3.13 | Yes |
| | *Wnt7a* | -1.05 | 5.31 | Yes |

**Table 2.4.** $m^6A$-seq and RNA-seq results showing transcripts involved in key signaling oligodendrocyte pathways were significantly altered and $m^6A$ marked in oligodendrocytes (n=3; $log_2$ |FC|>1, $log_2$ |CPM|>1, q-value<0.001, Z-score>0).

**Table 2.5. mRNA and protein levels comparison of selected key factors in oligodendrocytes development. Relate to Figure 2.6.**

| Gene name | mRNA (Mutant/control) | Protein (Mutant/control) |
|---|---|---|
| *Myrf* | 13% | 26% |
| *Olig2* | 63% | 83% |
| *Mbp* | 8% | 2% |
| *Mag* | 9% | 13% |

**Table 2.5.** RNA-seq and western blot results showing mRNA levels correlated with the protein levels of selected key factors that are critical for oligodendrocyte development (n=3).

### 2.3.7 *Mettl14*'s possible mechanism of actions in oligodendrocyte lineage cells

We also wished to explore potential mechanism(s) of action of the m$^6$A mark in regulating oligodendrocyte lineage cell development and function in addition to the disruption of the cells' transcriptomes discussed above. Previous studies have shown m$^6$A's role in increasing the translational efficiency of the marked transcripts in various systems (Coots et al., 2017; Shi et al., 2017; Wang et al., 2015; Zhou et al., 2018). In order to investigate this potential mechanism, we compared transcriptional and translational levels of a subset of the m$^6$A marked transcripts that encode proteins critical for oligodendrocyte development (Bujalka et al., 2013; Zhou and Anderson, 2002). We found significantly decreased levels of these proteins both *in vivo* (Fig.2.3 H,I,J) and *in vitro* (Fig.2.4 F,G; Fig.S2.8 A,B), however, the observed reductions correlated with the levels of mRNA reduction found in the oligodendrocyte transcriptome (Table 2.5), suggesting that translational regulation may not be a key feature of m$^6$A gene regulation in oligodendrocyte lineage cells. Nevertheless, a more comprehensive proteomics assessment will be required to determine the global impact of the m$^6$A mark on translational efficiency in oligodendrocytes.

MBP, a predominant and critical protein of myelin, is translated locally in the myelin compartment (Colman et al., 1982), which requires the active transport of its mRNA into oligodendrocyte processes (Carson et al., 1997). This transport requires the RNA binding protein heterogeneous nuclear ribonucleoprotein (hnRNP) A2 (Hoek et al., 1998; Müller et al., 2013). Importantly, it was recently discovered that hnRNPA2B1, an isoform of hnRNPA2 that is expressed in oligodendrocyte lineage cells (Han et al., 2010), is an $m^6A$ reader (Alarcón et al., 2015), suggesting that the $m^6A$ mark might have a role in regulating *Mbp* mRNA transport in oligodendrocytes. In order to investigate this possibility, we used the RNAscope approach to determine the distribution of *Mbp* and *Myrf* mRNA in oligodendrocytes of the corpus callosum. In controls, *Myrf* mRNA is localized in the oligodendrocyte cell bodies; whereas, *Mbp* mRNA distributes to the complex, web-like oligodendrocyte processes (Fig.S2.3 A). In P18 *Mettl14$^{fl/fl}$;Olig2*-Cre mutant oligodendrocytes, *Myrf* and *Mbp* mRNA levels are clearly reduced (Fig.S2.3 B), as expected, but the distribution of these transcripts does not appear altered, suggesting that the absence of the $m^6A$ mark has not disrupted the transport of the *Mbp* mRNA into the myelin compartment. In addition to MBP mRNA, a number of key oligodendrocyte transcripts has been shown to be localized in the myelin sheath (Thakurela et al., 2016). A more extensive analysis of the myelin mRNA content of the *Mettl14* mutants will help determine the role of the $m^6A$ mark in the establishment of myelin transcriptome.

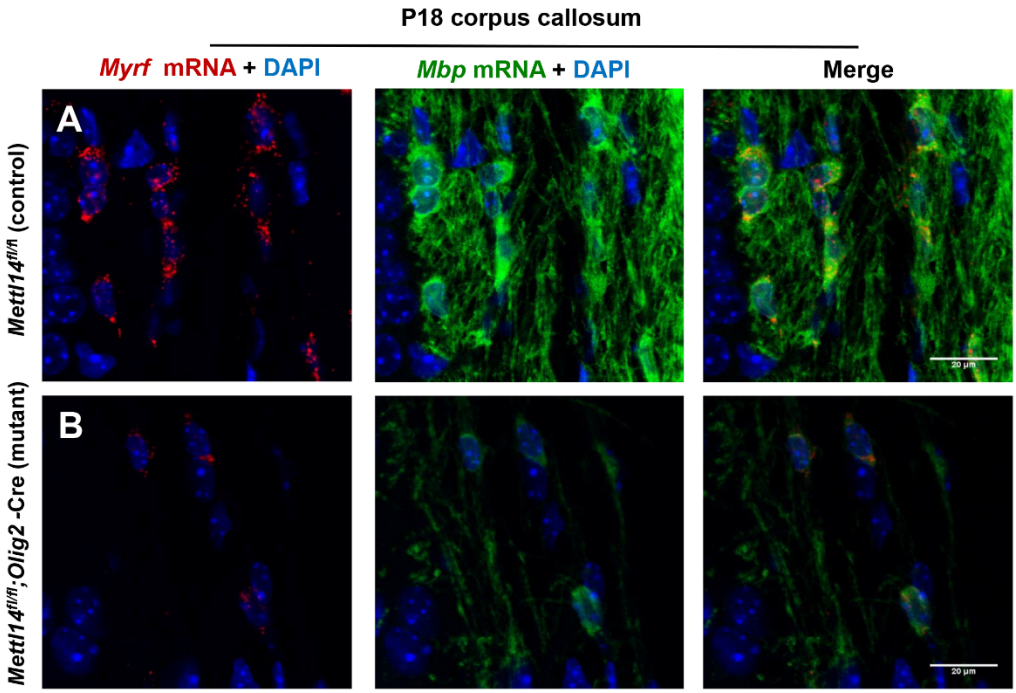


**Figure S2.3. *Mettl14* deletion does not inhibit *Mbp* mRNA transport to oligodendrocyte processes. Relate to Figure 2.7.**

**(A-B)** Representative RNAscope result demonstrating reduced *Myrf* (red) and *Mbp* (green) mRNA levels in *Mettl14$^{fl/fl}$;Olig2-Cre* P18 mutants compared to controls. (n=3, scale bar=20µm). *Myrf* mRNA localization is strictly perinuclear, whereas *Mbp* mRNA also extends into the processes.

Functional variant isoforms of myelin proteins are generated by alternative splicing to ensure precise oligodendrocyte lineage progression (Montague et al., 2006; Zhang et al., 2014; Zhao et al., 2010a). Previous studies have shown that m$^6$A plays a critical role in regulating mRNA splicing in various cellular systems (Haussmann et al., 2016; Xiao et al., 2016b; Zhao et al., 2014b; Zhou et al., 2019). In order to investigate the potential role of the m$^6$A mark in regulating differential splicing during oligodendrocyte development, we used LeafCutter (Li et al., 2018c) to identify altered splicing events in OPC and oligodendrocyte transcriptomes. LeafCutter identifies alternatively excised intron clusters and compares differentially excised intron levels between controls and mutants. Differential splicing is measured by changes in the percent spliced in (change,

or delta, dPSI) (Li et al., 2018c). Global comparison of alternative splicing events revealed numerous statistically significant changes in *Mettl14* ablated mutants versus controls (Stouffer's Z-score = 40.86 in OPCs and 105.76 in oligodendrocytes). In addition, we found that 1,372 splicing events in 364 genes in OPCs, and 1,930 splicing events in 485 genes in oligodendrocytes were differentially spliced upon *Mettl14* deletion ($q<0.01$). A number of significant differentially alternative spliced transcripts were previously shown to encode proteins with important functions in the myelinating process, such as protein tyrosine phosphate receptor type Z1(*Ptprz*) in OPCs (Harroch et al., 2002) and neurofascin (*Nfasc*) in oligodendrocytes (Table.2.6,2.7). Interestingly, the neurofascin protein (NF), which is essential in the establishment and maintenance of node of Ranvier domains (Howell et al., 2006; Pillai et al., 2009; Sherman et al., 2005; Thaxton et al., 2010; Zonta et al., 2008), has the most significantly altered isoforms and bears the highest differential dPSI level in the oligodendrocyte transcriptome (Fig.2.7 A, Table.2.7).

**Table 2.6. Top 10 dPSI aberrantly spliced transcripts (OPCs). Relate to Figure 2.7.**

| Gene | Intron | Log (Effect Size) | Control PSI | Mutant PSI | dPSI | q-value |
|---|---|---|---|---|---|---|
| *Hexdc* | chr11:121206774:121207639:clu_4231_+ | 1.48 | 0.13 | 0.74 | 0.61 | 6.14E-03 |
| *Ptprz1* | chr6:23000199:23007274:clu_3707_+ | 1.27 | 0.25 | 0.81 | 0.56 | 3.56E-04 |
| *Gm44503,Ccpg1* | chr9:73012992:73015332:clu_4610_+ | 1.29 | 0.28 | 0.84 | 0.56 | 5.25E-03 |
| *Mettl14* | chr3:123371485:123376145:clu_1176_- | 7.97 | 0.00 | 0.53 | 0.53 | 1.81E-06 |
| *Heca* | chr10:17908188:17915725:clu_7550_- | 2.49 | 0.01 | 0.51 | 0.50 | 5.94E-03 |
| *D11Wsu47e* | chr11:113684711:113687774:clu_4193_+ | 1.10 | 0.15 | 0.62 | 0.47 | 1.14E-03 |
| *NA* | chr8:69375432:69395441:clu_1976_- | 1.18 | 0.48 | 0.91 | 0.43 | 2.87E-02 |
| *Rfesd* | chr13:76008286:76017521:clu_7817_- | 0.97 | 0.42 | 0.83 | 0.42 | 9.94E-02 |
| *Dixdc1* | chr9:50695583:50701920:clu_2217_- | 0.92 | 0.41 | 0.81 | 0.41 | 7.23E-02 |
| *Ppcdc* | chr9:57415254:57420163:clu_2228_- | 0.86 | 0.31 | 0.72 | 0.40 | 1.76E-02 |

**Table 2.6.** LeafCutter analysis showing aberrantly spliced transcripts in *Mettl14$^{fl/fl}$;Olig2*-Cre mutant OPCs. Listed are the top 10 transcripts that have the highest dPSI values, with their chromosome intron locations and $Log_2$ effect sizes. (dPSI: changes/or delta in the percent spliced in; n=3)

**Table 2.7. Top 10 dPSI aberrantly spliced transcripts (oligodendrocytes). Relate to Figure 2.7.**

| Gene | Intron | Log (Effect Size) | Control PSI | Mutant PSI | dPSI | q-value |
|---|---|---|---|---|---|---|
| *Mettl14* | chr3:123371485:123376145:clu_874_- | 15.62 | 0.00 | 0.93 | 0.93 | 7.45E-08 |
| *Fhl3* | chr4:124700851:124705613:clu_2216_+ | 2.35 | 0.05 | 0.85 | 0.80 | 1.59E-03 |
| *Wdr91* | chr6:34892534:34893842:clu_6172_- | 1.45 | 0.07 | 0.57 | 0.50 | 5.71E-05 |
| *Pms2* | chr5:143925501:143928099:clu_4550_+ | 1.08 | 0.22 | 0.70 | 0.49 | 1.94E-04 |
| *Sh3bp2* | chr5:34549796:34551561:clu_4359_+ | 1.34 | 0.08 | 0.55 | 0.47 | 5.61E-04 |
| *Atp9a* | chr2:168710976:168741682:clu_7631_- | 1.49 | 0.41 | 0.86 | 0.46 | 9.58E-06 |
| *Nfasc* | chr1:132576417:132595484:clu_5208_- | 1.34 | 0.33 | 0.79 | 0.45 | 1.92E-07 |
| *Aasdh* | chr5:76884201:76884312:clu_7746_- | 1.02 | 0.17 | 0.61 | 0.44 | 2.33E-03 |
| *Lpgat1* | chr1:191718205:191719354:clu_2621_+ | 0.97 | 0.20 | 0.63 | 0.43 | 5.69E-03 |
| *Mapk8ip1* | chr2:92391141:92392157:clu_7491_- | 0.91 | 0.27 | 0.70 | 0.43 | 1.13E-05 |

**Table 2.7.** LeafCutter analysis showing aberrantly spliced transcripts in *Mettl14*$^{fl/fl}$*;Olig2*-Cre mutant oligodendrocytes. Listed are the top 10 transcripts that have the highest dPSI values, with their chromosome intron locations and Log2 effect sizes. (n=3)

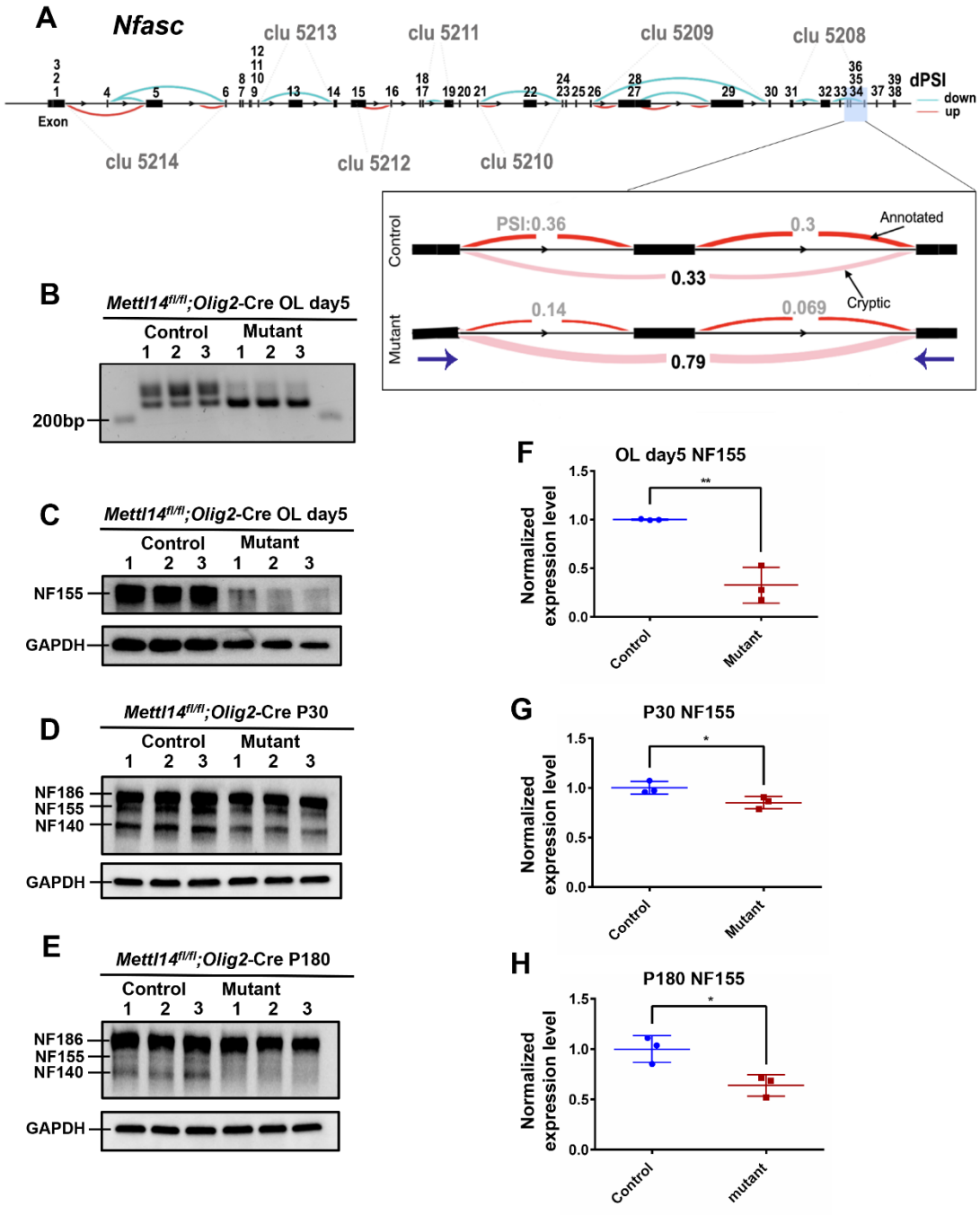


**Figure 2.7. *Mettl14* deletion differentially alters *Nfasc155* alternative splicing and expression.**

**(A)** Schematic view of differentially spliced sites in the *Nfasc* gene in control versus *Mettl14*$^{fl/fl}$*;Olig2*-Cre mutant day5 oligodendrocytes. The 39 *Nfasc* exons are labeled above the exons. Each cluster (i.e. abbreviated as "clu X") represents a group of introns that display alternative excision events. Specifically, these are introns that share a donor site (canonical 5'

splice site, AT) or acceptor site (canonical 3' splice site, GA). Blue curves represent cases that have fewer splicing events in the mutants, while the red represent cases with more splicing events in the mutants ($p<0.05$). The magnified window shows the sample cluster (clu 5208) that we examined for the presence of aberrant spliced isoforms in the mutants in panel B. Purple arrows represent the start points for reverse and forward primers that we used for RT-PCR in (B). **(B)** Differentially spliced *Nfasc* isoform were detected by RT-PCR and agarose gel electrophoresis in the *Mettl14$^{fl/fl}$;Olig2*-Cre day5 oligodendrocyte mutants (218kb). (Primers used: Forward: ACTGGGAAAGCAGATGGTGG Reverse: ACATGAGCCCGATGAACCAG). **(C-E)** Western blot results of NFASC *in vitro* (C) and *in vivo* (D:P30, E:P180). **(F-H)** Quantification of NF155 expression *in vitro* (F) and *in vivo* (G:P30, H:P180). NF155 expression level was normalized to GAPDH expression level. NF155 had significant reduction in both P30 and P180 *Mettl14$^{fl/fl}$;Olig2-Cre* mutants. Values represent mean ± SEM (n=3; $^{*}p<0.05$; $^{**}p<0.01$; unpaired Student's t test). **See also Figure S2.3, Table 2.6-2.7.**

To further investigate the role of m$^6$A mRNA methylation in regulating the distribution of NF isoforms during development, we used RT-PCR to confirm the differential distribution of distinct splicing products (Fig.2.7 B) in purified oligodendrocyte mRNA from mutants and controls. This analysis confirmed the presence of the predicted altered spliced *Nfasc* mRNA product in the mutant oligodendrocytes. Since NF155 is the glial NF isoform that is required for the assembly of paranodal domains (Sherman et al., 2005), we examined NF155 expression levels in different developmental stages *in vitro* and *in vivo*. *Mettl14$^{fl/fl}$;Olig2*-Cre mutant oligodendrocytes that had been cultured in differentiation media for 5 days had a significant reduction of NF155 expression compared to controls (Fig.2.7 C,F). *In vivo*, 1-month old animals (P30) showed significantly decreased NF155 levels in the *Mettl14$^{fl/fl}$;Olig2*-Cre mutants (Fig.2.7 D,G). To further analyze nodal and paranodal domains with immunohistochemistry we used antibodies to the voltage gated sodium channel (NaCh) and Caspr to identify the nodal and paranodal domains, respectively (Fig.2.8 A,B). We found a significant reduction in the number of nodes at P30 in the mutants compared to controls (Fig.2.8 E). We also used pan-NF antibody to characterize NF localization and morphology in both nodal and paranodal domains (Fig.2.8 A,B). We found no difference in node and paranodal size in the mutants as compared to controls (Fig.2.8 F).

We further investigated whether NF155 expression abnormalities persist to adulthood (P180) in *Mettl14*$^{fl/fl}$*;Olig2*-Cre mutants. Western blot results revealed significantly reduced expression levels of NF155 in P180 mutants (Fig.2.7 E,H). Next, we measured nodal and paranodal domains via immunohistochemistry in these animals (Fig.2.8 C,D). We found significant reduction of node numbers in the mutants (Fig.2.8 G). In addition, both nodal and paranodal domains showed significantly increased sizes in the mutants (Fig.2.8 H), suggesting widespread pathological changes at the node of Ranvier in adult *Mettl14*$^{fl/fl}$*;Olig2*-Cre mutants.

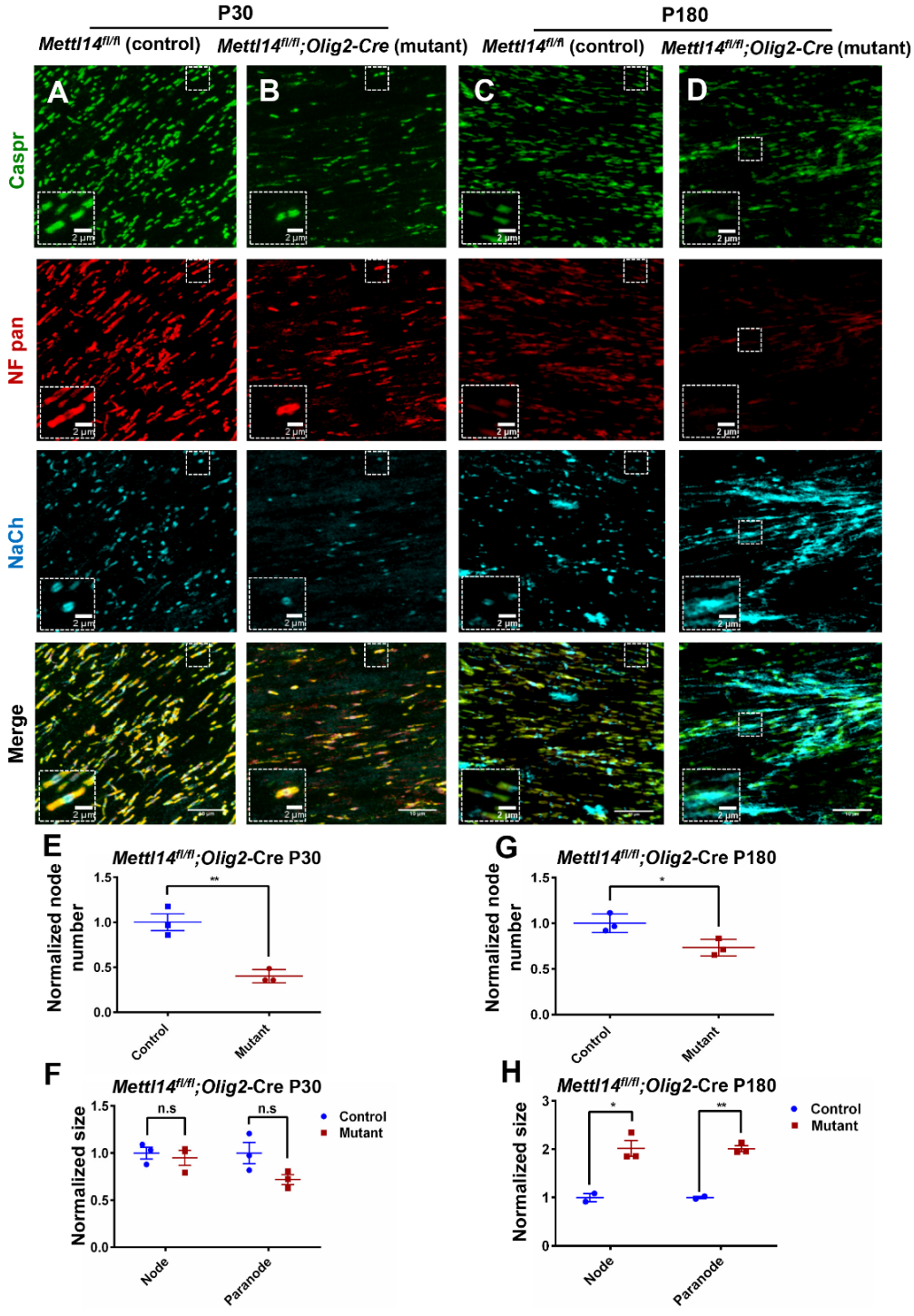


**Figure 2.8. *Mettl14* deletion results in aberrant node and paranode morphology.**

**(A-B)** Representative immunostaining with Caspr, Nfasc and NaCh in P30 *Mettl14$^{fl/fl}$;Olig2*-Cre control and mutant corpus callosum. Representative node(s) of Ranvier are shown in magnified windows. (Scale bar=10μm, 2μm). **(C-D)** Representative immunostaining with Caspr, Nfasc and NaCh in P180 *Mettl14$^{fl/fl}$;Olig2*-Cre control and mutant corpus callosum. Representative node(s)

of Ranvier are are shown in magnified windows. (Scale bar=10μm, 2μm). **(E, G)** Quantification of node number (NaCh positive) in P30(E) and P180(G) *Mettl14$^{fl/fl}$;Olig2*-Cre control and mutant corpus callosum. Normalized number = mutant count / control count (=1) (n=3; $^{*}p<0.05$; $^{**}p<0.01$, unpaired Student's t-test). **(F, H)** Quantification of node (Caspr, NaCh positive) and paranode (Nfasc, Caspr double positive) size in P30 (F) and P180 (H) *Mettl14$^{fl/fl}$;Olig2*-Cre control and mutant corpus callosum. Normalized size = mutant size / control size (=1) (control n=2 mutant n=3; $^{*}p<0.05$; $^{**}p<0.01$, unpaired Student's t-test).

## 2.4 Discussion

RNA modifications have recently emerged as critical post-transcriptional regulatory mechanism to modulate gene expression (Frye et al., 2018). Among all post-transcriptional mRNA modifications, m$^6$A is the most abundant internal alteration found in eukaryotic mRNA (Yue et al., 2015). In contrast to DNA and protein methylation, m$^6$A methylation has the potential to have a very rapid influence on transcriptome changes during cell state transitions (Frye et al., 2018; Zhao and He, 2017).

In this report we show that oligodendrocyte lineage progression is accompanied by changes in m$^6$A modification on numerous transcripts. We also show that *Mettl14*, which encodes an essential m$^6$A writer component, is critical in regulating oligodendrocyte development and CNS myelination. We demonstrate altered oligodendrocyte numbers and hypomyelination in both oligodendrocyte lineage cell specific *Mettl14* ablated mice. Nevertheless, OPC numbers were not altered by *Mettl14* ablation. We also show that *Mettl14* ablated OPCs lacked the ability to differentiate into mature MBP-positive myelin-forming oligodendrocytes in vitro. These results indicate that the m$^6$A RNA modification is essential for post-mitotic oligodendrocyte differentiation.

Interestingly, our data revealed a more severe developmental phenotype *in vitro* than *in vivo*, suggesting communication with other CNS cell types may mitigate the effects of the *Mettl14*

deletion *in vivo*. In addition, it is curious that when we cultured *Mettl14*$^{fl/fl}$*;CNP*-Cre OPCs (data not shown), in which the *Mettl14* gene is inactivated later in the oligodendrocyte lineage, the mutant cells had the capacity to differentiate into MBP-positive, mature oligodendrocytes as efficiently as control cells, suggesting that the severe block in maturation that occurs in the *Mettl14*$^{fl/fl}$*;Olig2*-Cre OPCs *in vitro* is the result of an m$^6$A deficiency early in the oligodendrocyte lineage. This is supported by the failure of enforced METTL14 expression in the *Mettl14*$^{fl/fl}$*;Olig2*-Cre OPCs to fully rescue the severe *in vitro* differentiation phenotype (Fig. S2.4). Our future efforts will be devoted to elucidating the effects of the m$^6$A mark at distinct stages of the oligodendrocyte lineage.

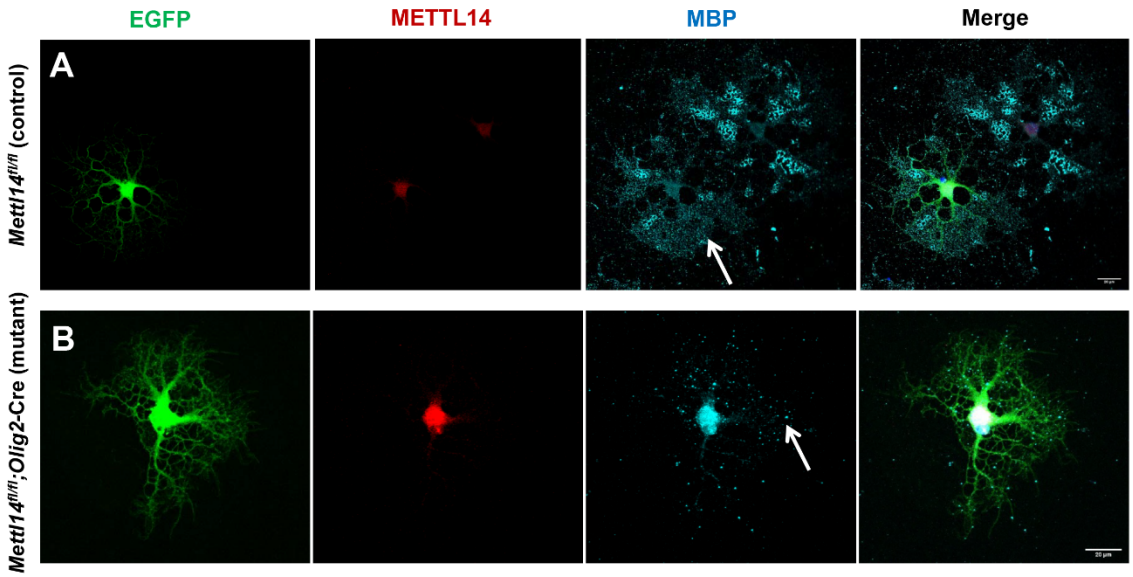


**Figure S2.4. METTL14 partially rescues *Mettl14*$^{fl/fl}$*;Olig2*-Cre oligodendrocytes. Relate to Figure 2.4.**

**(A)** Representative METTL14 (red), MBP (cyan) immunostaining of day 5 *Mettl14*$^{fl/fl}$ oligodendrocytes after electroporation with *Mettl14 and EGFP* plasmids. White arrow shows control oligodendrocytes normally express MBP after electroporation. (n=3, scale bar=20μm). **(B)** Representative METTL14 (red), MBP (cyan) immunostaining of *Mettl14*$^{fl/fl}$*;Olig2*-Cre oligodendrocytes showing partially restored (white arrow) MBP expression with METTL14 expression. (n=3, scale bar=20μm).

Oligodendrocyte differentiation involves many steps that must be regulated in time and space (Zuchero and Barres, 2013). Our RNA-seq and m$^6$A-seq data revealed changes of the m$^6$A marked status on numerous transcripts that encode critical transcription factors in OPCs and oligodendrocytes, suggesting that m$^6$A mRNA modification contributes to transcriptional changes during oligodendrocyte development. Indeed, emerging studies have shown that the turnover and/or translation of transcripts during cell-state transitions regulated by the m$^6$A mark represent an important developmental mechanism (Frye et al., 2018).

The functional role of various histone modifiers in oligodendrocyte differentiation is stage-dependent, yet the underlying regulatory role of these factors is unknown (Copray et al., 2009; Hernandez and Casaccia, 2015). Our study revealed that transcripts that encode a number of histone modifiers are dynamically marked by m$^6$A in OPCs and oligodendrocytes (Table 2.2), suggesting that m$^6$A RNA modifications may play a role in regulating the expression of epigenetic modifiers at distinct oligodendrocyte lineage stages. Consistent with this possibility, a recent study revealed cross-talk between m$^6$A RNA modification and histone modification (Wang et al., 2018).

In addition, we also found numerous oligodendrocyte lineage signaling pathway transcripts that are dynamically marked by m$^6$A and expressed at significantly altered levels in the absence of METTL14. The alternation of m$^6$A marked transcripts is accompanied by significant alterations of other important pathway transcripts that do not bear an m$^6$A mark, suggesting that m$^6$A RNA modification may have a primary or secondary effect on gene expression. Together, our RNA-seq and m$^6$A-seq results indicate that m$^6$A RNA modifications modulate the expression of multiple transcriptional regulators, DNA epigenetic modifiers and signaling pathways to facilitate oligodendrocyte lineage progression.

In addition to the effect on mRNA levels discussed above, we examined several additional potential functions of the m$^6$A mark on gene expression in oligodendrocyte lineage cells. We explored whether the m$^6$A mark affects translational efficiency of important myelin genes and their regulators, since it had previously been shown that translational efficiently of marked transcripts is increased (Shi et al., 2017; Wang et al., 2015). Surprisingly, we did not detect dramatic alternations of protein levels when compared with mRNA levels of m$^6$A marked transcripts. The m$^6$A mark has also been shown to play a role in intracellular mRNA transport (Roundtree et al., 2017). Therefore, we examined the transport of *Mbp* mRNA into oligodendrocyte processes, which has been shown to be critical for CNS myelination. Nevertheless, using RNAscope we were unable to detect a significant decrease in the efficiency with which the *Mbp* mRNA is transported into the myelin domain in the *Mettl14* mutant animals. Although these initial efforts did not reveal a role for the m$^6$A mark in mRNA translation or sub-cellular transport, more thorough analyses may uncover alterations in these processes in the *Mettl14* mutant oligodendrocytes.

We did, however, detect widespread changes in the *Mettl14* mutant oligodendrocyte lineage cells that were related to aberrant RNA splicing. In fact, 283 out of 364 (~78%) aberrantly spliced OPC transcripts, and 311 out of 485 (~64%) aberrantly spliced oligodendrocyte transcripts are marked by m$^6$A. Many of these altered transcripts have been described as crucial for oligodendrocyte lineage development and function, such as *Ptprz1*, *Gsn* (Brown and Verden, 2017) and *Map2* (Müller et al., 1997). Importantly, we discovered the transcript encoding NF, a critical cell adhesion protein involved in node of Ranvier establishment and maintenance, was differentially spliced under the regulation of m$^6$A. The mouse *Nfasc* gene contains 39 exons, and the inclusion or exclusion of different *Nfasc* exons results in transcripts that encode functionally distinct

isoforms (Suzuki et al., 2017). NF186 is expressed by neurons and is critical for node assembly, and NF155, which is expressed by the myelinating cells, is critical to the stability of the paranodal domain (Howell et al., 2006; Kawamura et al., 2013; Kira et al., 2018; Pomicter et al., 2010). The disruption of NF isoform distribution results in pathological changes in myelinated axons (Howell et al., 2006; Pillai et al., 2009; Thaxton et al., 2010). We identified aberrantly spliced *Nfasc* RNA isoforms in the *Mettl14* deleted oligodendrocytes, and provided *in vivo* evidence of altered NF155 protein expression that correlated with morphological abnormalities of the paranodal domain. In particularly, the CNS nodes of Ranvier of adult *Mettl14*$^{fl/fl}$*;Olig2*-Cre mutants displayed widespread abnormalities, strikingly reminiscent of NF155-deficient mice (Pillai et al., 2009). These results indicate m$^6$A RNA methylation regulates *Nfasc155* splicing, and plays a role in establishing and maintaining normal function of critical axonal-oligodendrocyte interactions. Interestingly, changes in NF155 expression have recently been suggested to be central to adult myelin remodeling associated with altered impulse transmission (Fields and Dutta, 2019). This raises an intriguing possibility that the m$^6$A epigenetic mark plays a critical role in activity-dependent myelin remodeling.

A recent study reported that the proline rich coiled-coil 2 A (Prrc2a) protein is an m$^6$A reader that participates in oligodendrocyte specification and myelination by regulating the stability of its critical downstream target *Olig2* (Wu et al., 2019). Nevertheless, the clinical and pathological phenotypes of the oligodendrocyte-specific mouse mutants of *Prrc2a* are considerably more severe than that observed for the *Mett14* writer mutants described here, and the alteration in *Olig2* expression is also much more significant in the *Prrc2a* mutants. This raises the possibility that Prrc2a participates in other functions in addition to its putative role as an m$^6$A reader in oligodendrocyte lineage cells.

In conclusion, our study demonstrates that m$^6$A RNA modification is essential for normal oligodendrocyte maturation and CNS myelination. We show that the m$^6$A mark plays an important role in regulating various aspects of gene expression in oligodendrocyte lineage cells, with the most profound effects on mRNA levels and splicing. Rapid alterations to the m$^6$A landscape have the potential to quickly modify a cell's phenotypic properties (Geula et al., 2015; Licht and Jantsch, 2016; Yoon et al., 2017) . Therefore, in addition to its critical role during development, the m$^6$A mark may participate in oligodendrocyte plasticity in adults. Future characterization of m$^6$A RNA epigenetic regulation should provide important insight to our growing understanding of the myelination process and demyelinating diseases.

## 2.5 Materials and methods

### 2.5.1 Animals

All animals were housed under pathogen-free conditions, and all animal procedures and animal care were conducted in accordance with guidelines approved by the University of Chicago's Institutional Animal Care and Use Community (IACUC). All mice were on the C57BL/6 background, and both female and male mice were used.

*Mettl14*$^{fl/fl}$ mice (Koranda et al., 2018; Weng et al., 2018b; Yoon et al., 2017) were crossed with *Olig2*-Cre mice (Schüller et al., 2008), and *CNP*-Cre mice (Lappe-Siefke et al., 2003). *Mettl14*$^{fl/fl}$*;Olig2*-Cre and littermate control *Mettl14*$^{fl/fl}$ mice as well as *Mettl14*$^{fl/fl}$*;CNP*-Cre and littermate control *Mettl14*$^{fl/fl}$ mice were used for experiments.

### 2.5.2 OPC isolation and culture

OPCs were isolated and purified (95% purity) from postnatal day 6 (P6) mouse brains using an immunopanning protocol (Emery and Dugas, 2013). In brief, mice pups (both female and male) were genotyped and marked at P4-P5. At P6, pups were deeply anaesthetized on ice and cortices were collected, diced and digested with papain at 37$^{o}$ C. Cells were then triturated into a single cell suspension, then sequentially immunopanned in Ran-2, GalC, and O4 antibodies from hybridomal supernatant. The remaining $O4^{+}GalC^{-}$ cells (OPCs) were then trypsinized and plated in poly-d-Lysine (PDL)-coated plates with proliferation media. Once OPCs numbers reach sufficient amount, they were split and plated in differentiation media.

### 2.5.3 OPC electroporation

Amaxa cell nucleofector II device and an electroporation kit for primary mammalian glial cells (Lonza, Cat# VPI-1006) were used as per the manufacturer's instructions for OPC electroporation. For each biological replicate, 5 million OPCs were collected and transfected with both pmaxGFP Vector (Lonza, Cat# VPI-1006) and *Mettl14* plasmid (Origene, Cat# MR207291) or pmaxGFP Vector alone. Transfected OPCs were then plated in PDL coated plates with differentiation media. Transfection efficiency was about 40%, measured by GFP positive cell number versus total cell number after 72 hours of electroporation.

### 2.5.4 Immunohistochemistry and cell counts

Mice were deeply anaesthetized with 2.5% avertin (Cat#T48402, Sigma Aldrich) in dH2O. Upon the loss of nociceptive reflexes, mice were transcardially perfused with 0.9% saline followed by ice-cold 4% paraformaldehyde (PFA). Brains were collected and post-fixed overnight in 4% PFA at 4$^{o}$C, followed by incubation in 30% sucrose until saturation. Tissues were then embedded in

optimal cutting temperature compound (OCT) and sectioned at 10µm. Prior to Rabbit-anti-METTL14 (1:300, Sigma, Cat# HPA038002), Goat-anti-PDGFR-α (1:100, R and D systems, Cat# AF1062), Rabbit-anti-Ki67 (1:100, Abcam, cat# ab15580) ,Chicken-anti-Neurofascin (1:50, R and D systems, Cat# AF3235) , Mouse-anti-sodium channel (1:100, Sigma, Cat# S8809) and Rabbit-anti-Caspr (1:300, Abcam, Cat# ab34151) immunostaining, tissue sections were processed with an antibody retrieval protocol in which sections were treated with 10 mM trisodium citrate buffer (pH 6.0) at 90 $^{o}$C for 30 minutes. After cooling at room temperature (RT) for 30 minutes, sections were then incubated in 10 mM glycine (in TBS with 0.25% Triton X-100) for 1hour at RT. Slices were then blocked with TBS containing 5% normal donkey serum, 1% BSA and 0.25% Triton X-100 (blocking buffer) for 2 hours at RT, followed by incubation in primary antibody(s) diluted in blocking buffer for 48 hours at 4$^{o}$C. Immunohistochemistry with Rabbit-anti-MBP (1:500, Abcam, Cat# ab40390), Mouse-anti-CC1 (1:50, Milipore, Cat# OP80), Mouse-anti-Olig2 (1:100, Milipore, Cat# MABN50) and Rabbit-anti-ChAT (1:300, Milipore, Cat# AB144P) antibodies, were followed by immunostaining protocol without antigen retrieval.

Stained tissue sections were imaged with a Mariana Yokogawa-type spinning disk confocal microscope or Leica TCS SP5 two-photon confocal microscope. All experimental and littermate control tissues were imaged with the same parameters, followed with the same adjustments in Image J (NIH). Cells counts data was converted to cells/100µm$^2$.

### 2.5.5 Immunocytochemistry

Cells cultured on cover slips were rinsed with PBS and fixed with ice cold 4% PFA for 10 minutes at RT, washed with PBS, then air dried and stored at -80$^{o}$C until immunostaining. The primary antibodies used were Rabbit-anti-MBP (1:500, Abcam, Cat# ab40390), Goat-anti-PDGFR-α

(1:100, R and D systems, Cat# AF1062) and Mouse-anti-O1 (1:100, R and D systems, Cat# MAB1327). Immunocytochemistry was conducted using the normal immunostaining protocol as described above, without the antigen retrieval process.

### 2.5.6 RNA scope

Mouse *Myrf* mRNA probe (ACDbio, Cat# 524061), mouse *Mbp* mRNA probe (ACDbio, Cat# 451491) and RNAscope Multiplex Fluorescent Reagent Kit V2 assay (ACDbio, Cat# 323110) were purchased from ACDbio company. Fluorophores were purchased from Akoya biosciences (Opal 520: Cat# FP1487001KT, Opal 620: Cat# FP1495001KT). Mice were processed for RNAscope as follows. Deeply anesthetized animals were transcardially perfused with 0.9% saline followed by ice-cold 4% PFA as described above. Brains were immediately dissected out and transferred to 10% NB formalin solution (Sigma, Cat# HT5011) at RT for exactly 24 hours. Brains were then transferred to freshly made 70% ethanol for 24 hours at RT and processed for paraffin embedding. Sections were cut at 5 □m. RNAscope assay was performed as per manufacturer's specifications.

### 2.5.7 Electron Microscopy (EM) and analysis

Mice were deeply anesthetized with 2.5% avertin, followed by perfusion with 0.9% saline and 0.1M sodium cacodylate buffer containing 4% PFA and 2.5% glutaraldehyde (EM buffer). Corpus callosum and optic nerve were then post-fixed overnight at 4$^{o}$C. Tissues were dissected and washed with 0.1M sodium cacodylate buffer for 3 times, followed by post fixation with 1% osmium tetroxide (diluted with 0.1M sodium cacodylate) for 2 hours and another 3 times of wash with 0.1M sodium cacodylate buffer. These tissue samples then went through dehydration steps with

30%, 50%, 70%, 90%, 95%,100% ethanol and propylene oxide (PO), followed by permeation with 1:1 PO/Epon 812 and 1:2 PO/Epon 812 for 2 hours each, and in Epon 812 overnight at RT. The next morning, samples were permeated with Epon 812 for another 4 hours at RT, and then embedded with labeled paper strips in fresh Epon 812. These samples were then cured for 48 hours in a 60$^{o}$C oven. After EM processing steps, samples were sectioned (1μm) and stained with toluidine blue, before sectioned into ultrathin slices (60-90nm) and stained with uranyl acetate-lead citrate. FEI Tecnai F30 scanning transmission electron microscope (FEI company) was used to take EM images. Image J was used to analyze the EM images for g-ratio and axon counting.

### 2.5.8 Total protein isolation

Cells in culture were rinsed with sterile PBS 2 times, then lysed with ice-cold RIPA buffer containing protease inhibitors (Thermo Fisher Scientific, Cat# 78430) and phosphatase inhibitors (Sigma, Cat# P2850 and P5726) (lysis buffer), and then scraped and collected in microcentrifuge tubes for 10 min incubation on ice. Cell lysates were then centrifuged at 13,000 g for 15 min at 4°C, and supernatant was collected and stored in -80$^{o}$C until measurement. To collect brain tissues, mice were deeply anesthetized with 2.5% avertin and perfused with ice-cold sterile PBS, followed by brain isolation into microcentrifuge tubes and immediately frozen in liquid nitrogen. Brain samples were then stored in -80$^{o}$C until homogenization. Brain tissue protein lysates were prepared as follows: homogenized in lysis buffer, incubated on ice for 15 min and centrifuged at 13,000g for 15 min at 4°C, then collect supernatants. Protein concentration was determined by using a BCA Protein Assay Kit (Thermo Fisher Scientific, Cat# 23255) as per the manufacturer's instructions.

### 2.5.9 Western blot

Protein lysates were boiled for 5 min in Laemmli sample buffer (Bio-Rad, Cat# 161-0737) with β-mercaptoethanol (Sigma, Cat# M6250), seperated by SDS-PAGE, transferred to nitrocellulose membrane and immunoblotted. The primary antibodies used were Rabbit-anti-METTL14 (1:1000, Sigma, Cat# HPA038002); Rabbit-anti-MBP (1:1000, Abcam, Cat# ab40390), Rabbit-anti-MAG (1:1000, Thermo Fisher Scientific, Cat# AB_2533179), Mouse-anti-Olig2 (1:1000, Millipore, Cat# MABN50), Mouse-anti-MYRF (1:5000, gift from Dr. Ben Emery), GAPDH (1:2000, Cell signaling, Cat# 2118S). Western blot bands were analyzed in Image Lab software (Bio-Rad laboratories).

### 2.5.10 RNA isolation

Cell and tissue RNA samples were prepared and isolated following the manufacture's protocol (Bio-Rad, Cat# 732-6820). RNA quality was confirmed by 2100 Bioanalyzer using a model 6000 Nano kit (Agilent technologies, Cat# 5067-1511). Samples with RNA integrity number >8 were used.

### 2.5.11 RNA-seq and analysis

Bulk RNA-seq was performed on RNA isolated from cultured OPCs and oligodendrocytes as previously described (Aaker et al., 2016). Libraries were prepared and sequenced using the Illumina HiSeq 4000 at the University of Chicago Genomics Core facility. Reads were mapped using both STAR v2.6.1a and Kallisto v.0.44.0 using bowtie 2 aligner (Bray et al., 2016; Dobin et al., 2013). Mapped reads were further analyzed with the Bioconductor suite v3.7 by the University of Illinois at Chicago Bioinformatics Core facility (Huber et al., 2015).Q-values were determined as false discovery rate adjusted p-values using the method previously described (Benjamini and

Yekutieli, 2005). Results were compared with the m$^6$A-SMART-Seq analysis and visualized in R v.3.5.1 using the plot.ly, ggplot2, and venn.diagram packages. Values for expression, fold change and statistical significance were adapted for visualization using a $\log_2$ transformation.

### 2.5.12 m$^6$A-SMART-seq and analysis

mRNA from total RNA of OPCs and oligodendrocytes was purified with Dynabeads Oligo $(dT)_{25}$ (Thermo Fisher Scientific, Cat# 61006). The purified mRNA was then processed for m$^6$A-SMART-seq and analyzed as previously described (Weng et al., 2018b). Z scores were calculated for each m$^6$A mark and filtered with a threshold value of 0.

### 2.5.13 Differential alternative splicing analysis

Differential splicing analysis was performed between OPCs versus OPCs lacking *Mettl14* and oligodendrocytes versus oligodendrocytes lacking *Mettl14*. In brief, exon-exon junctions from mapped RNA-seq reads, which are representative of introns that are removed from pre-mRNA, were extracted. Next, alternatively excised introns, which are comprised of two more overlapping introns (e.g. introns that share a splice site), were clustered together. Finally, differential intron excision events across conditions were tested using LeafCutter (Li et al., 2018c).

### 2.5.14 Statistical analysis

All immunohistochemistry and electron microscopy data obtained from experimental and control mice were compared with a two-tailed unpaired Student's t-test. Data were presented as mean $\pm$

SEM. A p value of less-than 0.05 was considered significant. Analysis was done using GraphPad Prism version 6.00 for Windows (GraphPad Software) and Microsoft Office Excel 2010.

### 2.5.15 Data availability

The sequencing data have been deposited to the National Center for Biotechnology Information Gene Expression Omnibus (GEO) database under accession number: GSE124244.

### 2.5.16 Reagents

**Table 2.8. Reagents table**

| REAGENT or RESOURCE | SOURCE | IDENTIFIER |
|---|---|---|
| **Antibodies** | | |
| Rabbit anti-METTL14 | Sigma-Aldrich | Cat# HPA038002; RRID: AB_10672401 |
| Goat anti-PDGFR-α | R&D Systems | Cat# AF1062; RRID: AB_2236897 |
| Rabbit anti-MBP | Abcam | Cat# ab40390; RRID: AB_1141521 |
| Mouse anti-CC1 | Millipore | Cat# OP80; RRID: AB_2057371 |
| Mouse anti-Olig2 | Millipore | Cat# MABN50; RRID: AB_10807410 |
| Mouse anti-O1 | R&D Systems | Cat# MAB1327; RRID: AB_357618 |
| Rabbit anti-Ki67 | Abcam | Cat# AB15580; RRID: AB_805388 |
| Rabbit anti-MAG | Thermo Fisher Scientific | Cat# 34-6200, RRID: AB_2533179 |
| Mouse anti-MBP | BioLegend | Cat# SMI 99; RRID: AB_2314771 |
| Mouse anti-MYRF | Generous gift from Dr. Ben Emery | Cat# 4G4; RRID: AB_2814997 |
| Mouse anti-GAPDH | Cell Signaling | Cat# 2118; RRID: AB_561053 |
| To be continued in the next page | | |

| | | |
|---|---|---|
| Chicken anti-Neurofascin, pan | R&D Systems | Cat# AF3235; RRID: AB_10890736 |
| Rabbit anti-Caspr | Abcam | Cat# ab34151; RRID: AB_869934 |
| Mouse anti-Sodium channel, pan | Sigma-Aldrich | Cat# S8809; RRID: AB_477552 |
| Rabbit anti-Choline acetyltransferase (ChAT) | Millipore | Cat# AB144P; RRID: AB_2079751 |
| Goat anti-mouse IgG+IgM | Jackson ImmunoResearch | Cat# 115-055-044; RRID: AB_2338532 |
| Goat anti-mouse IgM | Jackson ImmunoResearch | Cat# 115-005-020; RRID: AB_2338450 |
| Mouse IgG HRP Linked Whole Antibody | GE Healthcare | Cat# NA931; RRID: AB_772210 |
| Rabbit IgG HRP-Linked Whole Antibody | GE Healthcare | Cat# NA934; RRID: AB_772206 |
| Rabbit anti-Chicken IgY (H+L) Secondary Antibody, HRP | Thermo Fisher Scientific | Cat# 31401; RRID: AB_228385 |
| Donkey Anti-mouse IgG (H+L), Alexa Fluor 488 | Thermo Fisher Scientific | Cat# A-21202; RRID: AB_141607 |
| Donkey Anti-Rabbit IgG (H+L) Antibody, Alexa Fluor 488 | Thermo Fisher Scientific | Cat# A-21206; RRID: AB_2535792 |
| Donkey Anti-Mouse IgG (H+L), Alexa Fluor 594 | Thermo Fisher Scientific | Cat# A-21203; RRID: AB_2535789 |
| Donkey Anti-Goat IgG (H+L), Alexa Fluor 594 | Thermo Fisher Scientific | Cat# A-11058; RRID: AB_2534105 |
| Donkey Anti-Rabbit IgG (H+L), Alexa Fluor 594 | Thermo Fisher Scientific | Cat# A-21207; RRID: AB_141637 |
| Goat anti-Chicken IgY (H+L) Secondary Antibody, Alexa Fluor 594 | Thermo Fisher Scientific | Cat# A-11042; RRID: AB_2534099 |
| **Chemicals, Peptides, and Recombinant Proteins** | | |
| RNAscope Probe –Mm-Myrf | ACD bio | Cat# 524061 |
| RNAscope Probe –Mm-Mbp | ACD bio | Cat# 451491 |
| Dynabeads Oligo(dT)25 | Thermo Fisher Scientific | Cat# 61006 |
| Dynabeads Protein A | Thermo Fisher Scientific | Cat# 1001D |
| N6-Methyladenosine 5′-monophosphate sodium salt | Sigma-Aldrich | Cat# M2780 |
| Poly-D-lysine | Sigma-Aldrich | Cat# P6407 |
| Platelet derived growth factor | PeproTech | Cat# 100-13A |
| Neurotrophin-3 | PeproTech | Cat# 450-03 |
| To be continued in the next page | | |

| | | |
|---|---|---|
| Ciliary neurotrophic factor | PeproTech | Cat# 450-13 |
| Forskolin | Sigma-Aldrich | Cat# F6886 |
| B27 | Life technologies | Cat# 17504044 |
| Fetal bovine serum | Atlanta Biologicals | Cat# S11050 |
| Normal donkey serum | Jackson ImmunoResearch | Cat# 017-000-121 |
| Protease inhibitor cocktail | Thermo Fisher Scientific | Cat# 78430 |
| Phosphatase inhibitors | Sigma-Aldrich | Cat# P2850 and P5726 |
| Laemmli sample buffer | Bio-Rad Laboratories | Cat# 161-0737 |
| β-mercaptoethanol | Sigma-Aldrich | Cat# M6250 |
| Trizol reagent | Thermo Fisher Scientific | Cat# 15596018 |
| Triiodothyronine | Sigma-Aldrich | Cat# T6397 |
| Trypsin 0.05% | Thermo Fisher Scientific | Cat# 25300-054 |
| Trypsin 2.5% | Thermo Fisher Scientific | Cat# 15090046 |
| Trypsin inhibitor | Worthington | Cat# LS003086 |
| Deoxyribonuclease I | Worthington | Cat# LS002007 |
| Papain | Worthington | Cat# LS003126 |
| Apo transferrin | Sigma-Aldrich | Cat# T1147 |
| ProLong gold abtifade reagent with DAPI | Life Technologies | Cat# P36931 |
| Paraformadehyde | Thermo Fisher Scientific | Cat# T353-500 |
| Osmium Tetroxide | Electron Microscopy Science | Cat# 19152 |
| Propylene Oxide | Electron Microscopy Science | Cat# 20401 |
| Sodium Cacodylate Buffer | Electron Microscopy Science | Cat# 11652 |
| Epon 812 | Electron Microscopy Science | Cat# 14900 |
| **Critical Commercial Assays** | | |
| BCA Protein Assay Kit | Thermo Fisher Scientific | Cat# 23255 |
| To be continued in the next page | | |

| | | |
|---|---|---|
| Aurum Total RNA mini Kit | Bio-Rad Laboratories | Cat# 732-6820 |
| Agilent RNA 6000 Nano kit with chips | Agilent | Cat# 5067-1511 |
| RNA Clean & Concentrator | Zymo | Cat# R1015 |
| NEBNext Ultra RNA library Prep kit for Illumina | New England Biolabs | Cat# 61011 |
| RNA Fragmentation Reagents | Thermo Fisher Scientific | Cat# AM8740 |
| Dynabeads Oligo(dT)25 | Thermo Fisher Scientific | Cat# 61006 |
| SuperSignal West Dura Extended Duration Substrate | Thermo Fisher Scientific | Cat# 34076 |
| Pierce™ ECL Western Blotting Substrate | Thermo Fisher Scientific | Cat# 32209 |
| SMARTScribe Reverse Transcriptase | Clontech | Cat# 639537 |
| Protein A Dynabeads | Thermo Fisher Scientific | Cat# 0002D |
| Advantage 2 Polymerase Mix | Thermo Fisher Scientific | Cat# 639201 |
| Agencourt AMPure XP | Beckman Coulter | Cat# A63880 |
| RNAScope Multiplex Fluorescent V2 Assay kit | ACD bio | Cat# 323110 |
| Basic NucleofectorTM Kit for Primary Mammalian Glial Cells | Lonza | Cat# VPI-1006 |
| Opal™ 520 | Akoya Biosciences | Cat# FP1487001KT |
| Opal™ 620 | Akoya Biosciences | Cat# FP1495001KT |
| **Deposited Data** | | |
| Raw and analyzed data | This paper | GEO: GSE124244 |
| **Experimental Models: Organisms/Strains** | | |
| Mouse: *Mettl14fl/fl* | Generous gift from Dr. Xiaoxi Zhuang | Koranda et al., 2018, Weng et al., 2018b, Yoon et al., 2017 |
| Mouse: *Olig2*-Cre | Generous gift from Dr. David Rowitch | The Jackson Laboratory: 011103 |
| Mouse: *CNP*-Cre | Generous gift from Dr. Klaus Amin Nave | MGI: 3051635 |
| **Oligonucleotides** | | |
| To be continued in the next page | | |

| | | |
|---|---|---|
| RT-PCR primers for *Nfasc* aberrant spliced locus: | | |
| Forward: ACTGGGAAAGCAGATGGTGG | | |
| Reverse: ACATGAGCCCGATGAACCAG | This paper | Figure 7 |
| **Recombinant DNA** | | |
| Mettl14 (NM_201638) Mouse Tagged ORF Clone | OriGene | Cat# MR207291 |
| pmaxGFP™ vector | Lonza | Cat# VPI-1006 |
| **Software and Algorithms** | | |
| ImageJ | National Institutes of Health | RRID: SCR_003070 |
| Image Lab | Bio-Rad Laboratories | RRID: SCR_014210 |
| R v3.5.1 | R core team | RRID: SCR_001905 |
| Bioconductor v.3.7 | Huber et al., 2015 | RRID: SCR_006442 |
| STAR v2.6.1a | Dobin et al., 2013 | RRID: SCR_015899 |
| Trimmomatic | Bolger et al., 2014 | RRID: SCR_011848 |
| Kallisto v0.44.0 | Bray et al., 2016 | RRID: SCR_016582 |
| GraphPad Prism 6 | GraphPad Software | RRID: SCR_002798 |
| LeafCutter | Li et al.,2018 | RRID: SCR_017639 |

## 2.6 References


Aaker, J.D., Elbaz, B., Wu, Y., Looney, T.J., Zhang, L., Lahn, B.T., and Popko, B. (2016). Transcriptional fingerprint of hypomyelination in zfp191null and shiverer (mbpshi) mice. ASN Neuro *8*.

Alarcón, C.R., Goodarzi, H., Lee, H., Liu, X., Tavazoie, S., and Tavazoie, S.F. (2015). HNRNPA2B1 Is a Mediator of m(6)A-Dependent Nuclear RNA Processing Events. Cell *162*, 1299–1308.

Batista, P.J., Molinie, B., Wang, J., Qu, K., Zhang, J., Li, L., Bouley, D.M., Lujan, E., Haddad, B., Daneshvar, K., et al. (2014). m(6)A RNA modification controls cell fate transition in mammalian embryonic stem cells. Cell Stem Cell *15*, 707–719.

Benjamini, Y., and Yekutieli, D. (2005). False discovery rate–adjusted multiple confidence intervals for selected parameters. J. Am. Stat. Assoc. *100*, 71–81.

Bergles, D.E., and Richardson, W.D. (2015). Oligodendrocyte development and plasticity. Cold Spring Harb. Perspect. Biol. *8*, a020453.

Bray, N.L., Pimentel, H., Melsted, P., and Pachter, L. (2016). Near-optimal probabilistic RNA-seq quantification. Nat. Biotechnol. *34*, 525–527.

Brockschnieder, D., Lappe-Siefke, C., Goebbels, S., Boesl, M.R., Nave, K.-A., and Riethmacher, D. (2004). Cell depletion due to diphtheria toxin fragment A after Cre-mediated recombination. Mol. Cell. Biol. *24*, 7636–7642.

Brown, T.L., and Verden, D.R. (2017). Cytoskeletal regulation of oligodendrocyte differentiation and myelination. J. Neurosci. *37*, 7797–7799.

Bujalka, H., Koenning, M., Jackson, S., Perreau, V.M., Pope, B., Hay, C.M., Mitew, S., Hill, A.F., Lu, Q.R., Wegner, M., et al. (2013). MYRF is a membrane-associated transcription factor that autoproteolytically cleaves to directly activate myelin genes. PLoS Biol. *11*, e1001625.

Carson, J.H., Worboys, K., Ainger, K., and Barbarese, E. (1997). Translocation of myelin basic protein mRNA in oligodendrocytes requires microtubules and kinesin. Cell Motil. Cytoskeleton *38*, 318–328.

Colman, D.R., Kreibich, G., Frey, A.B., and Sabatini, D.D. (1982). Synthesis and incorporation of myelin polypeptides into CNS myelin. J. Cell Biol. *95*, 598–608.

Coots, R.A., Liu, X.-M., Mao, Y., Dong, L., Zhou, J., Wan, J., Zhang, X., and Qian, S.-B. (2017). m6A Facilitates eIF4F-Independent mRNA Translation. Mol. Cell *68*, 504–514.e7.
Copray, S., Huynh, J.L., Sher, F., Casaccia-Bonnefil, P., and Boddeke, E. (2009). Epigenetic mechanisms facilitating oligodendrocyte development, maturation, and aging. Glia *57*, 1579–1587.

Dobin, A., Davis, C.A., Schlesinger, F., Drenkow, J., Zaleski, C., Jha, S., Batut, P., Chaisson, M., and Gingeras, T.R. (2013). STAR: ultrafast universal RNA-seq aligner. Bioinformatics *29*, 15–21.

Elbaz, B., and Popko, B. (2019). Molecular control of oligodendrocyte development. Trends Neurosci. *42*, 263–277.

Emery, B., and Dugas, J.C. (2013). Purification of oligodendrocyte lineage cells from mouse cortices by immunopanning. Cold Spring Harb. Protoc. *2013*, 854–868.

Fields, R.D., and Dutta, D.J. (2019). Treadmilling model for plasticity of the myelin sheath. Trends Neurosci. *42*, 443–447.

Frye, M., Harada, B.T., Behm, M., and He, C. (2018). RNA modifications modulate gene expression during development. Science *361*, 1346–1349.

Fu, Y., Dominissini, D., Rechavi, G., and He, C. (2014). Gene expression regulation mediated through reversible $m^6A$ RNA methylation. Nat. Rev. Genet. *15*, 293–306.

Geula, S., Moshitch-Moshkovitz, S., Dominissini, D., Mansour, A.A., Kol, N., Salmon-Divon, M., Hershkovitz, V., Peer, E., Mor, N., Manor, Y.S., et al. (2015). Stem cells. m6A mRNA methylation facilitates resolution of naïve pluripotency toward differentiation. Science *347*, 1002–1006.

Han, S.P., Friend, L.R., Carson, J.H., Korza, G., Barbarese, E., Maggipinto, M., Hatfield, J.T., Rothnagel, J.A., and Smith, R. (2010). Differential subcellular distributions and trafficking functions of hnRNP A2/B1 spliceoforms. Traffic *11*, 886–898.

Harroch, S., Furtado, G.C., Brueck, W., Rosenbluth, J., Lafaille, J., Chao, M., Buxbaum, J.D., and Schlessinger, J. (2002). A critical role for the protein tyrosine phosphatase receptor type Z in functional recovery from demyelinating lesions. Nat. Genet. *32*, 411–414.

Haussmann, I.U., Bodi, Z., Sanchez-Moran, E., Mongan, N.P., Archer, N., Fray, R.G., and Soller, M. (2016). m6A potentiates Sxl alternative pre-mRNA splicing for robust Drosophila sex determination. Nature *540*, 301–304.

Hernandez, M., and Casaccia, P. (2015). Interplay between transcriptional control and chromatin regulation in the oligodendrocyte lineage. Glia *63*, 1357–1375.

Hoek, K.S., Kidd, G.J., Carson, J.H., and Smith, R. (1998). hnRNP A2 selectively binds the cytoplasmic transport sequence of myelin basic protein mRNA. Biochemistry *37*, 7021–7029.

Howell, O.W., Palser, A., Polito, A., Melrose, S., Zonta, B., Scheiermann, C., Vora, A.J., Brophy, P.J., and Reynolds, R. (2006). Disruption of neurofascin localization reveals early changes preceding demyelination and remyelination in multiple sclerosis. Brain *129*, 3173–3185.

Huber, W., Carey, V.J., Gentleman, R., Anders, S., Carlson, M., Carvalho, B.S., Bravo, H.C., Davis, S., Gatto, L., Girke, T., et al. (2015). Orchestrating high-throughput genomic analysis with Bioconductor. Nat. Methods *12*, 115–121.

Ivanova, I., Much, C., Di Giacomo, M., Azzi, C., Morgan, M., Moreira, P.N., Monahan, J., Carrieri, C., Enright, A.J., and O'Carroll, D. (2017). The RNA m6A Reader YTHDF2 Is Essential for the Post-transcriptional Regulation of the Maternal Transcriptome and Oocyte Competence. Mol. Cell *67*, 1059–1067.e4.

Kawamura, N., Yamasaki, R., Yonekawa, T., Matsushita, T., Kusunoki, S., Nagayama, S., Fukuda, Y., Ogata, H., Matsuse, D., Murai, H., et al. (2013). Anti-neurofascin antibody in patients with combined central and peripheral demyelination. Neurology *81*, 714–722.

Kira, J.-I., Yamasaki, R., and Ogata, H. (2018). Anti-neurofascin autoantibody and demyelination. Neurochem. Int. 104360.

Koranda, J.L., Dore, L., Shi, H., Patel, M.J., Vaasjo, L.O., Rao, M.N., Chen, K., Lu, Z., Yi, Y., Chi, W., et al. (2018). Mettl14 is essential for epitranscriptomic regulation of striatal function and learning. Neuron *99*, 283–292.e5.

Koreman, E., Sun, X., and Lu, Q.R. (2018). Chromatin remodeling and epigenetic regulation of oligodendrocyte myelination and myelin repair. Mol. Cell. Neurosci. *87*, 18–26.

Lappe-Siefke, C., Goebbels, S., Gravel, M., Nicksch, E., Lee, J., Braun, P.E., Griffiths, I.R., and Nave, K.-A. (2003). Disruption of Cnp1 uncouples oligodendroglial functions in axonal support and myelination. Nat. Genet. *33*, 366–374.

Li, H., and Richardson, W.D. (2009). Genetics meets epigenetics: HDACs and Wnt signaling in myelin development and regeneration. Nat. Neurosci. *12*, 815–817.

Li, Y.I., Knowles, D.A., Humphrey, J., Barbeira, A.N., Dickinson, S.P., Im, H.K., and Pritchard, J.K. (2018). Annotation-free quantification of RNA splicing using LeafCutter. Nat. Genet. *50*, 151–158.

Li, Z., Weng, H., Su, R., Weng, X., Zuo, Z., Li, C., Huang, H., Nachtergaele, S., Dong, L., Hu, C., et al. (2017). FTO Plays an Oncogenic Role in Acute Myeloid Leukemia as a N6-Methyladenosine RNA Demethylase. Cancer Cell *31*, 127–141.

Licht, K., and Jantsch, M.F. (2016). Rapid and dynamic transcriptome regulation by RNA editing and RNA modifications. J. Cell Biol. *213*, 15–22.

Liu, J., Yue, Y., Han, D., Wang, X., Fu, Y., Zhang, L., Jia, G., Yu, M., Lu, Z., Deng, X., et al. (2014). A METTL3-METTL14 complex mediates mammalian nuclear RNA N6-adenosine methylation. Nat. Chem. Biol. *10*, 93–95.

Liu, J., Moyon, S., Hernandez, M., and Casaccia, P. (2016). Epigenetic control of oligodendrocyte development: adding new players to old keepers. Curr. Opin. Neurobiol. *39*, 133–138.

Marin-Husstege, M., Muggironi, M., Liu, A., and Casaccia-Bonnefil, P. (2002). Histone deacetylase activity is necessary for oligodendrocyte lineage progression. J. Neurosci. *22*, 10333–10345.

Mitew, S., Hay, C.M., Peckham, H., Xiao, J., Koenning, M., and Emery, B. (2014). Mechanisms regulating the development of oligodendrocytes and central nervous system myelin. Neuroscience *276*, 29–47.

Montague, P., McCallion, A.S., Davies, R.W., and Griffiths, I.R. (2006). Myelin-associated oligodendrocytic basic protein: a family of abundant CNS myelin proteins in search of a function. Dev Neurosci *28*, 479–487.

Moyon, S., and Casaccia, P. (2017). DNA methylation in oligodendroglial cells during developmental myelination and in disease. Neurogenesis (Austin) *4*, e1270381.

Müller, C., Bauer, N.M., Schäfer, I., and White, R. (2013). Making myelin basic protein -from mRNA transport to localized translation. Front. Cell Neurosci. *7*, 169.

Müller, R., Heinrich, M., Heck, S., Blohm, D., and Richter-Landsberg, C. (1997). Expression of microtubule-associated proteins MAP2 and tau in cultured rat brain oligodendrocytes. Cell Tissue Res. *288*, 239–249.

Nave, K.-A., and Werner, H.B. (2014). Myelination of the nervous system: mechanisms and functions. Annu. Rev. Cell Dev. Biol. *30*, 503–533.

Nishiyama, A., Komitova, M., Suzuki, R., and Zhu, X. (2009). Polydendrocytes (NG2 cells): multifunctional cells with lineage plasticity. Nat. Rev. Neurosci. *10*, 9–22.

Picelli, S., Faridani, O.R., Björklund, A.K., Winberg, G., Sagasser, S., and Sandberg, R. (2014). Full-length RNA-seq from single cells using Smart-seq2. Nat. Protoc. *9*, 171–181.

Pillai, A.M., Thaxton, C., Pribisko, A.L., Cheng, J.-G., Dupree, J.L., and Bhat, M.A. (2009). Spatiotemporal ablation of myelinating glia-specific neurofascin (Nfasc NF155) in mice reveals gradual loss of paranodal axoglial junctions and concomitant disorganization of axonal domains. J. Neurosci. Res. *87*, 1773–1793.

Pomicter, A.D., Shroff, S.M., Fuss, B., Sato-Bigbee, C., Brophy, P.J., Rasband, M.N., Bhat, M.A., and Dupree, J.L. (2010). Novel forms of neurofascin 155 in the central nervous system: alterations in paranodal disruption models and multiple sclerosis. Brain *133*, 389–405.

Ravanelli, A.M., and Appel, B. (2015). Motor neurons and oligodendrocytes arise from distinct cell lineages by progenitor recruitment. Genes Dev. *29*, 2504–2515.

Roundtree, I.A., Luo, G.-Z., Zhang, Z., Wang, X., Zhou, T., Cui, Y., Sha, J., Huang, X., Guerrero, L., Xie, P., et al. (2017). YTHDC1 mediates nuclear export of N6-methyladenosine methylated mRNAs. Elife *6*.

Rowitch, D.H. (2004). Glial specification in the vertebrate neural tube. Nat. Rev. Neurosci. *5*, 409–419.

Schüller, U., Heine, V.M., Mao, J., Kho, A.T., Dillon, A.K., Han, Y.-G., Huillard, E., Sun, T., Ligon, A.H., Qian, Y., et al. (2008). Acquisition of granule neuron precursor identity is a critical determinant of progenitor cell competence to form Shh-induced medulloblastoma. Cancer Cell *14*, 123–134.

Sherman, D.L., Tait, S., Melrose, S., Johnson, R., Zonta, B., Court, F.A., Macklin, W.B., Meek, S., Smith, A.J.H., Cottrell, D.F., et al. (2005). Neurofascins are required to establish axonal domains for saltatory conduction. Neuron *48*, 737–742.

Shi, H., Wang, X., Lu, Z., Zhao, B.S., Ma, H., Hsu, P.J., Liu, C., and He, C. (2017). YTHDF3 facilitates translation and decay of N6-methyladenosine-modified RNA. Cell Res. *27*, 315–328.

Simons, M., and Nave, K.-A. (2015). Oligodendrocytes: myelination and axonal support. Cold Spring Harb. Perspect. Biol. *8*, a020479.

Sommer, and Schachner (1981). Monoclonal Antibodies (01 to 04) to Oligodendrocyte Cell Surfaces: An lmmunocytological Study in the Central Nervous System. Dev. Biol. *83*.

Suzuki, S., Ayukawa, N., Okada, C., Tanaka, M., Takekoshi, S., Iijima, Y., and Iijima, T. (2017). Spatio-temporal and dynamic regulation of neurofascin alternative splicing in mouse cerebellar neurons. Sci. Rep. *7*, 11405.

Thakurela, S., Garding, A., Jung, R.B., Müller, C., Goebbels, S., White, R., Werner, H.B., and Tiwari, V.K. (2016). The transcriptome of mouse central nervous system myelin. Sci. Rep. 6, 25828.

Thaxton, C., Pillai, A.M., Pribisko, A.L., Labasque, M., Dupree, J.L., Faivre-Sarrailh, C., and Bhat, M.A. (2010). In vivo deletion of immunoglobulin domains 5 and 6 in neurofascin (Nfasc) reveals domain-specific requirements in myelinated axons. J. Neurosci. *30*, 4868–4876.

Wang, X., Lu, Z., Gomez, A., Hon, G.C., Yue, Y., Han, D., Fu, Y., Parisien, M., Dai, Q., Jia, G., et al. (2014). N6-methyladenosine-dependent regulation of messenger RNA stability. Nature *505*, 117–120.

Wang, X., Zhao, B.S., Roundtree, I.A., Lu, Z., Han, D., Ma, H., Weng, X., Chen, K., Shi, H., and He, C. (2015). N(6)-methyladenosine Modulates Messenger RNA Translation Efficiency. Cell *161*, 1388–1399.

Wang, Y., Li, Y., Yue, M., Wang, J., Kumar, S., Wechsler-Reya, R.J., Zhang, Z., Ogawa, Y., Kellis, M., Duester, G., et al. (2018). N6-methyladenosine RNA modification regulates embryonic neural stem cell self-renewal through histone modifications. Nat. Neurosci. *21*, 195–206.

Weng, H., Huang, H., Wu, H., Qin, X., Zhao, B.S., Dong, L., Shi, H., Skibbe, J., Shen, C., Hu, C., et al. (2018a). METTL14 Inhibits Hematopoietic Stem/Progenitor Differentiation and Promotes Leukemogenesis via mRNA m6A Modification. Cell Stem Cell *22*, 191–205.e9.

Weng, Y.-L., Wang, X., An, R., Cassin, J., Vissers, C., Liu, Y., Liu, Y., Xu, T., Wang, X., Wong, S.Z.H., et al. (2018b). Epitranscriptomic m6a regulation of axon regeneration in the adult mammalian nervous system. Neuron *97*, 313–325.e6.

Wu, R., Li, A., Sun, B., Sun, J.-G., Zhang, J., Zhang, T., Chen, Y., Xiao, Y., Gao, Y., Zhang, Q., et al. (2019). A novel m6A reader Prrc2a controls oligodendroglial specification and myelination. Cell Res. *29*, 23–41.

Xiao, W., Adhikari, S., Dahal, U., Chen, Y.-S., Hao, Y.-J., Sun, B.-F., Sun, H.-Y., Li, A., Ping, X.-L., Lai, W.-Y., et al. (2016). Nuclear m(6)A Reader YTHDC1 Regulates mRNA Splicing. Mol. Cell *61*, 507–519.

Xu, K., Yang, Y., Feng, G.-H., Sun, B.-F., Chen, J.-Q., Li, Y.-F., Chen, Y.-S., Zhang, X.-X., Wang, C.-X., Jiang, L.-Y., et al. (2017). Mettl3-mediated m6A regulates spermatogonial differentiation and meiosis initiation. Cell Res. *27*, 1100–1114.

Ye, F., Chen, Y., Hoang, T., Montgomery, R.L., Zhao, X., Bu, H., Hu, T., Taketo, M.M., van Es, J.H., Clevers, H., et al. (2009). HDAC1 and HDAC2 regulate oligodendrocyte differentiation by disrupting the beta-catenin-TCF interaction. Nat. Neurosci. *12*, 829–838.

Yoon, K.-J., Ringeling, F.R., Vissers, C., Jacob, F., Pokrass, M., Jimenez-Cyrus, D., Su, Y., Kim, N.-S., Zhu, Y., Zheng, L., et al. (2017). Temporal control of mammalian cortical neurogenesis by m6a methylation. Cell *171*, 877–889.e17.

Yue, Y., Liu, J., and He, C. (2015). RNA N6-methyladenosine methylation in post-transcriptional gene expression regulation. Genes Dev. *29*, 1343–1355.

Zhang, C., Chen, Y., Sun, B., Wang, L., Yang, Y., Ma, D., Lv, J., Heng, J., Ding, Y., Xue, Y., et al. (2017). m6A modulates haematopoietic stem and progenitor cell specification. Nature *549*, 273–276.

Zhang, Y., Chen, K., Sloan, S.A., Bennett, M.L., Scholze, A.R., O'Keeffe, S., Phatnani, H.P., Guarnieri, P., Caneda, C., Ruderisch, N., et al. (2014). An RNA-sequencing transcriptome and splicing database of glia, neurons, and vascular cells of the cerebral cortex. J. Neurosci. *34*, 11929–11947.

Zhao, B.S., and He, C. (2017). Gamete On" for m(6)A: YTHDF2 Exerts Essential Functions in Female Fertility. Mol. Cell *67*, 903–905.

Zhao, L., Mandler, M.D., Yi, H., and Feng, Y. (2010a). Quaking I controls a unique cytoplasmic pathway that regulates alternative splicing of myelin-associated glycoprotein. Proc. Natl. Acad. Sci. USA *107*, 19061–19066.

Zhao, X., He, X., Han, X., Yu, Y., Ye, F., Chen, Y., Hoang, T., Xu, X., Mi, Q.-S., Xin, M., et al. (2010b). MicroRNA-mediated control of oligodendrocyte differentiation. Neuron *65*, 612–626.

Zhao, X., Yang, Y., Sun, B.-F., Shi, Y., Yang, X., Xiao, W., Hao, Y.-J., Ping, X.-L., Chen, Y.-S., Wang, W.-J., et al. (2014). FTO-dependent demethylation of N6-methyladenosine regulates mRNA splicing and is required for adipogenesis. Cell Res. *24*, 1403–1419.

Zhou, Q., and Anderson, D.J. (2002). The bHLH transcription factors OLIG2 and OLIG1 couple neuronal and glial subtype specification. Cell *109*, 61–73.

Zhou, J., Wan, J., Shu, X.E., Mao, Y., Liu, X.-M., Yuan, X., Zhang, X., Hess, M.E., Brüning, J.C., and Qian, S.-B. (2018). N6-Methyladenosine Guides mRNA Alternative Translation during Integrated Stress Response. Mol. Cell *69*, 636–647.e7.

Zhou, K.I., Shi, H., Lyu, R., Wylder, A.C., Matuszek, Ż., Pan, J.N., He, C., Parisien, M., and Pan, T. (2019). Regulation of Co-transcriptional Pre-mRNA Splicing by m6A through the Low-Complexity Protein hnRNPG. Mol. Cell *76*, 70–81.e9.

Zonta, B., Tait, S., Melrose, S., Anderson, H., Harroch, S., Higginson, J., Sherman, D.L., and Brophy, P.J. (2008). Glial and neuronal isoforms of Neurofascin have distinct roles in the assembly of nodes of Ranvier in the central nervous system. J. Cell Biol. *181*, 1169–1177.

Zuchero, J.B., and Barres, B.A. (2013). Intrinsic and extrinsic control of oligodendrocyte development. Curr. Opin. Neurobiol. *23*, 914–920.

Zuchero, J.B., and Barres, B.A. (2015). Glia in mammalian development and disease. Development *142*, 3805–3809.

# CHAPTER 3

# $M^6A$ mRNA methylation

# Is essential for remyelination

## 3.1 Abstract

In the CNS, oligodendrocytes form the myelin sheath to allow rapid propagation of action potentials and to provide metabolic support to axons. Under pathological conditions such as traumatic injury and demyelinating diseases, CNS axons are demyelinated, which causes impaired axon action potential transmission and ultimately leads to impaired CNS functions. To repair the demyelination injury, CNS spontaneously initiates remyelination process, which involves rapid propagation of OPCs, followed by migration, differentiation and myelination of demyelinated axons. In patients with debilitating neurological diseases such as multiple sclerosis (MS), failure of remyelination is a prominent feature that contributes to disability. Therefore, it's critical to promote therapeutic strategies to enhance remyelination. Nevertheless, the mechanisms that regulate remyelination process are still unclear. Our previous study suggests that a post-transcriptional mechanism, N6-methyladenosine ($m^6A$) modification in mRNA, is essential for oligodendrocyte maturation and CNS myelination during development. In this study, we ask whether $m^6A$ mRNA modification mechanism plays a role in regulating remyelination in adults. Using a mouse model that deletes a core $m^6A$ writer component, METTL14, in the adult OPCs, we found that animals showed remyelination deficits at both early and late stages after demyelination. These results suggest $m^6A$ modification, a novel post-transcriptional mechanism, is critical for remyelination process.

## 3.2 Introduction

### 3.2.1 Myelination and demyelination in the adult brains

In the CNS, myelin is produced by oligodendrocytes that differentiate from OPCs. During development, OPCs migrate out of the embryonic neural tube and distribute evenly throughout the CNS. In the adulthood, production of new OPCs continues by proliferation of existing OPCs and specification by neural progenitor cells in subventricular zone (El Waly et al., 2014). Over the past decade, studies revealed myelination is a dynamic process, it continues throughout adult life and plays a critical role in neural circuits formation (Xin and Chan, 2020). The differentiation of OPCs and myelination are crucial in language learning, motor skill learning and fear memory formation in the adult brain (Del Maschio et al., 2020; McKenzie et al., 2014; Pan et al., 2020; Xiao et al., 2016a), suggesting complex roles of oligodendrocyte lineage cells in important adult CNS functions. In the CNS, oligodendrocytes bear the highest metabolic rate among all the CNS cell types, to produce and maintain high volumes of membranes that represent up to 100 times of the cell weight. Due to this extensive energy consuming property, oligodendrocytes are highly susceptible to the environmental insults and cues (El Waly et al., 2014; 1984). After myriad CNS injuries or diseases, oligodendrocytes die and myelin falls apart, a process called demyelination. Besides being a hallmark of demyelination diseases such as multiple sclerosis (MS), demyelination is also a common feature in pathological conditions such as traumatic brain injury, stroke and spinal cord injury (McDonald and Belegu, 2006; Shi et al., 2015). Moreover, white matter loss is also a pathological character in neurodegenerative diseases such as Alzheimer's disease, Parkinson's disease, and Huntington disease, as well as normal aging (Casella et al., 2020; Chiang et al., 2017; de la Fuente et al., 2020; Papuć and Rejdak, 2020; Peters, 2009). In addition, brain irradiation therapy also contributes to demyelination, with discrete sensitivity of myelin damage

that contributes to selective cognitive dysfunction (Nazem-Zadeh et al., 2012). JC virus infection in immunocompromised patients or patients requiring immunosuppressive treatments can cause severe demyelination disease called progressive multifocal leukoencephalopahty (PML) (Cortese et al., 2021).

### 3.2.2 Remyelination in the adult brain

Remyelination is a spontaneous process that restores myelin sheaths to demyelinated axons. It's a neuroprotective response that restores saltatory conduction, and resolves functional deficits (Franklin and Ffrench-Constant, 2008). The remyelination process involves activation of adult OPCs to proliferate and migrate to the areas of demyelination, followed by differentiation and myelination. During remyelination, oligodendrocyte lineage cells come from the stem and precursor cells of the SVZ and migration of parenchymal OPCs to local sites. The activation of adult OPCs is the first step of the remyelination process that involves not only morphological changes but also a switch in gene expression profiles, such as *IL1β* and *CCL2*, which enhance OPCs mobilization (Moyon et al., 2015). The translatome of oligodendrocyte lineage cells during remyelination in experimental autoimmune encephalomyelitis (EAE) revealed upregulation of cholesterol-synthesis gene expression (Voskuhl et al., 2019). The efficiency of remyelination depends on different factors and conditions, such as demyelination severity, lesion location, and aging. In ischemic/hypoxia white matter demyelination, even though there is active OPC proliferation, the remyelination is poor (Segovia et al., 2008; Shi et al., 2015). Recurrent episodes of demyelination and inflammation in chronic MS, exhaustion of the precursor cells and environmental factors leads to the failure of cell recruitment and differentiation (Franklin, 2002). In addition, the efficiency of remyelination deteriorates with age. The age-associated effects are mainly associated with decreased rate of OPC recruitment and OPC differentiation. The underlying

basis of aging effect is also associated with extrinsic signals such as lack of macrophage clearance and dysregulation of growth factors, and intrinsic signals such as epigenetic regulators (Franklin, 2002). In the past decade, epigenetic mechanisms have been revealed to play vital roles in oligodendrocyte remyelination. It has been shown that histone deacetylates (HDACs) are necessary for remyelination. HDACs downregulate the oligodendrocyte differentiation inhibitors and neural stem cell markers to promote oligodendrocyte differentiation and new myelin synthesis. Its regulation efficiency is age-dependent (Shen et al., 2008). microRNAs are also critical for remyelination. miR-219 accelerates the differentiation of mouse embryonic stem cells into OPCs (miR219-OPCs). The transplantation of these mi-219-overexpression OPCs enhanced remyelination and functional recovery in a oligodendrocyte toxin cuprizone (CPZ) induced chronic demyelination mouse model (Fan et al., 2017). miR-146a, which inactivates interleukin-1 receptor-associated kinase1 (IRAK1), promotes oligodendrocyte differentiation and enhances remyelination in CPZ mouse model (Zhang et al., 2017b). However, the picture of understanding epigenetic mechanisms in myelination and remyelination is incomplete.

In chapter 2, we demonstrated that $m^6A$ RNA modification is essential for oligodendrocyte development and CNS myelination. In the study, we showed that $m^6A$ is critical oligodendrocyte lineage progression, and may collaborate with various epigenetic mechanisms such as HDACs to regulate oligodendrocyte differentiation (Xu et al., 2020). Thus we hypothesis that in the adult brain, $m^6A$ may also play a role in regulating the remyelination process, which involves the activation of oligodendrocyte lineage cells. In this chapter, I will show the preliminary results to validate this hypothesis and discuss future perspectives to advance our understanding of $m^6A$ 's role in remyelination. Using a mouse model that deletes a core $m^6A$ writer component, METTL14,

in the adult OPCs, the animals that underwent demyelination process with CPZ diet experience remyelination deficits at both early and late stages after demyelination.

## 3.3 Results

### 3.3.1 *Mettl14* ablation in adult OPCs does not alter oligodendrocyte lineage cell numbers

In order to study the m$^6$A RNA modification's role during remyelination, we developed an inducible Cre mouse line *Mettl14$^{fl/fl}$;PDGFR α*-CreERT that specifically ablates an m$^6$A writer component, METTL14, in the OPCs after tamoxifen injection. The experimental paradigm is described in Figure 3.1. Briefly, when *Mettl14$^{fl/fl}$;PDGFR α*-CreERT mutant mice and their littermate controls reached adulthood at 6 weeks old, tamoxifen was injected for continuous 5 days to activate Cre recombination. In order to exclude the effect of tamoxifen on the CNS, we waited 2 weeks for sufficient clearance of tamoxifen and its metabolites (Valny et al., 2016). When animals reached 9 weeks old, both mutant and control tissues were collected as baseline controls before starting the CPZ chow to induce demyelination. After 3 weeks of CPZ chow, 12 weeks old animals were at peak disease and their tissues were collected. At 14 weeks old, when animals had CPZ chow for 5 weeks, CPZ was discontinued and followed by the normal chow. After having the normal chow for 2 weeks, 16 weeks old animals experienced early remyelination (Karttunen et al., 2017). After having normal chow for 3 weeks, 17 weeks old animals experienced full remyelination. Tissues were collected at these time points for further identification.

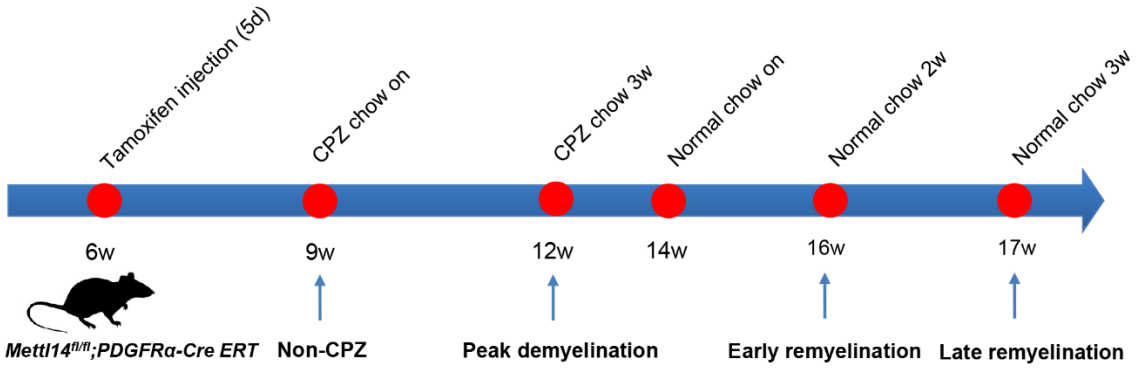


**Figure 3.1. Experimental paradigm**
*Mettl14$^{fl/fl}$;PDGFRα-Cre ERT* mutant and littermate control mice were injected tamoxifen at 6weeks old for continuous five days (5d). A two- weeks period was placed for sufficient Cre recombination and tamoxifen elimination out animals' circulation system before starting cuprizone (CPZ) chow at nine weeks (9w) old. Non-CPZ animals are measured as baseline levels. Peak demyelination is measured at twelve weeks (12w) old, when animals finished CPZ diet for three weeks. At fourteen weeks (14w), animals finished five weeks of CPZ chow, and started the normal chow. Early remyelination is measured at sixteen weeks (16w) old, when animals finished five-weeks (5w) CPZ chow + two-weeks (2w) normal chow. Full remyelination is measured at seventeen-weeks (17w) old, when animals finished five weeks (5w) CPZ chow + three-weeks (3w) normal chow.

To characterize the effects of *Mett14* deletion in adult OPCs at baseline level, we first measured the efficiency of *Mett14* gene inactivation via identification of METTL14 expression in the oligodendrocyte lineage cells with immunohistochemistry (Fig 3.2). We used Olig2 as the oligodendrocyte lineage cell marker, and detected no difference of Olig2+ cells in the mutants compared to the controls (Fig 3.2 A, B, E). Moreover, we observed a significant reduction of METTL14 expression in the Olig2+ cells in the mutants (Fig 3.2 C, D, F). To understand whether *Mett14* gene inactivation results in differential impacts on oligodendrocyte lineage cells at different stages, we further analyzed the OPCs, proliferating OPCs, early myelinating cells, and mature oligodendrocytes in the corpus callosum using immunohistochemistry (Fig 3.2 G-W). With PDGFR-α marker, we found there was no significant difference of OPCs numbers between

*Mettl14*$^{fl/fl}$*;PDGFRα*-CreERT mutants and controls in the corpus callosum (Fig 3.2 G, H, S), while METTL14 was significantly knocked out in the mutants (Fig 3.2 I, J, T). These result suggests *Mett14* deletion in the adult OPCs have no effects on their survival. In addition, using double staining of Ki67 and PDGFR-α, we detected no difference of proliferating OPCs between mutants and controls (Fig 3.2 K, L, U). In addition, we explored the number of early myelinating cells using double staining of an oligodendrocyte lineage marker SOX10, and BCAS1, a marker recently found that is specific to myelinating oligodendrocytes at early stage (Fard et al., 2017). We did not detect difference of early myelinating cells between mutants and controls (Fig 3.2 M, N, V). We also used CC1 to detect mature oligodendrocyte numbers, and we found no differences between mutants and controls (Fig 3.2 Q, R, W). MBP, a myelin marker showed no observable signal change in the corpus callosum (Fig 3.2 O, P). To further examine *Mettl14'*s effects on the myelin, we examined *Mettl14*$^{fl/fl}$*;PDGFR α*-CreERT mice' corpus callosum using the electron microscopy (EM). We analyzed the g-ratio, which represents the thickness of myelin sheath and found no difference between mutants and controls (Fig 3.3 A, B). We also observed no difference of non-myelinated axon percentage, indicating that *Mettl14* deletion in the OPCs has no effects on myelination (Fig 3.3 A, C). In summary, these results suggest *Mett14* deletion in adult OPCs does not affect the oligodendrocyte lineage number at baseline level.

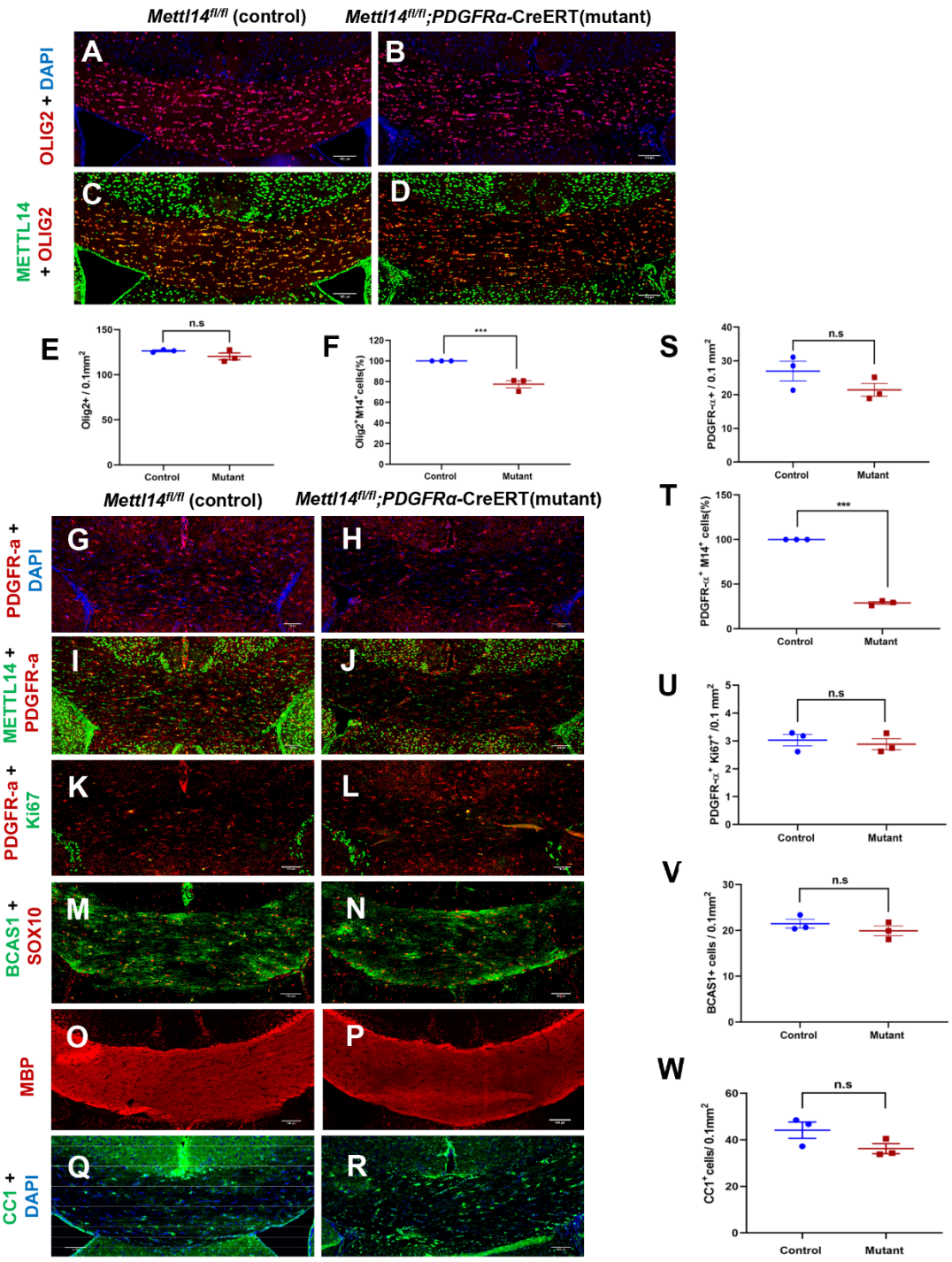


**Figure 3.2. *Mettl14* ablation in adult OPCs does not alter oligodendrocyte lineage cell numbers**

(A-D) Representative METTL14 (green) and Olig2 (red) immunostaining in the corpus callosum of non-CPZ *Mettl14$^{fl/fl}$;PDGFRα-Cre ERT* control (A, C) and mutant (B, D) mice (scale bar = 100μm). (E) Quantification analysis showing no significant difference of total oligodendrocyte

lineage cells ($Olig2^+$ cells) in the mutants. Values represent mean ± SEM (n=3; p>0.05; unpaired Student's t- test). (F) Quantification analysis showing statistical significant reduction of $Olig2^+METTL14^+$ double positive cells in the mutants. Values represent mean ± SEM (n=3; $^{***}p<0.001$; unpaired Student's t-test). (G-H) Representative PDGFR-α (red) and DAPI (blue) immunostaining in the corpus callosum of non-CPZ *Mettl14$^{fl/fl}$;PDGFRα-Cre ERT* control (G) and mutant (H) (scale bar = 100µm). (I-J) Representative PDGFR-α (red) and METTL14 (green) immunostaining in the corpus callosum of non-CPZ *Mettl14$^{fl/fl}$;PDGFRα-Cre ERT* control (I) and mutant (J) (scale bar = 100µm). (K-L) Representative PDGFR-α (red) and Ki67 (green) immunostaining in the corpus callosum of non-CPZ *Mettl14$^{fl/fl}$;PDGFRα-Cre ERT* control (K) and mutant (L) (scale bar = 100µm). (M-N) Representative SOX10 (red) and BCAS1 (green) immunostaining in the corpus callosum of non-CPZ *Mettl14$^{fl/fl}$;PDGFRα-Cre ERT* control (M) and mutant (N) (scale bar = 100µm). (O-P) Representative MBP (red) immunostaining in the corpus callosum of non-CPZ *Mettl14$^{fl/fl}$;PDGFRα-Cre ERT* control (O) and mutant (P) (scale bar = 100µm). (Q-R) Representative CC1 (green) and DAPI (blue) immunostaining in the corpus callosum of non-CPZ *Mettl14$^{fl/fl}$;PDGFRα-Cre ERT* control (Q) and mutant (R) (scale bar = 100µm). (S) Quantification showing no significant difference between mutant and control numbers of PDGFR-$\alpha^+$ cells (OPCs) in non-CPZ *Mettl14$^{fl/fl}$;PDGFRα-Cre ERT* mice (n=3; p>0.05; unpaired Student's t-test). (T) Quantification showing significant reduction of mutant PDGFR-$\alpha^+METTL14^+$ double positive cells in the mutants in non-CPZ *Mettl14$^{fl/fl}$;PDGFRα-Cre ERT* mice (n=3; $^{***}p<0.001$; unpaired Student's t-test). (U) Quantification showing no significant difference between control and mutant numbers of PDGFR-$\alpha^+$ and $Ki67^+$ double positive cells in non-CPZ *Mettl14$^{fl/fl}$;PDGFRα-Cre ERT* mice (n=3; p>0.05; unpaired Student's t-test). (V) Quantification showing no significant difference between control and mutant numbers of $BCAS1^+$ $SOX10^+$ double positive cells in non-CPZ *Mettl14$^{fl/fl}$;PDGFRα-Cre ERT* mice (n=3; p>0.05; unpaired Student's t-test). (W) Quantification showing no significant difference between control and mutant numbers of CC1+ cells in non-CPZ *Mettl14$^{fl/fl}$;PDGFRα-Cre ERT* mice (n=3; p>0.05; unpaired Student's t-test).

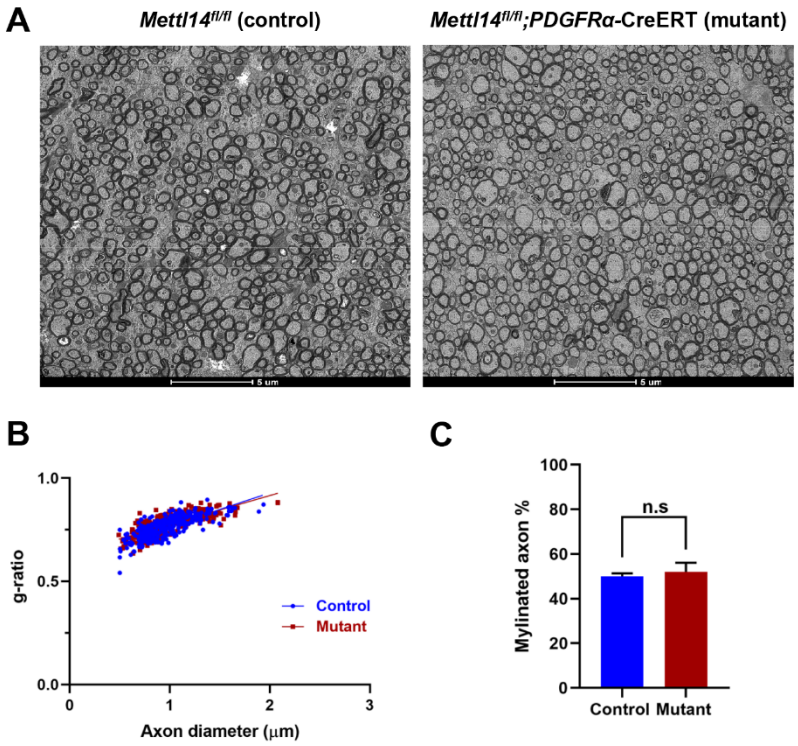


**Figure 3.3. *Mettl14* ablation in adult OPCs does not lead to myelin pathology**
(A) Representative EM images of corpus callosum non-CPZ *Mettl14$^{fl/fl}$;PDGFRα-Cre ERT* control and mutant animals (Scale bar = 5μm). (B) g-ratio analyze showing no significant difference between non-CPZ *Mettl14$^{fl/fl}$;PDGFRα-Cre ERT* control and mutant animals (n = 3; p>0.05; unpaired Student's t test). (C) Percentage of myelinated axons in corpus callosum showing no difference between non-CPZ *Mettl14$^{fl/fl}$;PDGFRα-Cre ERT* control and mutant animals (N=3, p>0.05; unpaired Student's t test)

### 3.3.2 *Mettl14* ablation leads to severe demyelination at peak disease

To determine the role of *Mettl14* in OPCs during demyelination stage, we examined oligodendrocyte lineage at different lineage stages using immunohistochemistry in *Mettl14$^{fl/fl}$;PDGFRα*-CreERT mice' corpus callosum. We used PDGFR-α to detect OPCs. Surprisingly, we found the OPCs are significantly decreased in the mutants when compared to controls (Fig 3.4 A, B, C, D, M). However, proliferating OPCs were not changed in the mutants, as shown by the quantification of PDGFR-α and Ki67 double staining cells (Fig 3.4 E, F, N). It

suggests that *Mettl14* deletion may impair the ability of OPCs' survival in the inhibitory environment created by demyelination (Saraswat et al., 2021), while not affecting the proliferating OPCs. We also examined the early myelinating cells using SOX10 and BCAS1 double staining, and we found that there was no difference of this cell population (Fig 3.4 G, H, O). Interestingly, we found there was significant reduction of CC1+ cells at peak demyelination stage, even though there was no detectable signal loss in the myelin (Fig 3.4 K, L, P). To further examine the myelin pathology, we applied EM analysis. In accordance with oligodendrocyte loss, mutants have significantly higher percentage of non-myelinated axons (Fig 3.4 Q, S). In addition the myelin in the mutants was significantly thinner, reflected by the quantification of g-ratio (Fig 3.4 Q, R). These results indicate that *Mettl14* deletion in the OPCs may affect the survival of mature oligodendrocytes and myelin stability. Studies have shown OPCs collaborate with other glia cells, and crosstalk with neurons upon injury (Fernandez-Castaneda and Gaultier, 2016). They can actively participate in the amplification of pathology in the demyelination mouse model (Kang et al., 2013). Further studies are required to elucidate how $m^6A$ dysregulation results in severe demyelination at peak disease.

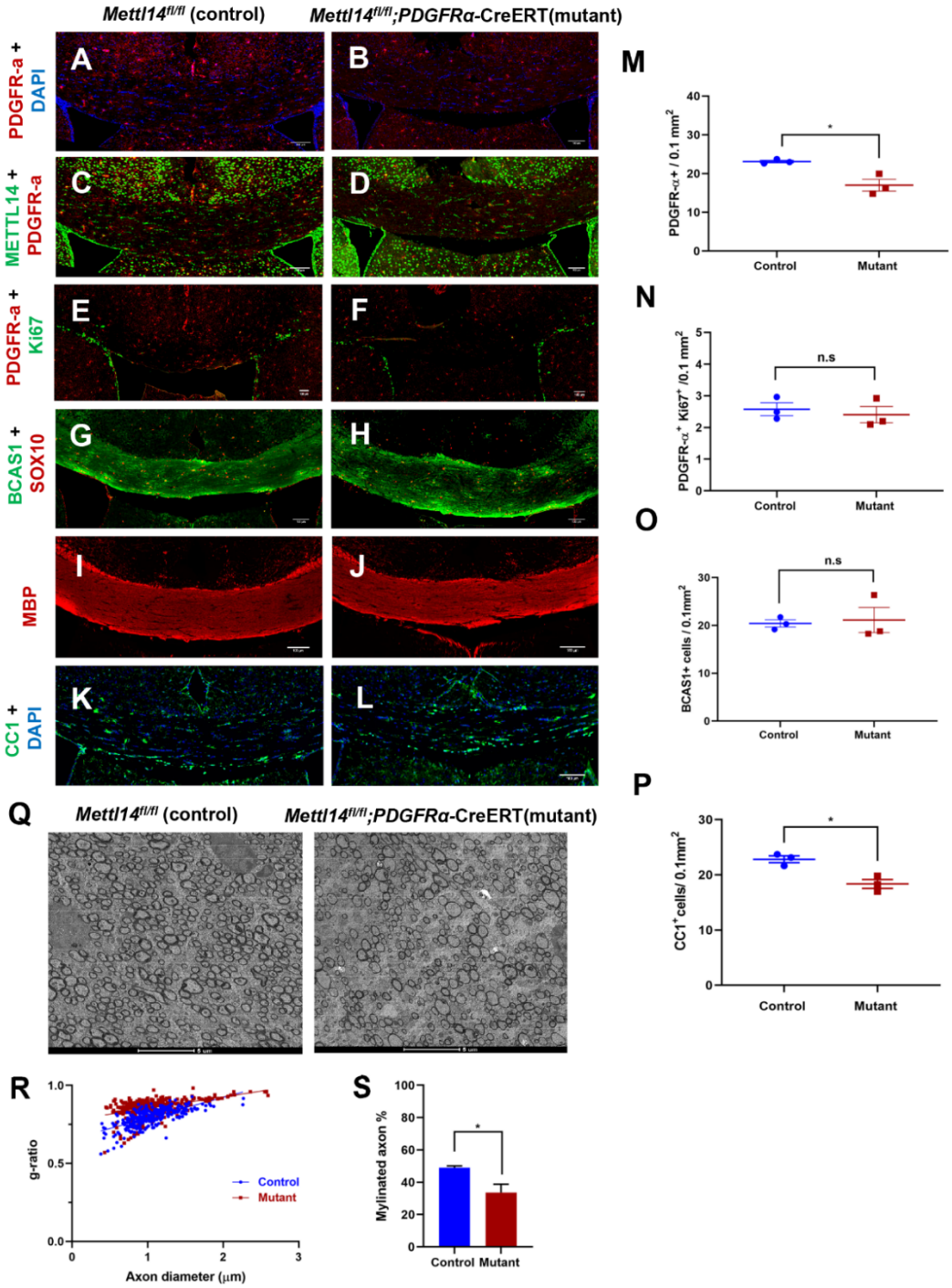


**Figure 3.4. *Mettl14* ablation in adult OPCs leads to severe demyelination at peak disease**
(A-B) Representative PDGFR-α (red) and DAPI (blue) immunostaining in the corpus callosum of peak disease *Mettl14$^{fl/fl}$;PDGFRα-Cre ERT* control (A) and mutant (B) (scale bar = 100μm). (C-D) Representative PDGFR-α (red) and METTL14 (green) immunostaining in the corpus callosum of peak disease *Mettl14$^{fl/fl}$;PDGFRα-Cre ERT* control (C) and mutant (D) (scale bar = 100μm).

(E-F) Representative PDGFR-α (red) and Ki67 (green) immunostaining in the corpus callosum of peak disease *Mettl14$^{fl/fl}$;PDGFRα-Cre ERT* control (K) and mutant (L) (scale bar = 100µm). (G-H) Representative SOX10 (red) and BCAS1 (green) immunostaining in the corpus callosum of peak disease *Mettl14$^{fl/fl}$;PDGFRα-Cre ERT* control (M) and mutant (N) (scale bar = 100µm). (I-J) Representative MBP (red) ) immunostaining in the corpus callosum of peak disease *Mettl14$^{fl/fl}$;PDGFRα-Cre ERT* control (O) and mutant (P) (scale bar = 100µm). (K-L) Representative CC1 (green) and DAPI (blue) immunostaining in the corpus callosum of peak disease *Mettl14$^{fl/fl}$;PDGFRα-Cre ERT* control (Q) and mutant (R) (scale bar = 100µm). (M) Quantification showing significant reduction of PDGFR-α$^{+}$ cells in mutant peak disease *Mettl14$^{fl/fl}$;PDGFRα-Cre ERT* mice (n=3; $p^{*}<0.05$; unpaired Student's t-test). (N) Quantification showing no significant difference between control and mutant numbers of PDGFR-α$^{+}$ and Ki67$^{+}$ double positive cells in peak disease *Mettl14$^{fl/fl}$;PDGFRα-Cre ERT* mice (n=3; $p>0.05$; unpaired Student's t-test). (O) Quantification showing no significant difference between control and mutant numbers of BCAS1$^{+}$ SOX10$^{+}$ double positive cells in peak disease *Mettl14$^{fl/fl}$;PDGFRα-Cre ERT* mice (n=3; $p>0.05$; unpaired Student's t-test). (P) Quantification showing significant reduction of CC1+ cells in the mutant peak disease *Mettl14$^{fl/fl}$;PDGFRα-Cre ERT* mice (n=3; $p^{*}<0.05$; unpaired Student's t-test). (Q) Representative EM images of corpus callosum of peak disease *Mettl14$^{fl/fl}$;PDGFRα-Cre ERT* control and mutant animals (Scale bar = 5µm). (R) g-ratio analyze showing significant increased g-ratio in mutant peak disease *Mettl14$^{fl/fl}$;PDGFRα-Cre ERT* animals (n = 3; $p^{**}<0.01$; unpaired Student's t test) (S). Percentage of myelinated axons in corpus callosum showing significant reduction in mutant peak disease *Mettl14$^{fl/fl}$;PDGFRα-Cre ERT* animals (N=3, $p^{*}<0.05$; unpaired Student's t test)

### 3.3.3 *Mettl14* ablation leads to early remyelination abnormalities

In order to characterize the effects of *Mettl14* deletion in the OPCs at early remyelination stage, we examined the oligodendrocyte lineage cells at different stages. We observed no difference of OPCs numbers between mutants and controls using PDGFR-α (Fig 3.5 A, B, C, D, M). And we did not observe difference of proliferating OPCs numbers with PDGFR-α and Ki67 double staining (Fig 3.5 E, F, N). Interestingly, we did not detect difference of early myelinating cells between mutants and controls (Figure 3.5 G, H, O). However, we detected significantly reduced numbers of mature oligodendrocytes marked with CC1 (Fig 3.5 K, L, P). These results indicate *Mettl14* deletion in the OPCs impairs the oligodendrocytes maturation during early remyelination stage. In

accordance with this result, we found significant thinner myelin quantified by g-ratio, and significantly lower percentage of myelinated axons in the corpus callosum by EM (Fig 3.5 Q, R, S).

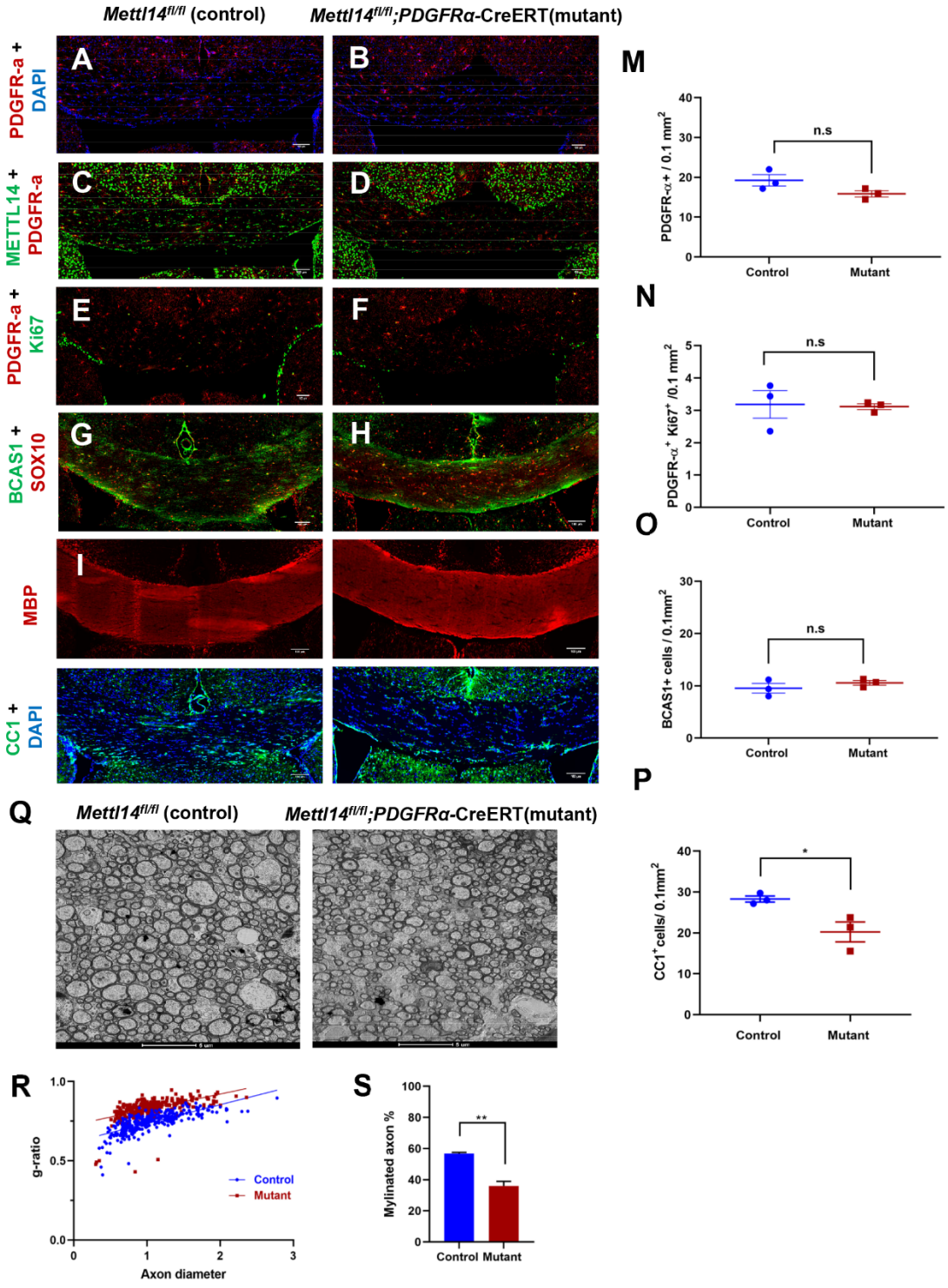


**Figure 3.5. *Mettl14* ablation in adult OPCs leads to early remyelination abnormalities**
(A-B) Representative PDGFR-α (red) and DAPI (blue) immunostaining in the corpus callosum of early remyelination *Mettl14$^{fl/fl}$;PDGFRα-Cre ERT* control (A) and mutant (B) (scale bar = 100µm).

(C-D) Representative PDGFR-α (red) and METTL14 (green) immunostaining in the corpus callosum of early remyelination *Mettl14$^{fl/fl}$;PDGFRα-Cre ERT* control (C) and mutant (D) (scale bar = 100μm). (E-F) Representative PDGFR-α (red) and Ki67 (green) immunostaining in the corpus callosum of early remyelination *Mettl14$^{fl/fl}$;PDGFRα-Cre ERT* control (K) and mutant (L) (scale bar = 100μm). (G-H) Representative SOX10 (red) and BCAS1 (green) immunostaining in the corpus callosum of early remyelination *Mettl14$^{fl/fl}$;PDGFRα-Cre ERT* control (M) and mutant (N) (scale bar = 100μm). (I-J) Representative MBP (red) immunostaining in the corpus callosum of early remyelination *Mettl14$^{fl/fl}$;PDGFRα-Cre ERT* control (O) and mutant (P) (scale bar = 100μm). (K-L) Representative CC1 (green) and DAPI (blue) immunostaining in the corpus callosum of early remyelination *Mettl14$^{fl/fl}$;PDGFRα-Cre ERT* control (Q) and mutant (R) (scale bar = 100μm). (M) Quantification showing no significant difference between mutant and control numbers of PDGFR-α$^{+}$ cells in early remyelination *Mettl14$^{fl/fl}$;PDGFRα-Cre ERT* mice (n=3; p>0.05; unpaired Student's t-test). (N) Quantification showing no significant difference between control and mutant numbers of PDGFR-α$^{+}$ Ki67$^{+}$ double positive cells in early remyelination *Mettl14$^{fl/fl}$;PDGFRα-Cre ERT* mice (n=3; p>0.05; unpaired Student's t-test). (O) Quantification showing no significant difference between control and mutant numbers of BCAS1$^{+}$ SOX10$^{+}$ double positive cells in early remyelination *Mettl14$^{fl/fl}$;PDGFRα-Cre ERT* mice (n=3; p>0.05; unpaired Student's t-test). (P) Quantification showing significant reduction of CC1+ cells in the mutant early remyelination *Mettl14$^{fl/fl}$;PDGFRα-Cre ERT* mice (n=3; p$^{*}$<0.05; unpaired Student's t-test). (Q) Representative EM images of corpus callosum of early remyelination *Mettl14$^{fl/fl}$;PDGFRα-Cre ERT* control and mutant animals (Scale bar = 5μm). (R) g-ratio analyze showing significant increased g-ratio in mutant early remyelination *Mettl14$^{fl/fl}$;PDGFRα-Cre ERT* animals (n = 3; p$^{***}$<0.001; unpaired Student's t test) (S) Percentage of myelinated axons in corpus callosum showing significant reduction in mutant early remyelination *Mettl14$^{fl/fl}$;PDGFRα-Cre ERT* animals (N=3, p$^{**}$<0.01; unpaired Student's t test)

### 3.3.4 *Mettl14* ablation leads to late remyelination abnormalities

To further examine the effects of *Mettl14* deletion in the OPCs at full remyelination stage, we also detected oligodendrocyte lineage cells at different remyelination stages by immunohistochemistry. There was no difference of OPCs numbers between mutants and controls using PDGFR-α (Fig 3.6 A, B, C, D, M). And we did not observe difference of proliferating OPCs numbers, either, by PDGFR-α and Ki67 double staining (Fig 3.6 E, F, N). Similar to what we observed at early remyelinating stage, we did not detect difference of early myelinating cells (Fig 3.6 G, H, O). We

also detected significantly reduced numbers of mature oligodendrocytes using CC1 staining (Fig 3.6 K, L, P). EM results showed significant thinner myelin, quantified by g-ratio, and significantly lower percentage of myelinated axons in the corpus callosum (Fig 3.6 Q, R, S). These results suggest *Mettl14* deletion in the adult OPCs impairs oligodendrocyte maturation, but not early myelinating cells, at full remyelination stage. Interestingly, our previous data showed that after *Mettl14* deletion in the oligodendrocyte lineage cells, OPCs could not form MBP+ cells and could not develop into mature oligodendrocytes during development (Xu et al., 2020). This is highly correlated with the results we observed in the remyelinating brains with *Mettl14* deleted in adult OPCs, suggesting that $m^6A$ modification affects the post-mitotic oligodendrocytes maturation at both developmental stage and adulthood.

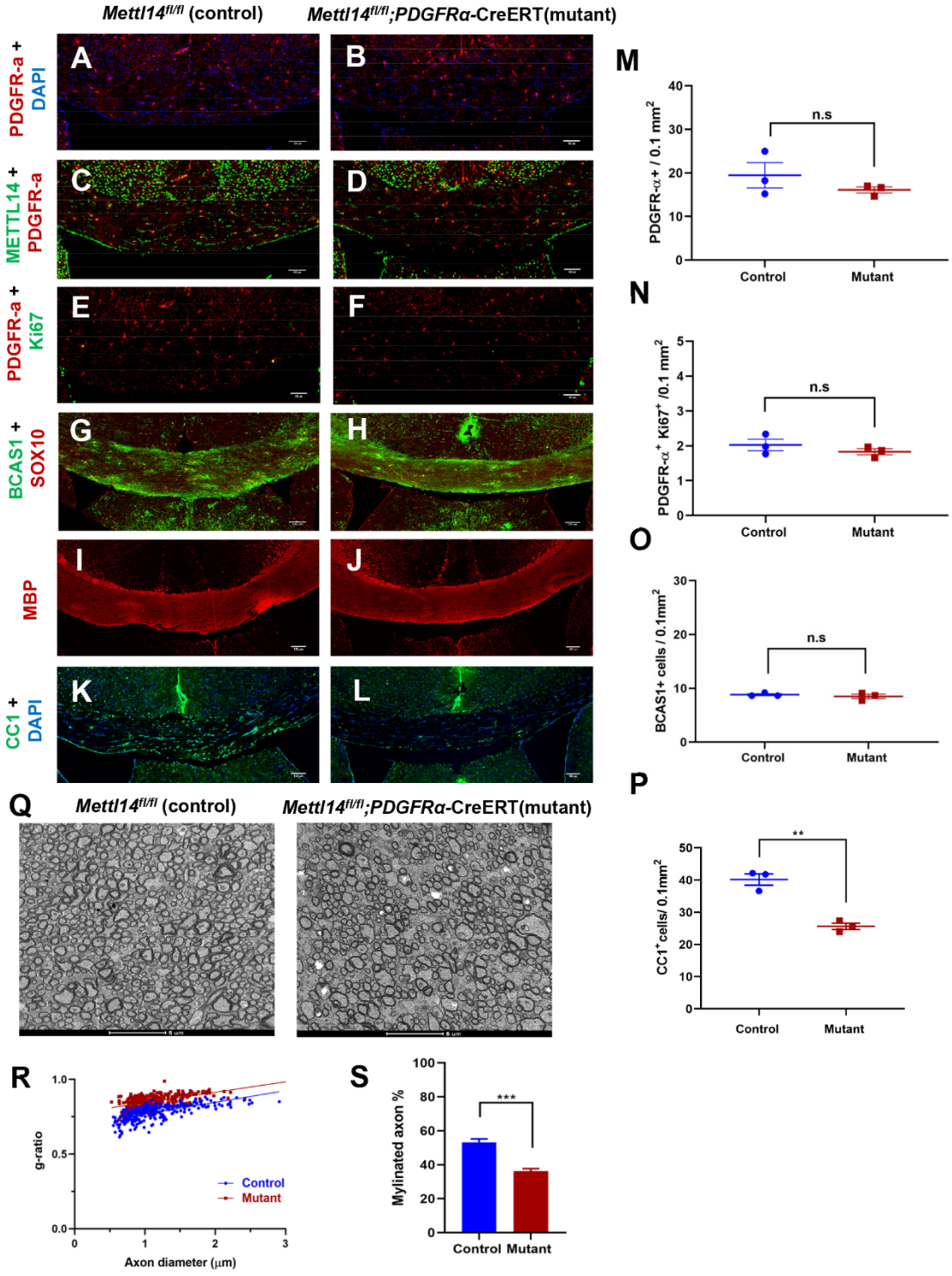


**Figure 3.6. *Mettl14* ablation in adult OPCs leads to late remyelination abnormalities**
(A-B) Representative PDGFR-α (red) and DAPI (blue) immunostaining in the corpus callosum of late remyelination *Mettl14$^{fl/fl}$;PDGFRα-Cre ERT* control (A) and mutant (B) (scale bar = 100μm). (C-D) Representative PDGFR-α (red) and METTL14 (green) immunostaining in the corpus

callosum of late remyelination *Mettl14$^{fl/fl}$;PDGFRα-Cre ERT* control (C) and mutant (D) (scale bar = 100μm).(E-F) Representative PDGFR-α (red) and Ki67 (green) immunostaining in the corpus callosum of late remyelination *Mettl14$^{fl/fl}$;PDGFRα-Cre ERT* control (K) and mutant (L) (scale bar = 100μm).(G-H) Representative SOX10 (red) and BCAS1 (green) immunostaining in the corpus callosum of late remyelination *Mettl14$^{fl/fl}$;PDGFRα-Cre ERT* control (M) and mutant (N) (scale bar = 100μm).(I-J) Representative MBP (red) immunostaining in the corpus callosum of late remyelination *Mettl14$^{fl/fl}$;PDGFRα-Cre ERT* control (O) and mutant (P) (scale bar = 100μm).(K-L) Representative CC1 (green) and DAPI (blue) immunostaining in the corpus callosum of late remyelination *Mettl14$^{fl/fl}$;PDGFRα-Cre ERT* control (Q) and mutant (R) (scale bar = 100μm).(M) Quantification showing no significant difference between mutant and control numbers of PDGFR-α$^{+}$ cells in late remyelination *Mettl14$^{fl/fl}$;PDGFRα-Cre ERT* mice (n=3; p>0.05; unpaired Student's t-test).(N) Quantification showing no significant difference between control and mutant numbers of PDGFR-α$^{+}$ Ki67$^{+}$ double positive cells in late remyelination *Mettl14$^{fl/fl}$;PDGFRα-Cre ERT* mice (n=3; p>0.05; unpaired Student's t-test).(O) Quantification showing no significant difference between control and mutant numbers of BCAS1$^{+}$ SOX10$^{+}$ double positive cells in late remyelination *Mettl14$^{fl/fl}$;PDGFRα-Cre ERT* mice (n=3; p>0.05; unpaired Student's t-test).(P) Quantification showing significant reduction of CC1+ cells in the mutant late remyelination *Mettl14$^{fl/fl}$;PDGFRα-Cre ERT* mice (n=3; p$^{***}$<0.001; unpaired Student's t-test).(Q) Representative EM images of corpus callosum of late remyelination *Mettl14$^{fl/fl}$;PDGFRα-Cre ERT* control and mutant animals (Scale bar = 5μm). (R) g-ratio analyze showing significant increased g-ratio in mutant late remyelination *Mettl14$^{fl/fl}$;PDGFRα-Cre ERT* animals (n = 3; p$^{***}$<0.001; unpaired Student's t test).(S) Percentage of myelinated axons in corpus callosum showing significant reduction in mutant late remyelination *Mettl14$^{fl/fl}$;PDGFRα-Cre ERT* animals (N=3, p$^{**}$<0.01; unpaired Student's t test)

### 3.4 Discussion

Effective remyelination is essential in restoring demyelinated nerve fibers and CNS deficits after demyelination. It is important to understand the molecular mechanisms that regulate the remyelination process, which relies on the generation of newly formed mature oligodendrocytes from OPCs (Franklin and Ffrench-Constant, 2008) and involves OPC proliferation, migration and differentiation. Increasing evidence indicate epigenetic mechanisms such as histone modification and microRNAs play important roles in the remyelination process (Fan et al., 2017; Shen et al., 2008; Zhang et al., 2017b). Recently m$^{6}$A mRNA modification emerged as a critical post-

transcriptional mechanism that regulates cell lineage progression (Furlan et al., 2019; Weng et al., 2018b; Xu et al., 2020; Zhang et al., 2017a). We reported that $m^6A$ is accompanied with oligodendrocyte lineage progression and is critical for OPCs maturation during development in the CNS (Xu et al., 2020). Mechanistically, compared to DNA and protein methylation, $m^6A$ RNA modification has the potential for rapid transition of transcriptomes to drive cell lineage progression (Boo and Kim, 2020; Jiang et al., 2021).

In this study, we show that *Mettl14* deletion in adult OPCs impairs remyelination. Using *Mettl14*$^{fl/fl}$*;PDGFRα*-CreERT mouse line, we were able to examine different stages of oligodendrocyte lineage cells at different time points following demyelination and remyelination. We used CPZ, a copper chelator that disturbs mitochondrial enzymes that leads to apoptosis in the oligodendrocytes, to induce demyelination and spontaneous remyelination (Torkildsen et al., 2008). CPZ induces non-immune mediated oligodendrogliopathy and primary oligodendrocyte damage with preserved blood brain barrier (BBB) (Torkildsen et al., 2008). After *Mettl14* deletion in the adult OPCs following tamoxifen injection, we detected no difference of OPCs numbers before the onset of demyelination (Fig 3.7 A). This indicates *Mettl14* is not essential for adult OPCs survival. Nevertheless, we observed significant reduction of OPCs numbers at peak demyelination, when mice were undergone CPZ diet for 3 weeks. Since we did not observe the reduction of proliferating OPCs in the mutant animals (Fig 3.7 D), we hypothesis that *Mettl14* deletion could make non-proliferating OPCs more susceptible to inflammatory environment during demyelination (Praet et al., 2014). It's shown that CPZ activates astrocytes and microglial cells, which in turn promote pro-inflammatory cytokine secretion (Praet et al., 2014). The inflammatory cytokines could directly impact the functions and survival of the OPCs (Chew et al., 2005). Therefore, the heightened susceptibility of adult OPCs by the environment created by $m^6A$

dysregulation could be a possible explanation for the decreased OPCs in the mutants during demyelination. While CPZ is inducing demyelination, OPCs are proliferating and differentiating to remyelinate the axons (Sachs et al., 2014). As we showed in the immunohistochemistry and EM results, *Mettl14* deletion in the adult OPCs affect the remyelination process, which may explain the thinner myelin in the EM that we observed at peak disease (Fig 3.4 Q, R). In addition, the reduction of overall OPC (Fig 3.7 C) numbers at the demyelination and remyelination stages may reflect a temporary unbalanced homeostasis of OPCs production (Hughes et al., 2013) caused by the *Mettl14* deletion.

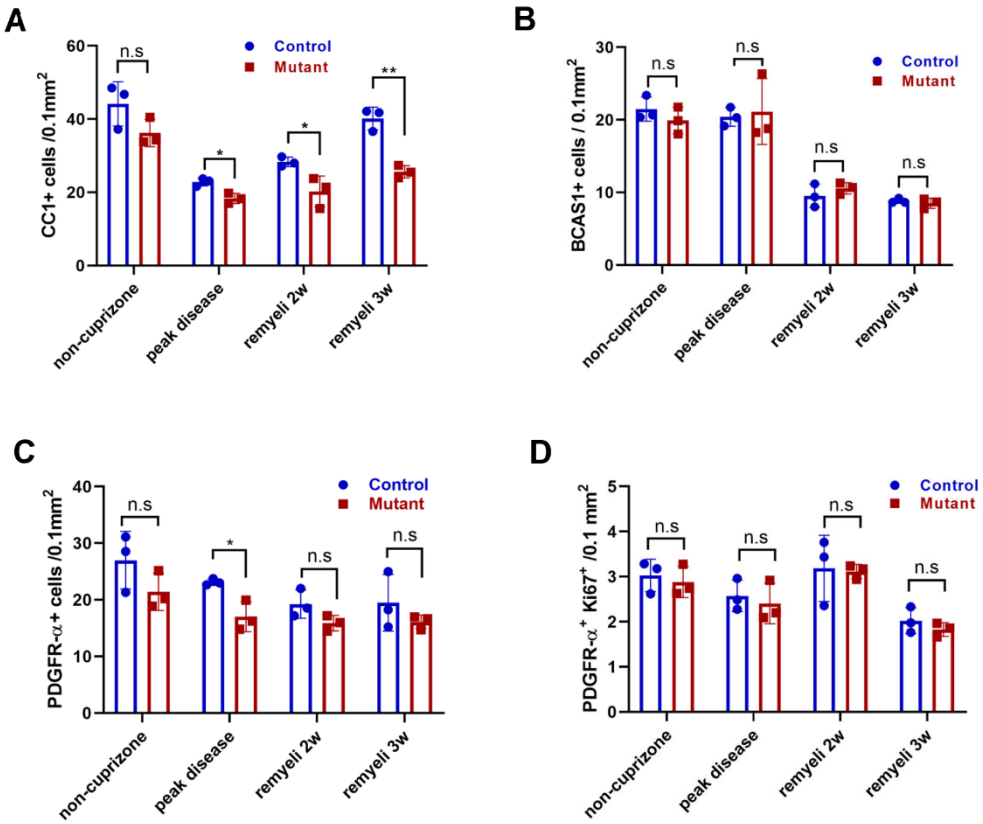


**Figure 3.7. Effects of *Mettl14* ablation in adult OPCs at different disease stages**
(A) Quantification of CC1+ cells in the mutant and control corpus callosum of *Mettl14$^{fl/fl}$;PDGFRα-Cre ERT* mice at different disease stages ($p^{*}<0.05$; $p^{**}<0.01$; unpaired Student's t-test). (B) Quantification of BCAS1$^{+}$ SOX10$^{+}$ double positive cells in the mutant and control corpus callosum of *Mettl14$^{fl/fl}$;PDGFRα-Cre ERT* mice at different disease stages ($p>0.05$;

unpaired Student's t-test). (C) Quantification of PDGFR-$\alpha^+$ cells in the mutant and control corpus callosum of *Mettl14$^{fl/fl}$;PDGFRα-Cre ERT* mice at different disease stages ($p>0.05$; $p^*<0.05$;unpaired Student's t-test). (D) Quantification of PDGFR-$\alpha^+$ Ki67$^+$ double positive cells in the mutant and control corpus callosum of *Mettl14$^{fl/fl}$;PDGFRα-Cre ERT* mice at different disease stages ($p>0.05$; unpaired Student's t-test).

The reduction of the mature oligodendrocytes at peak disease, early remyelination and late remyelination reflects the deficiency of mutant adult OPCs maturation (Fig 3.7 A), suggesting m$^6$A mRNA methylation is critical for the oligodendrocyte lineage progression during remyelination. Interestingly, we observed no difference of early myelinating oligodendrocytes at both demyelination and remyelination stages (Fig 3.7 B), suggesting m$^6$A mRNA regulation is more important for the late maturation stage than the early stage. In our previous study, we demonstrated that OPCs could not develop into mature oligodendrocytes after knocking out *Mettl14* in the lineage (*Mettl14$^{fl/fl}$;Olig2-Cre*) in vitro (Xu et al., 2020). However, when we cultured the cells that lack *Mettl14* only in the mature stage (*Mettl14$^{fl/fl}$;CNP-Cre*), the OPCs could differentiate into mature oligodendrocytes (unpublished data). We hypothesis that the severe block in maturation that occurs in the *Mettl14$^{fl/fl}$;Olig2-Cre* OPCs in vitro is the result of an m$^6$A deficiency early in the oligodendrocyte lineage (Xu et al., 2020). Our current data from *Mettl14$^{fl/fl}$;PDGFR α-CreERT* supports this hypothesis, that m$^6$A deficiency at OPCs stage is critical for the deficits of maturation. However, further studies are required to validate the potential differences of m$^6$A regulatory mechanisms in the oligodendrocyte lineage between development and adulthood. After all, m$^6$A modification displays dynamic regulation patterns during CNS development and aging at both temporal and spatial levels (Shafik et al., 2021). It will be interesting to study the dynamics of m$^6$A regulation by examining the adult oligodendrocyte lineage transcriptomes and the m$^6$A landscape of these transcriptomes at each stage during

demyelination and remyelination (Fig 3.1). To understand how m$^6$A deposition regulates post-transcriptional functions, multifaceted effects should be taken into consideration. Studies have found m$^6$A mark regulates alternative splicing, transcription, alternative polyadenylation, nuclear export, translation, mRNA degradation and mRNA stabilization (Han et al., 2017; He and He, 2021; Roundtree et al., 2017; Slobodin et al., 2017; Wang et al., 2014a; Xiao et al., 2016b; Zhou et al., 2018). It is important to look into these effects of m$^6$A dynamic deposition on oligodendrocyte lineage cell transcripts that are associated with remyelination. It will be particularly interesting to understand m$^6$A's effects on transcripts and their downstream targets that involve with important remyelination signaling pathways such as cholesterol-synthesis pathways (Voskuhl et al., 2019), and the collaborations with other remyelination-associated gene expression mechanisms such as histone modification, miRNAs and DNA methylation (Duffy and McCoy, 2020; Glaser, 2007; Moyon and Casaccia, 2017; Shen et al., 2008).

In summary, we showed that m$^6$A mRNA methylation is critical in regulating remyelination in the adult brain. This is the first study that identifies m$^6$A epigenetic mechanism's role during remyelination. It will be important and interesting to the field to further understand how m$^6$A regulates the remyelination process, which could ultimately contribute to identify the potential therapeutic targets for demyelination diseases such as MS.

## 3.5 Materials and methods

### 3.5.1 Animals

All animals were housed under pathogen-free conditions, and all animal procedures and animal care were conducted in accordance with guidelines approved by Northwestern Center of Comparative Medicine. All mice were on the C57BL/6 background, and both female and male mice were used. *Mettl14*$^{fl/fl}$ mice (Koranda et al., 2018; Weng et al., 2018b; Yoon et al., 2017) were

crossed with *PDGFRα-CreERT* (Generous gift from Dr.Dwight E Bergles, Johns Hopkins School of Medicine). *Mettl14*$^{fl/fl}$*;PDGFRα-CreERT* mutant littermate control *Mettl14*$^{fl/fl}$ mice were used.

### 3.5.2 Immunohistochemistry and cell counts

Mice were deeply anaesthetized with 2.5% avertin (Cat#T48402, Sigma Aldrich) in dH2O. Upon the loss of nociceptive reflexes, mice were transcardially perfused with 0.9% saline followed by ice-cold 4% paraformaldehyde (PFA). Brains were collected and post-fixed overnight in 4% PFA at 4ºC, followed by incubation in 30% sucrose until saturation. Tissues were then embedded in optimal cutting temperature compound (OCT) and sectioned at 10µm. Prior to Rabbit-anti-METTL14 (1:300, Sigma, Cat# HPA038002), Goat-anti-PDGFR-α (1:100, R and D systems, Cat# AF1062), Rabbit-anti-Ki67 (1:100, Abcam, cat# ab15580) , immunostaining, tissue sections were processed with an antibody retrieval protocol in which sections were treated with 10 mM trisodium citrate buffer (pH 6.0) at 90 ºC for 30 minutes. After cooling at room temperature (RT) for 30 minutes, sections were then incubated in 10 mM glycine (in TBS with 0.25% Triton X-100) for 1hour at RT. Slices were then blocked with TBS containing 5% normal donkey serum, 1% BSA and 0.25% Triton X-100 (blocking buffer) for 2 hours at RT, followed by incubation in primary antibody(s) diluted in blocking buffer for 48 hours at 4ºC. Immunohistochemistry with Rabbit-anti-MBP (1:500, Abcam, Cat# ab40390), Mouse-anti-CC1 (1:50, Milipore, Cat# OP80), and Mouse-anti-Olig2 (1:100, Milipore, Cat# MABN50) antibodies were followed by immunostaining protocol without antigen retrieval.

Stained tissue sections were imaged with a Mariana Yokogawa-type spinning disk confocal microscope or Leica TCS SP5 two-photon confocal microscope. All experimental and littermate control tissues were imaged with the same parameters, followed with the same adjustments in Image J (NIH). Cells counts data was converted to cells/100µm$^2$.

### 3.5.3 Electron Microscopy (EM) and analysis

Mice were deeply anesthetized with 2.5% avertin, followed by perfusion with 0.9% saline and 0.1M sodium cacodylate buffer containing 4% PFA and 2.5% glutaraldehyde (EM buffer). Corpus callosum and optic nerve were then post-fixed overnight at 4$^{o}$C. Tissues were dissected and washed with 0.1M sodium cacodylate buffer for 3 times, followed by post fixation with 1% osmium tetroxide (diluted with 0.1M sodium cacodylate) for 2 hours and another 3 times of wash with 0.1M sodium cacodylate buffer. These tissue samples then went through dehydration steps with 30%, 50%, 70%, 90%, 95%,100% ethanol and propylene oxide (PO), followed by permeation with 1:1 PO/Epon 812 and 1:2 PO/Epon 812 for 2 hours each, and in Epon 812 overnight at RT. The next morning, samples were permeated with Epon 812 for another 4 hours at RT, and then embedded with labeled paper strips in fresh Epon 812. These samples were then cured for 48 hours in a 60$^{o}$C oven. After EM processing steps, samples were sectioned (1μm) and stained with toluidine blue, before sectioned into ultrathin slices (60-90nm) and stained with uranyl acetate-lead citrate. FEI Tecnai F30 scanning transmission electron microscope (FEI company) was used to take EM images. Image J was used to analyze the EM images for g-ratio and axon counting.

### 3.5.4 Statistical analysis

All immunohistochemistry and electron microscopy data obtained from experimental and control mice were compared with a two-tailed unpaired Student's t-test. Data were presented as mean $\pm$ SEM. A p value of less-than 0.05 was considered significant. Analysis was done using GraphPad Prism version 8.00 for Windows (GraphPad Software) and Microsoft Office Excel 2016.

### 3.5.5 Reagents

**Table 3.1: Reagents table**

| REAGENT or RESOURCE | SOURCE | IDENTIFIER |
|---|---|---|
| **Antibodies** | | |
| Rabbit anti-METTL14 | Sigma-Aldrich | Cat# HPA038002; RRID: AB_10672401 |
| Goat anti-PDGFR-α | R&D Systems | Cat# AF1062; RRID: AB_2236897 |
| Rabbit anti-MBP | Abcam | Cat# ab40390; RRID: AB_1141521 |
| Mouse anti-CC1 | Millipore | Cat# OP80; RRID: AB_2057371 |
| Mouse anti-Olig2 | Millipore | Cat# MABN50; RRID: AB_10807410 |
| Mouse anti-BCAS1 | Santa Cruz | Cat# sc-136342; RRID: AB_10839529 |
| Rabbit anti-Ki67 | Abcam | Cat# AB15580; RRID: AB_805388 |
| Donkey Anti-mouse IgG (H+L), Alexa Fluor 488 | Thermo Fisher Scientific | Cat# A-21202; RRID: AB_141607 |
| Donkey Anti-Rabbit IgG (H+L) Antibody, Alexa Fluor 488 | Thermo Fisher Scientific | Cat# A-21206; RRID: AB_2535792 |
| Donkey Anti-Mouse IgG (H+L), Alexa Fluor 594 | Thermo Fisher Scientific | Cat# A-21203; RRID: AB_2535789 |
| Donkey Anti-Goat IgG (H+L), Alexa Fluor 594 | Thermo Fisher Scientific | Cat# A-11058; RRID: AB_2534105 |
| Donkey Anti-Rabbit IgG (H+L), Alexa Fluor 594 | Thermo Fisher Scientific | Cat# A-21207; RRID: AB_141637 |
| Fetal bovine serum | Atlanta Biologicals | Cat# S11050 |
| Normal donkey serum | Jackson ImmunoResearch | Cat# 017-000-121 |
| Paraformadehyde | Thermo Fisher Scientific | Cat# T353-500 |
| Osmium Tetroxide | Electron Microscopy Science | Cat# 19152 |
| Propylene Oxide | Electron Microscopy Science | Cat# 20401 |
| Sodium Cacodylate Buffer | Electron Microscopy Science | Cat# 11652 |
| Epon 812 | Electron Microscopy Science | Cat# 14900 |

### 3.6 References

Boo, S.H., and Kim, Y.K. (2020). The emerging role of RNA modifications in the regulation of mRNA stability. Exp Mol Med *52*, 400–408.

Casella, C., Lipp, I., Rosser, A., Jones, D.K., and Metzler-Baddeley, C. (2020). A critical review of white matter changes in huntington's disease. Mov. Disord. *35*, 1302–1311.

Chew, L.-J., King, W.C., Kennedy, A., and Gallo, V. (2005). Interferon-gamma inhibits cell cycle exit in differentiating oligodendrocyte progenitor cells. Glia *52*, 127–143.

Chiang, P.-L., Chen, H.-L., Lu, C.-H., Chen, P.-C., Chen, M.-H., Yang, I.-H., Tsai, N.-W., and Lin, W.-C. (2017). White matter damage and systemic inflammation in Parkinson's disease. BMC Neurosci. *18*, 48.

Cortese, I., Reich, D.S., and Nath, A. (2021). Progressive multifocal leukoencephalopathy and the spectrum of JC virus-related disease. Nat. Rev. Neurol. *17*, 37–51.

De la Fuente, A.G., Queiroz, R.M.L., Ghosh, T., McMurran, C.E., Cubillos, J.F., Bergles, D.E., Fitzgerald, D.C., Jones, C.A., Lilley, K.S., Glover, C.P., et al. (2020). Changes in the Oligodendrocyte Progenitor Cell Proteome with Ageing. Mol. Cell Proteomics *19*, 1281–1302.

Duffy, C.P., and McCoy, C.E. (2020). The role of micrornas in repair processes in multiple sclerosis. Cells *9*.

El Waly, B., Macchi, M., Cayre, M., and Durbec, P. (2014). Oligodendrogenesis in the normal and pathological central nervous system. Front. Neurosci. *8*, 145.

Fan, H.-B., Chen, L.-X., Qu, X.-B., Ren, C.-L., Wu, X.-X., Dong, F.-X., Zhang, B.-L., Gao, D.-S., and Yao, R.-Q. (2017). Transplanted miR-219-overexpressing oligodendrocyte precursor cells promoted remyelination and improved functional recovery in a chronic demyelinated model. Sci. Rep. *7*, 41407.

Fard, M.K., van der Meer, F., Sánchez, P., Cantuti-Castelvetri, L., Mandad, S., Jäkel, S., Fornasiero, E.F., Schmitt, S., Ehrlich, M., Starost, L., et al. (2017). BCAS1 expression defines a population of early myelinating oligodendrocytes in multiple sclerosis lesions. Sci. Transl. Med. *9*.

Fernandez-Castaneda, A., and Gaultier, A. (2016). Adult oligodendrocyte progenitor cells - Multifaceted regulators of the CNS in health and disease. Brain Behav. Immun. *57*, 1–7.

Franklin, R.J.M. (2002). Why does remyelination fail in multiple sclerosis? Nat. Rev. Neurosci. *3*, 705–714.

Franklin, R.J.M., and Ffrench-Constant, C. (2008). Remyelination in the CNS: from biology to therapy. Nat. Rev. Neurosci. *9*, 839–855.

Furlan, M., Galeota, E., de Pretis, S., Caselle, M., and Pelizzola, M. (2019). m6A-Dependent RNA Dynamics in T Cell Differentiation. Genes (Basel) *10*.

Glaser, K.B. (2007). HDAC inhibitors: clinical update and mechanism-based potential. Biochem. Pharmacol. *74*, 659–671.

Han, R., Slobodin, B., and Agami, R. (2017). The methylated way to translation. Oncotarget *8*, 93313–93314.

He, P.C., and He, C. (2021). m6 A RNA methylation: from mechanisms to therapeutic potential. EMBO J. *40*, e105977.

Hughes, E.G., Kang, S.H., Fukaya, M., and Bergles, D.E. (2013). Oligodendrocyte progenitors balance growth with self-repulsion to achieve homeostasis in the adult brain. Nat. Neurosci. *16*, 668–676.

Jiang, X., Liu, B., Nie, Z., Duan, L., Xiong, Q., Jin, Z., Yang, C., and Chen, Y. (2021). The role of m6A modification in the biological functions and diseases. Signal Transduct. Target. Ther. *6*, 74.

Kang, Z., Wang, C., Zepp, J., Wu, L., Sun, K., Zhao, J., Chandrasekharan, U., DiCorleto, P.E., Trapp, B.D., Ransohoff, R.M., et al. (2013). Act1 mediates IL-17-induced EAE pathogenesis selectively in NG2+ glial cells. Nat. Neurosci. *16*, 1401–1408.

Karttunen, M.J., Czopka, T., Goedhart, M., Early, J.J., and Lyons, D.A. (2017). Regeneration of myelin sheaths of normal length and thickness in the zebrafish CNS correlates with growth of axons in caliber. PLoS One *12*, e0178058.

Koranda, J.L., Dore, L., Shi, H., Patel, M.J., Vaasjo, L.O., Rao, M.N., Chen, K., Lu, Z., Yi, Y., Chi, W., et al. (2018). Mettl14 is essential for epitranscriptomic regulation of striatal function and learning. Neuron *99*, 283–292.e5.

Del Maschio, N., Sulpizio, S., Toti, M., Caprioglio, C., Del Mauro, G., Fedeli, D., and Abutalebi, J. (2020). Second language use rather than second language knowledge relates to changes in white matter microstructure. J. Cult. Cogn. Sci. *4*, 165–175.

McDonald, J.W., and Belegu, V. (2006). Demyelination and remyelination after spinal cord injury. J. Neurotrauma *23*, 345–359.

McKenzie, I.A., Ohayon, D., Li, H., de Faria, J.P., Emery, B., Tohyama, K., and Richardson, W.D. (2014). Motor skill learning requires active central myelination. Science *346*, 318–322.

Moyon, S., and Casaccia, P. (2017). DNA methylation in oligodendroglial cells during developmental myelination and in disease. Neurogenesis (Austin) *4*, e1270381.

Moyon, S., Dubessy, A.L., Aigrot, M.S., Trotter, M., Huang, J.K., Dauphinot, L., Potier, M.C., Kerninon, C., Melik Parsadaniantz, S., Franklin, R.J.M., et al. (2015). Demyelination causes adult CNS progenitors to revert to an immature state and express immune cues that support their migration. J. Neurosci. *35*, 4–20.

Nazem-Zadeh, M.-R., Chapman, C.H., Lawrence, T.L., Tsien, C.I., and Cao, Y. (2012). Radiation therapy effects on white matter fiber tracts of the limbic circuit. Med. Phys. *39*, 5603–5613.

Pan, S., Mayoral, S.R., Choi, H.S., Chan, J.R., and Kheirbek, M.A. (2020). Preservation of a remote fear memory requires new myelin formation. Nat. Neurosci. *23*, 487–499.

Papuć, E., and Rejdak, K. (2020). The role of myelin damage in Alzheimer's disease pathology. Arch. Med. Sci. *16*, 345–351.

Peters, A. (2009). The effects of normal aging on myelinated nerve fibers in monkey central nervous system. Front. Neuroanat. *3*, 11.

Praet, J., Guglielmetti, C., Berneman, Z., Van der Linden, A., and Ponsaerts, P. (2014). Cellular and molecular neuropathology of the cuprizone mouse model: clinical relevance for multiple sclerosis. Neurosci. Biobehav. Rev. *47*, 485–505.

Roundtree, I.A., Luo, G.-Z., Zhang, Z., Wang, X., Zhou, T., Cui, Y., Sha, J., Huang, X., Guerrero, L., Xie, P., et al. (2017). YTHDC1 mediates nuclear export of N6-methyladenosine methylated mRNAs. Elife *6*.

Sachs, H.H., Bercury, K.K., Popescu, D.C., Narayanan, S.P., and Macklin, W.B. (2014). A new model of cuprizone-mediated demyelination/remyelination. ASN Neuro *6*.

Saraswat, D., Shayya, H.J., Polanco, J.J., Tripathi, A., Welliver, R.R., Pol, S.U., Seidman, R.A., Broome, J.E., O'Bara, M.A., van Kuppervelt, T.H., et al. (2021). Overcoming the inhibitory microenvironment surrounding oligodendrocyte progenitor cells following experimental demyelination. Nat. Commun. *12*, 1923.

Segovia, K.N., McClure, M., Moravec, M., Luo, N.L., Wan, Y., Gong, X., Riddle, A., Craig, A., Struve, J., Sherman, L.S., et al. (2008). Arrested oligodendrocyte lineage maturation in chronic perinatal white matter injury. Ann. Neurol. *63*, 520–530.

Shafik, A.M., Zhang, F., Guo, Z., Dai, Q., Pajdzik, K., Li, Y., Kang, Y., Yao, B., Wu, H., He, C., et al. (2021). N6-methyladenosine dynamics in neurodevelopment and aging, and its potential role in Alzheimer's disease. Genome Biol. *22*, 17.

Shen, S., Sandoval, J., Swiss, V.A., Li, J., Dupree, J., Franklin, R.J.M., and Casaccia-Bonnefil, P. (2008). Age-dependent epigenetic control of differentiation inhibitors is critical for remyelination efficiency. Nat. Neurosci. *11*, 1024–1034.

Shi, H., Hu, X., Leak, R.K., Shi, Y., An, C., Suenaga, J., Chen, J., and Gao, Y. (2015). Demyelination as a rational therapeutic target for ischemic or traumatic brain injury. Exp. Neurol. *272*, 17–25.

Slobodin, B., Han, R., Calderone, V., Vrielink, J.A.F.O., Loayza-Puch, F., Elkon, R., and Agami, R. (2017). Transcription Impacts the Efficiency of mRNA Translation via Co-transcriptional N6-adenosine Methylation. Cell *169*, 326–337.e12.

Torkildsen, O., Brunborg, L.A., Myhr, K.M., and Bø, L. (2008). The cuprizone model for demyelination. Acta Neurol. Scand. Suppl *188*, 72–76.

Valny, M., Honsa, P., Kirdajova, D., Kamenik, Z., and Anderova, M. (2016). Tamoxifen in the Mouse Brain: Implications for Fate-Mapping Studies Using the Tamoxifen-Inducible Cre-loxP System. Front. Cell Neurosci. *10*, 243.

Voskuhl, R.R., Itoh, N., Tassoni, A., Matsukawa, M.A., Ren, E., Tse, V., Jang, E., Suen, T.T., and Itoh, Y. (2019). Gene expression in oligodendrocytes during remyelination reveals cholesterol homeostasis as a therapeutic target in multiple sclerosis. Proc. Natl. Acad. Sci. USA *116*, 10130–10139.

Wang, X., Lu, Z., Gomez, A., Hon, G.C., Yue, Y., Han, D., Fu, Y., Parisien, M., Dai, Q., Jia, G., et al. (2014). N6-methyladenosine-dependent regulation of messenger RNA stability. Nature *505*, 117–120.

Weng, Y.-L., Wang, X., An, R., Cassin, J., Vissers, C., Liu, Y., Liu, Y., Xu, T., Wang, X., Wong, S.Z.H., et al. (2018). Epitranscriptomic m6a regulation of axon regeneration in the adult mammalian nervous system. Neuron *97*, 313–325.e6.

Xiao, L., Ohayon, D., McKenzie, I.A., Sinclair-Wilson, A., Wright, J.L., Fudge, A.D., Emery, B., Li, H., and Richardson, W.D. (2016a). Rapid production of new oligodendrocytes is required in the earliest stages of motor-skill learning. Nat. Neurosci. *19*, 1210–1217.

Xiao, W., Adhikari, S., Dahal, U., Chen, Y.-S., Hao, Y.-J., Sun, B.-F., Sun, H.-Y., Li, A., Ping, X.-L., Lai, W.-Y., et al. (2016b). Nuclear m(6)A Reader YTHDC1 Regulates mRNA Splicing. Mol. Cell *61*, 507–519.

Xin, W., and Chan, J.R. (2020). Myelin plasticity: sculpting circuits in learning and memory. Nat. Rev. Neurosci. *21*, 682–694.

Xu, H., Dzhashiashvili, Y., Shah, A., Kunjamma, R.B., Weng, Y.-L., Elbaz, B., Fei, Q., Jones, J.S., Li, Y.I., Zhuang, X., et al. (2020). m6A mRNA Methylation Is Essential for Oligodendrocyte Maturation and CNS Myelination. Neuron *105*, 293–309.e5.

Yoon, K.-J., Ringeling, F.R., Vissers, C., Jacob, F., Pokrass, M., Jimenez-Cyrus, D., Su, Y., Kim, N.-S., Zhu, Y., Zheng, L., et al. (2017). Temporal control of mammalian cortical neurogenesis by m6a methylation. Cell *171*, 877–889.e17.

Zhang, C., Chen, Y., Sun, B., Wang, L., Yang, Y., Ma, D., Lv, J., Heng, J., Ding, Y., Xue, Y., et al. (2017a). m6A modulates haematopoietic stem and progenitor cell specification. Nature *549*, 273–276.

Zhang, J., Zhang, Z.G., Lu, M., Wang, X., Shang, X., Elias, S.B., and Chopp, M. (2017b). MiR-146a promotes remyelination in a cuprizone model of demyelinating injury. Neuroscience *348*, 252–263.

Zhou, J., Wan, J., Shu, X.E., Mao, Y., Liu, X.-M., Yuan, X., Zhang, X., Hess, M.E., Brüning, J.C., and Qian, S.-B. (2018). N6-Methyladenosine Guides mRNA Alternative Translation during Integrated Stress Response. Mol. Cell *69*, 636–647.e7.

(1984). Oligodendroglia (Boston, MA: Springer US).

# CHAPTER 4

# Conclusion and perspective

## 4.1 Summary

Oligodendrocytes are myelin-producing cells in the central nervous system (CNS) that play essential roles in CNS function, such as metabolic support to axons, motor circuits formation, learning, cognition and social behavior (Pepper et al., 2018). Defects in oligodendrocytes lineage cell generation, proliferation, differentiation, myelination and maintenance can cause severe neurological disorders such as leukodystrophies and multiple sclerosis (MS). To achieve proper myelination during development, preventing and recovering from diseases, it is critical to understand the molecular mechanisms that regulate oligodendrocyte lineage functions both under physiological and pathological conditions (Berry et al., 2020). Oligodendrocyte lineage progression is a highly orchestrated process that requires precise coordination of a series of external and internal cues in time and space. Thus an understanding of the mechanisms that move beyond the genetic code into epigenetics field is essential (Gregath and Lu, 2018; Koreman et al., 2018). Previous studies have identified several key epigenetic regulators that enable the fine tuning and gene expression reprogramming during oligodendrocyte development and regeneration in response to the changes of microenvironment (Berry et al., 2020). These epigenetic regulators include chromatin remodelers, DNA methylation modifiers, histone modifiers, microRNAs, and long non-coding RNAs.

### 4.1.1 $m^6A$ mRNA methylation is an emerging post-transcriptional mechanism in neurological diseases

In chapter 1, I reviewed the molecular mechanisms that govern oligodendrocyte development, CNS myelination and remyelination. Specifically, I discussed the recent progress and findings of epigenetic regulators' functions during oligodendrocyte lineage progression and their roles in neurobiology diseases. As an emerging post-transcriptional mechanism, $m^6A$ mRNA methylation is essential for myriad cell functions in various mammalian cell types (Frye et al., 2018). In the CNS, $m^6A$ is an abundant RNA modification to regulate brain development, neurogenesis, learning and memory, and axon regeneration (Li et al., 2018a; Shi et al., 2017, 2018; Weng et al., 2018b; Yoon et al., 2017). The known $m^6A$ modifiers, including writers, readers, and erasers functions have been implicated as essential for the homeostasis of brain functions. Dysregulation of these modifiers have been implicated in human neurological and psychiatric disorders, both acute and chronic, developmental and degenerative (Berry et al., 2020; Engel et al., 2018; Shafik et al., 2021; Wei et al., 2017; Yoon et al., 2017). While most of the studies were performed in mouse models and postmortem tissues, a recent study showed that in the patient peripheral blood, $m^6A$ level was found impaired in major depressive disorder patients after glucocorticoid stimulation. This indicates $m^6A$ may serve as a potential biomarker for the diagnosis of neurological diseases. Nevertheless, we have very limited knowledge of $m^6A$'s role in regulating glia cell development, function and disease pathogenesis in the CNS.

This leads to my Ph.D. thesis work that is mainly focused on understanding the epigenetic regulation in oligodendrocyte lineage progression in both developmental brain and adult brain.

### 4.1.2 $m^6A$ mRNA methylation regulation is an essential mechanism for regulating oligodendrocyte lineage progression and myelination

Here in my dissertation, I presented evidence that m$^6$A mRNA methylation regulation is essential for oligodendrocyte lineage progression during development and the remyelination response to toxicant-induced demyelination in adulthood. In chapter 2, my work focused on exploring the role of m$^6$A mRNA methylation in oligodendrocyte development and CNS myelination. Our major discoveries are:

- Dynamic changes of m$^6$A levels are accompanied with oligodendrocytes lineage progression.
- m$^6$A mRNA methylation is required for post-mitotic oligodendrocyte maturation and CNS myelination.
- m$^6$A mRNA methylation differentially regulates the transcriptomes of oligodendrocyte lineage cells at different lineage stages.
- m$^6$A mRNA methylation regulates alternative splicing of oligodendrocyte lineage transcriptomes. Proper mRNA splicing of essential oligodendrocyte maturation genes such as *neurofascin* requires m$^6$A methylation.

In the study, we hypothesized that m$^6$A mRNA methylation plays a role in regulating oligodendrocyte lineage progression. To test this hypothesis, we first examined m$^6$A marked transcriptome by combining the m$^6$A-seq and RNA-seq results from wildtype cultured OPCs and mature oligodendrocytes. Due to the limitation of conventional m$^6$A-seq technique, which requires large amount of RNA (400 μg mRNA or 2.5 mg total RNA) (Dominissini et al., 2012), we applied an updated novel approach that combined a single cell RNA-seq technique (SMART2-seq) (Picelli et al., 2014) and m$^6$A-seq method named m$^6$A-SMART-seq (Weng et al., 2018b) to overcome the low amount of RNA input from cultured cells (5 μg total RNA). We successfully detected m$^6$A

marked transcripts in both OPCs and mature oligodendrocytes. We observed dynamic changes of $m^6A$ marked status in the transcripts that are expressed in both OPC and maturation stages, which indicates $m^6A$ RNA methylation accompanied the OPC differentiation and maturation. We then examined the functions of these dynamic $m^6A$ marked transcripts with gene ontology, and we found these transcripts were involved with the oligodendrocyte-specific developmental signaling pathways, which further directs to the conclusion that $m^6A$ plays a role in regulating oligodendrocyte development.

To validate these results, we examined the pathological consequences that could be caused by dysregulation of $m^6A$ RNA methylation in the oligodendrocytes. We developed 2 mouse lines *Mettl14$^{fl/fl}$;Olig2*-Cre and *Mettl14$^{fl/fl}$;CNP*-Cre mice using Cre-LoxP genetic approach, that knocked out the $m^6A$ writer component METTL14 throughout the oligodendrocyte lineage and at post-mitotic developmental stage respectively. In both mouse lines, we observed neurological phenotypes such as hind limb paralysis, and tremor when animals were in their adulthood. *Mettl14$^{fl/fl}$;CNP*-Cre animals showed more severe phenotypes around 4 months old, which was about 2 months earlier than *Mettl14$^{fl/fl}$;Olig2*-Cre animals showed phenotypes. Since *Cnp* expression is present in both oligodendrocytes in CNS and Schwann cells in peripheral nervous system (PNS), we reasoned that $m^6A$ mRNA methylation may affect both oligodendrocyte lineage and Schwann cell lineage development. Indeed, we observed severe myelin pathology in the PNS sciatic nerves in the *Mettl14$^{fl/fl}$;CNP*-Cre mutants (data not shown) and another mouse line that specifically knocked out *Mettl14* in Schwann cells (*Mettl14$^{fl/fl}$;P0*-Cre) (data not shown). In the CNS, *Mettl14$^{fl/fl}$;Olig2*-Cre and *Mettl14$^{fl/fl}$;CNP*-Cre mutant animals showed similar pathology of myelin at the same myelination stages, measured with abnormalities of myelin sheath and

myelinated axon ratios under EM. Similarly in both mouse lines, the abnormalities of oligodendrocyte maturation were also detected by immunohistochemistry at the same myelination stages. Interestingly, we detected the pathology of oligodendrocyte maturation and myelination at very early stage of development (P12) in the mutant animals, even though neurological phenotypes appeared at much later time point. In addition, the myelin pathology got progressively worse during development. These results suggest dysregulation of $m^6A$ at early developmental stage in oligodendrocyte lineage cells could result in severe pathological consequences in later adult life.

In our study, we did not observe abnormalities of either OPCs or proliferating OPC numbers from *Mettl14*$^{fl/fl}$*;Olig2*-Cre mutants both in vivo and in vitro. However, we found that cultured mutant OPCs could not develop into mature oligodendrocytes and form myelin sheaths. These results strongly support the suggestion that $m^6A$ is essential for post-mitotic oligodendrocyte maturation and myelination.

To understand the mechanisms of $m^6A$'s role in regulating oligodendrocyte development and functions, we first compared the transcriptomes in purified OPCs and mature oligodendrocytes from both mutants and controls. We found there were dramatic differences of differentially expressed transcripts in these two lineage stages. We concluded that $m^6A$ differentially regulates the transcriptomes in OPCs and mature oligodendrocytes. This conclusion correlates with the dynamic $m^6A$ tagged status we observed in these two stages. In fact, studies have demonstrated that $m^6A$ levels and tagging status are indeed varied in time and space in the CNS (Chang et al., 2017). In addition, we discovered many key oligodendrocyte lineage regulators such as transcriptional factors, signaling pathways, and DNA epigenetic regulators, histone modifiers are

m$^6$A tagged, indicating the collaboration among these mechanisms to co-regulate the oligodendrocyte maturation and myelination. As a post-transcriptional mechanism, m$^6$A mRNA methylation regulates various aspects of RNA metabolism, such as RNA translation, mRNA splicing, nuclear export, RNA decay (He and He, 2021; Li et al., 2019; Wang et al., 2014a; Xiao et al., 2016b; Zhou et al., 2015). We looked into several potential aspects that were previously shown critical for oligodendrocyte development and myelination: 1. Translational efficiency control 2. mRNA transportation 3. mRNA splicing (Ainger et al., 1997; Hoek et al., 1998; Müller et al., 2013, 2015; White et al., 2012; Zhao et al., 2010a).

First, we compared the transcriptional and translational levels of a subset of m$^6$A marked transcripts that encode proteins critical for oligodendrocyte development. We did not detect the correlated levels of changes between mRNA and proteins, possibly due to the selection biases. Further studies are worth pursuing to elucidate the possible translational efficiency regulation by m$^6$A in the oligodendrocyte lineage cells. Combining comprehensive proteomics study might be helpful to clarify the associations of transcriptional and translational levels. A sophisticated systems biology analysis, which identifies the m$^6$A-tagging pattern with protein co-expression signature, followed with experimental validation, will be very helpful to understand the key targets that are regulated by m$^6$A at the pathway level (Swarup et al., 2020).

Second, we explored m$^6$A's role of the mRNA transportation in the oligodendrocytes. Since *Mbp* is one of the most important and abundant known transcripts that requires proper transportation and local expression in the oligodendrocytes (Meservey et al., 2021), we did preliminary examination on this transcript. To visualize the *Mbp* mRNA, we used RNAscope to label the

transcript with a fluorescent probe. We observed the reduction of *Mbp* mRNA florescence signal in the *Mettl14*$^{fl/fl}$*;Olig2*-Cre mutant oligodendrocytes. However, we were not able to determine whether the reduction was dominated by the overall reduction of *Mbp* mRNA expression, which was validated in the RNA-seq differential analysis, or the impairment of *Mbp* transcript transportation. It would be very helpful to compare the transportation rate and the relative amount of the *Mbp* mRNA in the mutants and controls in live cells. A florescent labeling system that allows visualization of mRNA under time-lapse procedure could promote our understanding m$^6$A's role in the mRNA transportation in the oligodendrocytes.

Third, we examined whether m$^6$A plays a role in alternative splicing Surprisingly, we found many aberrantly transcribed transcripts in *Mettl14*$^{fl/fl}$*;Olig2*-Cre mutant oligodendrocyte lineage cells. These transcripts include transcripts that are essential for oligodendrocyte development and myelination, for example, neurofascin (*Nfasc*) 155, a glia isoform that encodes essential protein in the establishment and maintenance of node of Ranvier domains. We experimentally validate the *Nfasc 155*'s transcriptional, translational levels and its pathological consequences of aberrant splicing in various time points in the mutants. These results indicate m$^6$A RNA methylation plays a role in establishing and maintaining normal function of critical axonal-oligodendrocyte interactions.

It's worth mentioning that even though we were able to detect the m$^6$A tagged status and tagged copies of transcripts, we were not able to locate the m$^6$A methylated nucleotides due to the limited resolution of m$^6$A-SMART-seq. Higher resolution of m$^6$A deposition patterns could reveal the distribution of m$^6$A peaks in each transcript (Zhang et al., 2019), which might help us to better

understand the possible modification machinery of $m^6A$ tagging in splicing. However, the fundamental rules that govern $m^6A$ deposition and functional annotations of the $m^6A$ deposition are still unclear (He and He, 2021). In addition, as an essential $m^6A$ writer, METTL14's deletion causes widespread $m^6A$ tagging deficits, which could lead to both primary and secondary effects on the transcriptome. Thus, we could not differentiate whether our targets of interest are directly or indirectly regulated by $m^6A$ marks. More studies are required to dive deeper to understand how $m^6A$ tagging impacts the key transcript or signaling pathways in the oligodendrocyte lineage and the direct pathological consequences. Molecular tools that can target and manipulate the $m^6A$ metabolism of specific transcripts could be helpful for these studies (Rauch et al., 2018).

### 4.1.3 $m^6A$ mRNA methylation regulation is an essential molecular mechanism for remyelination in the adult CNS

In chapter 3, I explored whether $m^6A$ mRNA methylation plays a role in the remyelination process in the adult CNS. Our major discoveries are:

- $m^6A$ mRNA methylation does not affect survival and proliferation of the adult OPCs
- $m^6A$ mRNA methylation may play a role in regulating OPCs' susceptibility to demyelination microenvironment in the adult CNS
- $m^6A$ mRNA methylation is essential for remyelination in the adult CNS

Remyelination is a crucial step for restoring demyelinated nerve fibers with new myelin, which involves the proliferation, migration, maturation and myelination of OPCs (Chen et al., 2021; Franklin and Goldman, 2015). Our study, for the first time, explored and addressed the $m^6A$ mRNA methylation's role on remyelination in adult brains. In our study, we detected the oligodendrocyte lineage cells at different stages in various time points. It is interesting that, similar

to their counterparts during development, oligodendrocyte lineage cells in adults also require proper m$^6$A mRNA methylation for maturation. The m$^6$A dysregulation does not impact OPCs maintenance and proliferation, or early myelinating cells, however it dramatically affects late stage oligodendrocyte maturation. These data suggests that an m$^6$A deficiency early in the oligodendrocyte lineage blocks late-stage oligodendrocyte maturation. Further studies are required to address the mechanisms of how m$^6$A plays a role in regulating the OPCs transcriptome to affect later lineage pathology. First, it will be helpful to compare the m$^6$A marked transcriptomes of wildtype adult OPCs in the demyelination and remyelination stages, which could reveal the m$^6$A landscape characters in the transcripts that respond to local microenvironment changes. Second, comparing the transcriptomes of adult OPCs between *Mettl14$^{fl/fl}$;PDGFRα-CreERT* mutants and controls in the demyelination and remyelination stages will be helpful to understand the qualitative (e.g: upregulation or downregulation) and quantitative (e.g: fold changes) differences of the transcripts by m$^6$A regulation. Third, proteomic studies that combined with the transcriptomic studies will be helpful to link the m$^6$A regulatory mechanisms with cellular functional levels at different oligodendrocyte lineage stages. Fourth, systemic analytical and validation studies (Chandran et al., 2016; Gandal et al., 2016) will be critical to understand the key regulation networks that are driven by m$^6$A regulation.

In conclusion, the result from this work highlights the critical role of m$^6$A mRNA methylation during remyelination in the adult brain. It is crucial to further study the mechanisms of how m$^6$A plays the role in regulating the remyelination process and validate the results in the human brains. These efforts could further promote the drug discovery for demyelinating diseases such as multiple sclerosis.

## 4.2 Future perspectives of m$^6$A mRNA methylation regulation mechanism in the oligodendrocyte lineage cells and myelination

My thesis research demonstrated the critical role of m$^6$A mRNA methylation in regulating oligodendrocyte lineage cell development, CNS myelination and adulthood remyelination. We explored how m$^6$A plays a role in regulating the transcriptome with various mechanistic perspectives. Nevertheless, it's only the beginning for us to understand this novel post-transcriptional mechanism in the oligodendrocyte lineage progression. More studies are required to expand our knowledge to understand and integrate m$^6$A mRNA methylation mechanism to a bigger picture of molecular regulation systems.

### 4.2.1 Potential collaboration of m$^6$A mRNA methylation with other regulatory mechanisms during oligodendrocyte lineage progression

One interesting finding in my thesis study is that there are changed m$^6$A marked status in a stage-dependent manner on numerous transcripts that encode transcriptional factors, histone modifiers, and signaling pathways that are essential for oligodendrocyte development. This finding suggest that there are collaborations between m$^6$A RNA modifications with other key regulators during the process of oligodendrocyte lineage progression. As a post-transcriptional mechanism, m$^6$A mRNA methylation regulates gene expression prior to translation, thus it is possible m$^6$A tagging guides these regulators to exert functions. Besides, compared to DNA and histone epigenetic regulators, m$^6$A mRNA methylation has the potential to turnover transcripts more rapidly during cell-state transitions (Frye et al., 2018). In turn, the changes of these regulators' expression may alter the efficiency of m$^6$A writing, reading and erasing (Aguilo et al., 2015; Chen et al., 2015; Wang et al.,

2018). In addition, we also found dramatic alterations of important signaling pathway transcripts and myelin-associated transcripts that do not bear any m$^6$A mark, suggesting that m$^6$A RNA modification may have a primary or secondary effect on gene expression. It is possible m$^6$A plays a role in mediating other regulators to exert secondary effects on gene expression. Further investigations are needed to elucidate how m$^6$A RNA methylation collaborates with other regulatory mechanisms during oligodendrocyte lineage progression.

### 4.2.2 m$^6$A mRNA methylation regulation in myelin plasticity

In this dissertation, our results demonstrated that m$^6$A is essential for oligodendrocyte maturation, not only during development, but also in the adult brain. Recent studies suggest that the plasticity of oligodendrocyte lineage and myelin sheath formation play a crucial role in forming neuronal circuits in life experience, learning and memory (Almeida and Lyons, 2017; Hughes et al., 2018; Pan et al., 2020; Pepper et al., 2018; Xin and Chan, 2020), in both developmental and adulthood. These findings trigger two important questions: 1. Does m$^6$A mRNA methylation regulation in oligodendrocytes play a role in forming early life experiences? 2. Is m$^6$A mRNA methylation regulation in oligodendrocytes required for skill learning in adulthood? In mice, P21-P35 is a critical period for social experience- dependent oligodendrocyte maturation and myelination (Makinodan et al., 2012). In our study, we showed that early embryonic m$^6$A dysregulation in the oligodendrocytes lineage (*Mettl14$^{fl/fl}$;Olig2*-Cre mice) leads to CNS hypomyelination before the critical period starts (P12, P18). In addition, our data from *Mettl14$^{fl/fl}$;PDGFRα-CreERT* indicates m$^6$A dysregulation after adulthood is critical for oligodendrocyte maturation. To answer the first question, it will be interesting to study the early life behaviors of mice that bear developmental stage-specific m$^6$A dysregulation (e.g. Cre induction during critical period in *Mettl14$^{fl/fl}$;PDGFRα-*

*CreERT* mice), followed by examining underlying cellular and molecular mechanisms that resulted from m$^6$A mRNA methylation. For example, interrogating m$^6$A mRNA methylation's potential role in molecular regulatory mechanisms such as neuregulin-1/ErbB3 signaling pathway, which is essential for prefrontal cortex myelination and social experience formation during critical period (Makinodan et al., 2012). To answer the second question, it will be interesting to examine the m$^6$A mRNA methylation's role in adulthood motor skill learning in a "complex wheel" system (McKenzie et al., 2014; Xiao et al., 2016a). Mice spontaneously run a normal wheel, however they need to master new motor skills in order to run on a "complex wheel" with irregular rung spacing (McKenzie et al., 2014; Xiao et al., 2016a). Early oligodendrocytes formation is required for the motor skill learning. And oligodendrocytes respond very rapidly to the novel experience, that is much faster than any other reported physiological or artificial stimuli (Xiao et al., 2016a). Since m$^6$A mRNA methylation regulates rapid changes of transcriptomes, and is required for oligodendrocyte maturation, we hypothesis that m$^6$A dysregulation could affect motor skill learning process. Nevertheless, the fundamental knowledge of how oligodendrocytes play a role in the motor skill learning is still rudimentary (Xiao et al., 2016a). More work is required to understand oligodendrocytes' role in neural plasticity, and m$^6$A mRNA methylation's role in regulating this process.

### 4.2.3 m$^6$A mRNA methylation's role in multiple sclerosis

In Chapter 3, I showed m$^6$A mRNA methylation is critical for the remyelination process in the adulthood. The study demonstrated the dysregulation of m$^6$A in the adult OPCs results in the impairment of oligodendrocyte maturation, thus leads to the remyelination deficits. Another interesting finding in this study is that *Mettl14* deletion in the adult OPCs leads to severe

demyelination at peak disease, suggesting cross-talks between oligodendrocyte lineage cells during CNS demyelination process. These results indicate the dysregulation of $m^6A$ mRNA methylation may play a role in the pathogenesis of demyelinating and remyelination diseases, such as multiple sclerosis (MS). In fact, recent evidence indicates that $m^6A$ mRNA methylation plays a role in enhancing Cap-independent translation in response to cellular stress (Meyer et al., 2015; Zhou et al., 2015). As we know, cell stress is a hallmark of oligodendrocyte pathology during demyelination (Chen et al., 2021; Clayton et al., 2017; Way and Popko, 2016; Way et al., 2015), thus it is reasonable to hypothesis $m^6A$ mRNA methylation plays a pivotal role in the rapid response of oligodendrocyte lineage cells to extracellular stimuli and/or perturbations that could lead to diseases. It will be very important to pursue our study described in Chapter 3, to elucidate the molecular mechanisms and downstream targets of $m^6A$ mRNA methylation modification. In addition, it will be interesting to explore $m^6A$ RNA methylation's role in another CNS demyelination model called experimental autoimmune encephalomyelitis (EAE). It is a model of MS in which CNS immune cell infiltration results in oligodendrocyte death and demyelination. The core pathological event in the MS and EAE CNS is the inflammatory environment that deteriorate the function and viability of oligodendrocytes. Our lab's previous studies have shown that mice in which oligodendrocytes have a diminished capacity to respond to stress experience have more severe EAE disease course that correlates with increased loss of oligodendrocytes and more severe demyelination (Hussien et al., 2014, 2015; Lin et al., 2005, 2007). However, mouse models in which the oligodendrocytes are more resistant to stress experience a less severe EAE phenotypes that is associated with diminished oligodendrocyte loss and demyelination (Lin et al., 2008, 2013; Way et al., 2015). Thus, it will be important to determine if $m^6A$ RNA methylation

plays a role in the response of oligodendrocytes to the stress associated with an inflammatory environment.

So far, there is only one study regarding $m^6A$ mRNA methylation modification in multiple sclerosis (Mo et al., 2019). Using genome wide associate studies (GWAS) in MS patients, the study found multiple $m^6A$ associated single nucleotide polymorphysisms ($m^6A$ -SNPs) (Zheng et al., 2018) are strongly associated with MS. Excitingly, the authors validated the associations of the $m^6A$ -SNPs with their gene expression levels in the peripheral blood samples from a group of Chinese Han individuals (Mo et al., 2019). However, the mechanisms of $m^6A$ mRNA methylation in the MS pathogenesis is still unclear. Further studies are required to elucidate how $m^6A$ regulation associated genetic variants contribute to MS as well as to develop potential diagnostic tools and treatments for MS patients.

### 4.2.4 $m^6A$ mRNA methylation's role in myelination at different stages and ages

One important finding in my thesis work is that $m^6A$ mRNA methylation differentially affects transcriptomes of OPCs and mature oligodendrocytes, suggesting $m^6A$ tagging plays distinct roles at different oligodendrocyte lineage progression stages during development. In addition, we observed similar oligodendrocyte lineage progression failure after $m^6A$ mRNA methylation is disrupted in adult OPCs. These results raise the question of whether $m^6A$ mRNA methylation plays a role and what the role it plays at different myelination stages and ages. It will be helpful to map the differences between developmental myelination and adult remyelination, a fundamental question in the field that is yet to be understood. While myelination requires the activation of OPCs proliferation, migration and differentiation in both developmental brains and

adult brains, the microenvironment for the myelination process is dramatically different. Glia cells including oligodendrocytes lineage cells were conventional thought as homogenous in the CNS, however, until recently, studies have found that these cells have different transcriptome and proteome at different ages across different brain regions. And the changes in -omics studies are strongly associated with aging (Soreq et al., 2017). A recent study showed OPCs' functions become regionally diverse and heterogeneous from development to adulthood, with significant shift of molecular features such as ion channel expression (Spitzer et al., 2019). These studies suggest distinct cellular regulatory molecular mechanisms or regulatory patterns exist between developmental myelination and adult remyelination. Nevertheless, while many remyelination studies focus on known transcriptional factors that influence developmental myelination, there is very little knowledge of factors with selective roles in the adult remyelination brains (Sock and Wegner, 2019). As a post-transcriptional mechanism, displays distinct regulatory pattern during oligodendrocyte lineage progression. A recent study has shown $m^6A$ mRNA methylation regulation is brain region, time and gene specific in the adult brains (Engel et al., 2018). Thus it is highly likely that it also regulates the myelination process at distinct stages and ages. Further studies are required to further understand how $m^6A$ mRNA methylation regulation plays a role across time and space during myelination.

### 4.3 Conclusion

$m^6A$ mRNA modifications have recently emerged as a critical post-transcriptional regulatory mechanism to modulate gene expression (Frye et al., 2018; He and He, 2021). In this dissertation, our data demonstrates that $m^6A$ mRNA modification is essential for normal oligodendrocyte maturation, CNS myelination during development and remyelination in

adulthood. We examined the potential mechanisms of $m^6A$ mRNA modification in regulating the oligodendrocyte lineage development. We showed that the $m^6A$ mark plays an important role in regulating various aspects of gene expression in oligodendrocyte lineage cells, with the most profound effects on mRNA levels and splicing. We also showed that $m^6A$ mRNA modification is critical for adult oligodendrocyte lineage cell maturation and CNS remyelination. Future studies that involve multi-faced mechanistic characterization of $m^6A$ mRNA epigenetic regulation in oligodendrocyte functions should provide important insight to our growing understanding of the myelination process and remyelinating process. In addition, using growing sequencing techniques, genetic and pharmaceutical tools may provide a unique opportunity for early diagnosis, prevention and treatment of demyelination diseases that are caused by $m^6A$ mRNA methylation dysregulation.

## 4.4 References


Aguilo, F., Zhang, F., Sancho, A., Fidalgo, M., Di Cecilia, S., Vashisht, A., Lee, D.-F., Chen, C.-H., Rengasamy, M., Andino, B., et al. (2015). Coordination of m(6)A mRNA Methylation and Gene Transcription by ZFP217 Regulates Pluripotency and Reprogramming. Cell Stem Cell *17*, 689–704.

Ainger, K., Avossa, D., Diana, A.S., Barry, C., Barbarese, E., and Carson, J.H. (1997). Transport and localization elements in myelin basic protein mRNA. J. Cell Biol. *138*, 1077–1087.

Almeida, R.G., and Lyons, D.A. (2017). On myelinated axon plasticity and neuronal circuit formation and function. J. Neurosci. *37*, 10023–10034.

Berry, K., Wang, J., and Lu, Q.R. (2020). Epigenetic regulation of oligodendrocyte myelination in developmental disorders and neurodegenerative diseases. [version 1; peer review: 2 approved]. F1000Res. *9*.

Chandran, V., Coppola, G., Nawabi, H., Omura, T., Versano, R., Huebner, E.A., Zhang, A., Costigan, M., Yekkirala, A., Barrett, L., et al. (2016). A Systems-Level Analysis of the Peripheral Nerve Intrinsic Axonal Growth Program. Neuron *89*, 956–970.

Chang, M., Lv, H., Zhang, W., Ma, C., He, X., Zhao, S., Zhang, Z.-W., Zeng, Y.-X., Song, S., Niu, Y., et al. (2017). Region-specific RNA m6A methylation represents a new layer of control in the gene regulatory network in the mouse brain. Open Biol *7*.

Chen, T., Hao, Y.-J., Zhang, Y., Li, M.-M., Wang, M., Han, W., Wu, Y., Lv, Y., Hao, J., Wang, L., et al. (2015). m(6)A RNA methylation is regulated by microRNAs and promotes reprogramming to pluripotency. Cell Stem Cell *16*, 289–301.

Chen, Y., Kunjamma, R.B., Weiner, M., Chan, J.R., and Popko, B. (2021). Prolonging the integrated stress response enhances CNS remyelination in an inflammatory environment. Elife *10*.

Clayton, B.L., Huang, A., Kunjamma, R.B., Solanki, A., and Popko, B. (2017). The integrated stress response in hypoxia-induced diffuse white matter injury. J. Neurosci.

Dominissini, D., Moshitch-Moshkovitz, S., Schwartz, S., Salmon-Divon, M., Ungar, L., Osenberg, S., Cesarkas, K., Jacob-Hirsch, J., Amariglio, N., Kupiec, M., et al. (2012). Topology of the human and mouse m6A RNA methylomes revealed by m6A-seq. Nature *485*, 201–206.

Engel, M., Eggert, C., Kaplick, P.M., Eder, M., Röh, S., Tietze, L., Namendorf, C., Arloth, J., Weber, P., Rex-Haffner, M., et al. (2018). The Role of m6A/m-RNA Methylation in Stress Response Regulation. Neuron *99*, 389–403.e9.

Franklin, R.J.M., and Goldman, S.A. (2015). Glia Disease and Repair-Remyelination. Cold Spring Harb. Perspect. Biol. *7*, a020594.

Frye, M., Harada, B.T., Behm, M., and He, C. (2018). RNA modifications modulate gene expression during development. Science *361*, 1346–1349.

Gandal, M.J., Leppa, V., Won, H., Parikshak, N.N., and Geschwind, D.H. (2016). The road to precision psychiatry: translating genetics into disease mechanisms. Nat. Neurosci. *19*, 1397–1407.

Gregath, A., and Lu, Q.R. (2018). Epigenetic modifications-insight into oligodendrocyte lineage progression, regeneration, and disease. FEBS Lett. *592*, 1063–1078.

He, P.C., and He, C. (2021). m6 A RNA methylation: from mechanisms to therapeutic potential. EMBO J. *40*, e105977.

Hoek, K.S., Kidd, G.J., Carson, J.H., and Smith, R. (1998). hnRNP A2 selectively binds the cytoplasmic transport sequence of myelin basic protein mRNA. Biochemistry *37*, 7021–7029.

Hughes, E.G., Orthmann-Murphy, J.L., Langseth, A.J., and Bergles, D.E. (2018). Myelin remodeling through experience-dependent oligodendrogenesis in the adult somatosensory cortex. Nat. Neurosci. *21*, 696–706.

Hussien, Y., Cavener, D.R., and Popko, B. (2014). Genetic inactivation of PERK signaling in mouse oligodendrocytes: normal developmental myelination with increased susceptibility to inflammatory demyelination. Glia *62*, 680–691.

Hussien, Y., Podojil, J.R., Robinson, A.P., Lee, A.S., Miller, S.D., and Popko, B. (2015). ER Chaperone BiP/GRP78 Is Required for Myelinating Cell Survival and Provides Protection during Experimental Autoimmune Encephalomyelitis. J. Neurosci. *35*, 15921–15933.

Koreman, E., Sun, X., and Lu, Q.R. (2018). Chromatin remodeling and epigenetic regulation of oligodendrocyte myelination and myelin repair. Mol. Cell. Neurosci. *87*, 18–26.

Li, J., Yang, X., Qi, Z., Sang, Y., Liu, Y., Xu, B., Liu, W., Xu, Z., and Deng, Y. (2019). The role of mRNA m6A methylation in the nervous system. Cell Biosci. *9*, 66.

Li, M., Zhao, X., Wang, W., Shi, H., Pan, Q., Lu, Z., Perez, S.P., Suganthan, R., He, C., Bjørås, M., et al. (2018). Ythdf2-mediated m6A mRNA clearance modulates neural development in mice. Genome Biol. *19*, 69.

Lin, W., Harding, H.P., Ron, D., and Popko, B. (2005). Endoplasmic reticulum stress modulates the response of myelinating oligodendrocytes to the immune cytokine interferon-gamma. J. Cell Biol. *169*, 603–612.

Lin, W., Bailey, S.L., Ho, H., Harding, H.P., Ron, D., Miller, S.D., and Popko, B. (2007). The integrated stress response prevents demyelination by protecting oligodendrocytes against immune-mediated damage. J. Clin. Invest. *117*, 448–456.

Lin, W., Kunkler, P.E., Harding, H.P., Ron, D., Kraig, R.P., and Popko, B. (2008). Enhanced integrated stress response promotes myelinating oligodendrocyte survival in response to interferon-gamma. Am. J. Pathol. *173*, 1508–1517.

Lin, W., Lin, Y., Li, J., Fenstermaker, A.G., Way, S.W., Clayton, B., Jamison, S., Harding, H.P., Ron, D., and Popko, B. (2013). Oligodendrocyte-specific activation of PERK signaling protects mice against experimental autoimmune encephalomyelitis. J. Neurosci. *33*, 5980–5991.

Makinodan, M., Rosen, K.M., Ito, S., and Corfas, G. (2012). A critical period for social experience-dependent oligodendrocyte maturation and myelination. Science *337*, 1357–1360.

McKenzie, I.A., Ohayon, D., Li, H., de Faria, J.P., Emery, B., Tohyama, K., and Richardson, W.D. (2014). Motor skill learning requires active central myelination. Science *346*, 318–322.

Meservey, L.M., Topkar, V.V., and Fu, M.-M. (2021). mRNA Transport and Local Translation in Glia. Trends Cell Biol.

Meyer, K.D., Patil, D.P., Zhou, J., Zinoviev, A., Skabkin, M.A., Elemento, O., Pestova, T.V., Qian, S.B., and Jaffrey, S.R. (2015). 5’ UTR m(6)A Promotes Cap-Independent Translation. Cell *163*, 999–1010.

Mo, X.-B., Lei, S.-F., Qian, Q.-Y., Guo, Y.-F., Zhang, Y.-H., and Zhang, H. (2019). Integrative analysis revealed potential causal genetic and epigenetic factors for multiple sclerosis. J. Neurol. *266*, 2699–2709.

Müller, C., Bauer, N.M., Schäfer, I., and White, R. (2013). Making myelin basic protein -from mRNA transport to localized translation. Front. Cell Neurosci. *7*, 169.

Müller, C., Schäfer, I., Luhmann, H.J., and White, R. (2015). Oligodendroglial Argonaute protein Ago2 associates with molecules of the Mbp mRNA localization machinery and is a downstream target of Fyn kinase. Front. Cell Neurosci. *9*, 328.

Pan, S., Mayoral, S.R., Choi, H.S., Chan, J.R., and Kheirbek, M.A. (2020). Preservation of a remote fear memory requires new myelin formation. Nat. Neurosci. *23*, 487–499.

Pepper, R.E., Pitman, K.A., Cullen, C.L., and Young, K.M. (2018). How do cells of the oligodendrocyte lineage affect neuronal circuits to influence motor function, memory and mood? Front. Cell Neurosci. *12*, 399.

Picelli, S., Faridani, O.R., Björklund, A.K., Winberg, G., Sagasser, S., and Sandberg, R. (2014). Full-length RNA-seq from single cells using Smart-seq2. Nat. Protoc. *9*, 171–181.

Rauch, S., He, C., and Dickinson, B.C. (2018). Targeted m6a reader proteins to study epitranscriptomic regulation of single rnas. J. Am. Chem. Soc. *140*, 11974–11981.

Shafik, A.M., Zhang, F., Guo, Z., Dai, Q., Pajdzik, K., Li, Y., Kang, Y., Yao, B., Wu, H., He, C., et al. (2021). N6-methyladenosine dynamics in neurodevelopment and aging, and its potential role in Alzheimer's disease. Genome Biol. *22*, 17.

Shi, H., Wang, X., Lu, Z., Zhao, B.S., Ma, H., Hsu, P.J., Liu, C., and He, C. (2017). YTHDF3 facilitates translation and decay of N6-methyladenosine-modified RNA. Cell Res. *27*, 315–328.

Shi, H., Zhang, X., Weng, Y.-L., Lu, Z., Liu, Y., Lu, Z., Li, J., Hao, P., Zhang, Y., Zhang, F., et al. (2018). m6A facilitates hippocampus-dependent learning and memory through YTHDF1. Nature *563*, 249–253.

Sock, E., and Wegner, M. (2019). Transcriptional control of myelination and remyelination. Glia *67*, 2153–2165.

Soreq, L., UK Brain Expression Consortium, North American Brain Expression Consortium, Rose, J., Soreq, E., Hardy, J., Trabzuni, D., Cookson, M.R., Smith, C., Ryten, M., et al. (2017). Major shifts in glial regional identity are a transcriptional hallmark of human brain aging. Cell Rep. *18*, 557–570.

Spitzer, S.O., Sitnikov, S., Kamen, Y., Evans, K.A., Kronenberg-Versteeg, D., Dietmann, S., de Faria, O., Agathou, S., and Káradóttir, R.T. (2019). Oligodendrocyte Progenitor Cells Become Regionally Diverse and Heterogeneous with Age. Neuron *101*, 459–471.e5.

Swarup, V., Chang, T.S., Duong, D.M., Dammer, E.B., Dai, J., Lah, J.J., Johnson, E.C.B., Seyfried, N.T., Levey, A.I., and Geschwind, D.H. (2020). Identification of conserved proteomic networks in neurodegenerative dementia. Cell Rep. *31*, 107807.

Wang, X., Lu, Z., Gomez, A., Hon, G.C., Yue, Y., Han, D., Fu, Y., Parisien, M., Dai, Q., Jia, G., et al. (2014). N6-methyladenosine-dependent regulation of messenger RNA stability. Nature *505*, 117–120.

Wang, Y., Li, Y., Yue, M., Wang, J., Kumar, S., Wechsler-Reya, R.J., Zhang, Z., Ogawa, Y., Kellis, M., Duester, G., et al. (2018). N6-methyladenosine RNA modification regulates embryonic neural stem cell self-renewal through histone modifications. Nat. Neurosci. *21*, 195–206.

Way, S.W., and Popko, B. (2016). Harnessing the integrated stress response for the treatment of multiple sclerosis. Lancet Neurol. *15*, 434–443.

Way, S.W., Podojil, J.R., Clayton, B.L., Zaremba, A., Collins, T.L., Kunjamma, R.B., Robinson, A.P., Brugarolas, P., Miller, R.H., Miller, S.D., et al. (2015). Pharmaceutical integrated stress response enhancement protects oligodendrocytes and provides a potential multiple sclerosis therapeutic. Nat. Commun. *6*, 6532.

Wei, W., Ji, X., Guo, X., and Ji, S. (2017). Regulatory Role of N6-methyladenosine (m6A) Methylation in RNA Processing and Human Diseases. J. Cell Biochem. *118*, 2534–2543.

Weng, Y.-L., Wang, X., An, R., Cassin, J., Vissers, C., Liu, Y., Liu, Y., Xu, T., Wang, X., Wong, S.Z.H., et al. (2018). Epitranscriptomic m6a regulation of axon regeneration in the adult mammalian nervous system. Neuron *97*, 313–325.e6.

White, R., Gonsior, C., Bauer, N.M., Krämer-Albers, E.-M., Luhmann, H.J., and Trotter, J. (2012). Heterogeneous nuclear ribonucleoprotein (hnRNP) F is a novel component of oligodendroglial RNA transport granules contributing to regulation of myelin basic protein (MBP) synthesis. J. Biol. Chem. *287*, 1742–1754.

Xiao, L., Ohayon, D., McKenzie, I.A., Sinclair-Wilson, A., Wright, J.L., Fudge, A.D., Emery, B., Li, H., and Richardson, W.D. (2016a). Rapid production of new oligodendrocytes is required in the earliest stages of motor-skill learning. Nat. Neurosci. *19*, 1210–1217.

Xiao, W., Adhikari, S., Dahal, U., Chen, Y.-S., Hao, Y.-J., Sun, B.-F., Sun, H.-Y., Li, A., Ping, X.-L., Lai, W.-Y., et al. (2016b). Nuclear m(6)A Reader YTHDC1 Regulates mRNA Splicing. Mol. Cell *61*, 507–519.

Xin, W., and Chan, J.R. (2020). Myelin plasticity: sculpting circuits in learning and memory. Nat. Rev. Neurosci. *21*, 682–694.

Yoon, K.-J., Ringeling, F.R., Vissers, C., Jacob, F., Pokrass, M., Jimenez-Cyrus, D., Su, Y., Kim, N.-S., Zhu, Y., Zheng, L., et al. (2017). Temporal control of mammalian cortical neurogenesis by m6a methylation. Cell *171*, 877–889.e17.

Zhang, Z., Chen, L.-Q., Zhao, Y.-L., Yang, C.-G., Roundtree, I.A., Zhang, Z., Ren, J., Xie, W., He, C., and Luo, G.-Z. (2019). Single-base mapping of m6A by an antibody-independent method. Sci. Adv. *5*, eaax0250.

Zhao, L., Mandler, M.D., Yi, H., and Feng, Y. (2010). Quaking I controls a unique cytoplasmic pathway that regulates alternative splicing of myelin-associated glycoprotein. Proc. Natl. Acad. Sci. USA *107*, 19061–19066.

Zheng, Y., Nie, P., Peng, D., He, Z., Liu, M., Xie, Y., Miao, Y., Zuo, Z., and Ren, J. (2018). m6AVar: a database of functional variants involved in m6A modification. Nucleic Acids Res. *46*, D139–D145.

Zhou, J., Wan, J., Gao, X., Zhang, X., Jaffrey, S.R., and Qian, S.-B. (2015). Dynamic m(6)A mRNA methylation directs translational control of heat shock response. Nature *526*, 591–594.